Platinum based bifunctional catalysts for carbon dioxide reforming of methane

Activity, stability and mechanism

J.H. Bitter

Leden van de promotiecommissie

Prof.dr. J.A. Lercher (promotor)

Dr. K. Seshan (assistent promotor)

Prof.dr. W.E. van der Linden (voorzitter/secretaris)

Prof.dr. W.F. Maier (Max Planck Institut für Kohlenforschung, Mülheim an der Ruhr)

Prof.dr. R.A. van Santen (TU Eindhoven)

Dr. W.H.J. Stork (Shell Research and Technology Centre Amsterdam)

Prof.dr.ir. W.P.M. van Swaaij (Universiteit Twente)

Prof.dr.ir. H. Verweij (Universiteit Twente)

The research described in this thesis was financially supported by the European Community (JOULE II programme, contract no. JOU2-CT92-0073)

ISBN 90-365-0963-7

PLATINUM BASED BIFUNCTIONAL CATALYSTS FOR CARBON DIOXIDE REFORMING OF METHANE

ACTIVITY, STABILITY AND MECHANISM

PROEFSCHRIFT

ter verkrijging van
de graad van doctor aan de Universiteit Twente,
op gezag van de rector magnificus
prof.dr. F.A. van Vught
volgens het besluit van het College voor Promoties
in het openbaar te verdedigen
op donderdag 12 juni 1997 te 13.15 uur.

door
Johannes Hendrik Bitter
geboren op 6 september 1969
te Zeist

Dit proefschrift is goedgekeurd door de promotor
prof.dr. J.A. Lercher

en de assistent promotor
dr. K. Seshan

Why worry, there should be laughter after pain
There should be sunshine after rain
These things have always been the same
So why worry now

Dire Straits
From the album “Brothers in Arms”

Enschede, 29 april 1997

Dankwoord

Deze bladzijde van het proefschrift is speciaal bestemd voor een ieder die op enigerlei wijze een bijdrage geleverd heeft aan de tot standkoming ervan. Een aantal mensen wil ik echter met name bedanken.

Allereerst pa en ma hartelijk dank voor alle steun die jullie de afgelopen jaren gegeven hebben. Helma van harte bedankt voor alle liefde en ondersteuning en voor het corrigeren van de meest vreselijke, door mij bedachte, zinsconstructies als er weer eens wat geschreven moest worden.

Het werk werd aanmerkelijk veraangenaamd door een aantal goede vrienden: Wilma, Barbara en Eric. Bij Wilma Busser kon ik altijd terecht met vragen over het onderzoek of voor een avond video/film kijken. De films werden door haar op een geheel eigen manier van commentaar voorzien wat een nieuwe dimensie aan het filmkijken toevoegde. Barbara Mojet vrolijkte altijd de logeerweekendjes op wanneer zij bij ons in Enschede was of wanneer wij in het 'verre' Utrecht waren. Eric Wessels wil ik hartelijk danken voor het dienen als help desk wanneer mijn computer weer eens niet naar mij wilde luisteren en het voor aanleveren van allerlei nuttige URL's.

Mijn dank gaat ook uit naar Prof. Lercher, Dr. Seshan en Dr. van Ommen voor de mogelijkheid die zij geboden hebben om onderzoek te kunnen verrichten in de katalyse groep. Tevens wil ik hen bedanken voor de begeleiding en sturing van het onderzoek.

Het was altijd erg gezellig in ons kantoor, daarvoor wil ik mijn (ex)kamergenoten André Steghuis, Willie Hally en Laurent Simon van harte bedanken. Verdere wil ik alle collega's van de katalyse groep van harte bedanken, ik kon altijd bij jullie binnenlopen om een praatje te maken waar ik dan ook dankbaar gebruik van gemaakt heb.

A special thanks to the EXAFS-colleagues (Saskia, Wilma, Andy, Martin, Walter) for keeping me (or was it the other way around?) awake during the long nights of measurements.

Naast de mensen die op wetenschappelijke wijze een bijdrage geleverd hebben aan het tot stand komen van dit werk wil ik ook de mensen bedanken die een niet-wetenschappelijk bijdrage hebben geleverd:
Bert Geerdink voor het leveren van creatieve oplossingen als de apparatuur weer eens niet wilde werken. En voor de zak met dropjes die op jouw buro te vinden was (alhoewel die snel leeg was nadat ik hem gevonden had). Karin Schildkamp voor het snel bestellen en leveren van de chemicaliën. Cis Twilt voor de nodige secretariële ondersteuning.

Er zijn zeker mensen die ik vergeten ben te noemen vandaar voor iedereen die een bijdrage aan het tot standkomen van dit proefschrift geleverd heeft: van harte bedankt!

Harry Bitter

Table of contents

1

1

General introduction

1.1 Synthesis gas, a general introduction

Synthesis gas (or syngas), a mixture of hydrogen and carbon monoxide is one of the most important feedstocks in the chemical industry. From syngas mixtures having different H_2/CO ratios a wide variety of products can be manufactured (Table 1) [1-3].

Table 1 *Sources of syngas and their applications*

H_2/CO ratio	Reaction	Application
1	$CH_4 + CO_2 \rightleftharpoons 2CO + 2H_2$	Oxoalcohols, polycarbonates, formaldehyde production
2	$CH_4 + 0.5O_2 \rightleftharpoons CO + 2H_2$	Methanol synthesis, Fischer-Tropsch synthesis
>3	$CH_4 + H_2O \rightleftharpoons CO + 3H_2$ &	H_2 production e.g. for
	$CO + H_2O \rightleftharpoons CO_2 + H_2$	ammonia synthesis

The compounds summarized in Table 1 are all derived from syngas produced from methane. Methane is the main component of natural gas although significant amounts of other gases such as ethane, propane, H_2S and CO_2 might be present. The composition of

Table 2 *Some compositions of natural gas (in volume %) [4]*

	Slochteren (The Netherlands)	Lacq (France)	Hass R'mel (Algeria)	Sarmas (Romania)	Dachave (former USSR)	Old Fields (Alberta)	Terrell County (Texas USA)
CH_4	81.9	69.4	83.5	99.2	98.0	52.3	45.7
C_2H_6	2.7	2.8	7.0	-	0.7	0.41	0.2
C_3H_8	0.38	1.5	2.0	-	-	0.14	-
C_4H_{10}	0.13	0.7	0.8	-	-	0.16	-
$>=C_5$	0.08	0.6	0.4	-	-	0.41	-
H_2S	-	15.2	-	-	-	35.79	-
CO_2	0.8	9.5	0.2	-	0.1	8.22	53.9
N_2	14	0.3	6.1	0.8	1.2	2.53	0.2

natural gas from different fields is compiled in Table 2 [2, 4]. The proven natural gas reserves have increased by a factor 4 during the last 25 years (see Figure 1) [1, 5-7]. Thus, a large amount of natural gas is available. The problem is however, that most of the natural gas is located in remote areas (see Figure 2) [8] and thus is difficult to access. The infrastructure necessary to transport gas over large distances requires a considerable investment [9]. Therefore on site conversion of the natural gas to more easily transportable (liquid, solid) or otherwise more valuable products is economically advantageous. In this respect different options are possible. Methane can be converted to higher hydrocarbons *via* the oxidative coupling of methane [10-12]. It can also be partially oxidized to methanol [13, 14] or formaldehyde [15]. However, for the direct conversion of methane to these products no commercial processes are available today. Another possibility is to convert natural gas to more valuable products *via* the production of syngas (Tables 1 and 3). Four different options to convert methane to syngas are summarized in Table 3 (steam reforming, partial oxidation, CO_2 reforming, autothermal reforming). These options will be discussed in the next paragraphs.

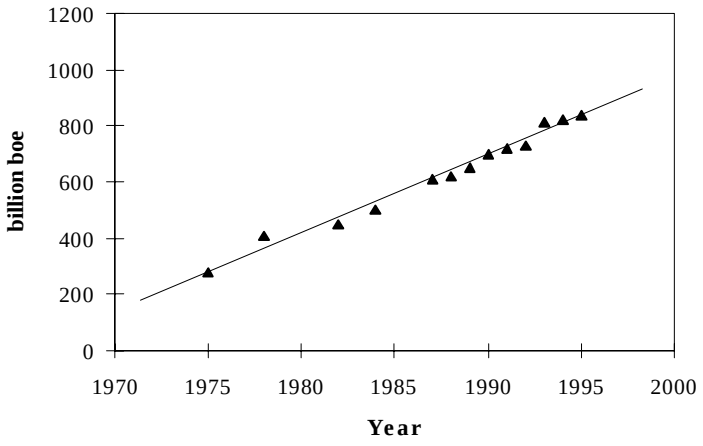

Figure 1 *The world proven reserves of natural gas (graph reproduced from ref [5]), boe=barrels oil equivalent*

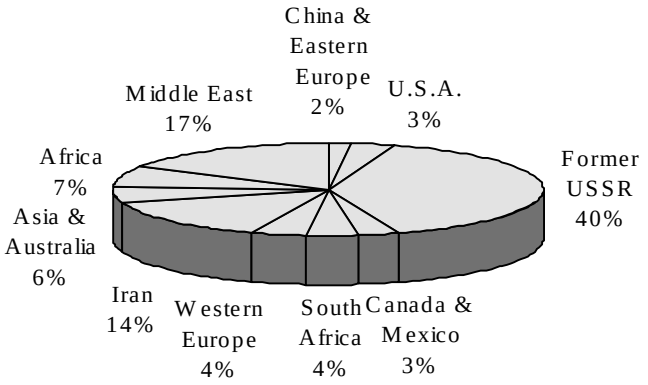

Figure 2 *Distribution of world proven gas reserves [6]*

Table 3 *Different reactions to produce syngas*

Reaction	equation		ΔH^{o}_{298} kJ/mol
steam reforming	$CH_4 + H_2O \rightleftharpoons CO + 3H_2$	**1**	206
partial oxidation	$CH_4 + 0.5\ O_2 \rightleftharpoons CO + 2H_2$	**2**	-36
CO_2 reforming	$CH_4 + CO_2 \rightleftharpoons 2CO + 2H_2$	**3**	247
autothermal reforming	$CH_4 + 2O_2 \rightarrow CO_2 + 2H_2O$ methane in excess	**4**	-802
	$CH_4 + H_2O \rightleftharpoons CO + 3H_2$ & $CH_4 + CO_2 \rightleftharpoons 2CO + 2H_2$	**1** **3**	206 247

1.2 Production of syngas

1.2.1 Steam reforming

The most widely used process for syngas production is steam reforming ($H_2O + CH_4 \rightleftharpoons CO + 3H_2$ (**1**); ΔH^0_{298K}=206kJ/mol) [16-18]. The process is typically operated at 15-30 bar and the outlet temperature of the reactor is typically 1123-1223K [19] with a H_2O/CH_4 ratio higher than 0.4. Steam reforming can be blended with CO_2-reforming to adjust the H_2/CO ratio in the produced syngas. In this case CO_2 is added in the range CO_2/CH_4 = 0.6-2.0 [19]. All group VIII metals show an appreciable activity for steam reforming. However, Rh and Ru show the highest activity but due to the poor availability of Rh and Ru, Ni is the most commonly used metal. To stabilize the surface area of the metal, oxidic materials with a low surface area (MgO, α-Al_2O_3) are used as supports because of their stability under reaction conditions (high temperatures (>1100K) and the presence of steam). SiO_2 is not a suitable support due to the possible formation of volatile $Si(OH)_4$ under reaction conditions [17, 20] which might cause a coverage of the metal particles with Si-containing species. Although steam reforming is the most widely used process to produce synthesis gas (mostly for methanol production) the alternative

processes described in the next paragraphs may have economic advantages [21], depending on the syngas stoichiometry needed or the availability of an oxygen plant (for oxidation of methane).

1.2.2 Partial oxidation

Partial oxidation of methane ($CH_4 + 0.5O_2 \rightleftharpoons CO + 2H_2$ (**2**); ΔH^0_{298K}=-36kJ/mol) converts methane in the presence of oxygen to syngas with a H_2/CO ratio of 2. Partial oxidation can be operated both non-catalytically [21-23] and catalytically [24-27]. In the non-catalytic process methane and oxygen typically react at 1350-1800K at a pressure ranging from atmospheric pressure to 140 bars [19]. These high temperatures require special expensive reactor materials. The advantage of the catalytic partial oxidation compared to the non-catalytic process is the possibility to carry out the reaction at lower temperatures (1000-1200K) [24-27] thus the requirements for the reactors are less stringent in this case. For the catalytic partial oxidation two pathways are suggested in which the reaction might proceed. In the first (indirect) pathway, methane is combusted to CO_2 and H_2O ($CH_4 + 2O_2 \rightarrow CO_2 + 2H_2O$ (**4**); ΔH^0_{298}=-802kJ/mol) followed by the reforming of the combustion products with the remaining methane ($CH_4 + H_2O \rightleftharpoons CO + 3H_2$ (**1**); ΔH^0_{298}=206kJ/mol, $CH_4 + CO_2 \rightleftharpoons 2CO + 2H_2$ (**3**); ΔH^0_{298}=247kJ/mol). However, large temperature gradients are present due to the high exothermicity (hot spot formation) of the oxidation reaction and the endothermicity of the reforming reactions. The large temperature gradient is not present in the second (direct) pathway because in this process methane is directly converted to H_2 and CO in the absence of the highly exothermic full combustion. However, discrimination between the two pathways can be difficult due to the difficulty of discrimination between primary and secondary products for these fast reactions. Direct partial oxidation is claimed to occur both on supported metal catalysts [24-25, 27] and oxidic materials [26]. The catalytic partial oxidation does not have an industrial application yet in contrast to the non-catalytic process which is, for example, used in the SMDS process (Shell Middle Distillate Synthesis) [28].

1.2.3 Autothermal reforming

Autothermal reforming is a special case of the above described indirect partial oxidation. In this process methane is non catalytically combusted (O_2/CH_4=0.55-0.6, also water can be added to the feed) to CO_2, CO and H_2O followed by a catalytic reforming step (on a Ni catalyst) which yields synthesis gas [21, 22, 29]. The process was developed at Haldor Topsøe to perform oxidation and reforming in one reactor. The oxidation step is operated at temperatures around 2200K whereas the temperature in the catalytic (reforming) zone is 1200-1400K and the pressure is 20-35 bar [21, 22]. Because the O_2/CH_4 ratio in this system is low (0.55-0.6) the excess of methane left after the combustion can decompose to carbon which can deposit down stream on the Ni catalyst causing severe operational problems (pressure build up, heat transfer problems).

1.2.4 CO_2 reforming

Because CO_2 reforming ($CH_4 + CO_2 \rightleftharpoons 2CO + 2H_2$ (**3**); ΔH^0_{298}=247kJ/mol) yields synthesis gas with a lower H_2/CO ratio compared to steam reforming (**1**), this reaction can be used to adjust the H_2/CO ratio in the product stream of steam reforming. Dry CO_2 reforming (i.e. in the absence of water) is industrially used to produce pure CO (CALCOR Process) [30, 31]. The major draw back of CO_2/CH_4 reforming is the possible formation of carbonaceous deposits on the catalyst which can cause significant deactivation of the catalyst [3]. Although CO_2/CH_4 reforming is a well documented reaction [see Ref 32 and 33 for excellent reviews] little is known about the reaction mechanism and the mechanism of carbon deposition and the parameters determining the stability of the catalyst.

1.3 Carbon dioxide reforming

1.3.1 Justification for CO_2/CH_4 reforming

As can be seen in Tables 1 and 3 dry CO_2 reforming yields syngas with a high CO concentration. In the CALCOR process, dry CO_2 reforming is used to produce pure CO [30, 31]. Michel [34] compared the costs of different syngas producing processes, i.e., steam reforming and CO_2 reforming of natural gas and partial oxidation of natural gas or heavy feedstocks, with each other. It was shown that, depending on the required H_2/CO ratio, CO_2 reforming can be economically advantageous over the other syngas producing processes. When a H_2/CO ratio in the range 0-0.5 is needed CO_2 reforming is preferred over the partial oxidation of natural gas or petroleum coke. For a H_2/CO ratio in the range 0.5-0.9 CO_2 reforming competes with the partial oxidation of bitumen. When higher H_2/CO ratios are required other processes are preferred over CO_2/CH_4 reforming. More over, an economic evaluation of the production of 100,000 tonnes of acetic acid showed that the use of CO_2 reforming to provide the syngas resulted in lower operating costs compared to steam reforming, partial oxidation or autothermal reforming [2]. As was shown before (§1.2.4) the major drawback of dry CO_2 reforming is the high thermodynamic driving force to produce coke. The above mentioned CALCOR process and the SPARG process (sulfur passivated reforming) have overcome the coking problem during reforming and will be described in the next paragraphs.

1.3.2 CALCOR Process

The CALCOR process aiming at production of high purity CO from natural gas or LPG [19, 30, 35] was developed to overcome problems involved in transportation of the toxic CO and the need for high product quality. These factors favour the production of CO on-site even for small capacities.

The CALCOR process operates under dry reforming conditions in an excess of CO_2. Details of catalysts used are proprietary. The prevention of carbon formation is

claimed to be achieved by using catalysts with different activities and shape and by their specific arrangement throughout the reformer tube. The CO produced contains less than 0.1% of methane. Two options for purification of CO produced are available: membrane purification leads to CO purity of about 98.9 vol%, while the low temperature pressure swing adsorption purification can yield CO with a purity higher than 99.4 vol%.

1.3.3 SPARG Process

The SPARG process was first commercialized at Sterling Chemical Inc., Texas, USA in 1987 in order to decrease the syngas H_2/CO ratio from 2.7 (obtained from steam reforming) to 1.8 without changing the steam reforming facility [3]. Because the use of CO_2 instead of steam lowers H/C ratios in the product, part of the steam was replaced by CO_2. The increased probability of carbon formation and the associated catalyst deactivation was minimized by introducing a partially sulfur-poisoned nickel catalyst. Carbon-free operation with sulfur-passivated nickel catalysts, at conditions that would otherwise favour carbon formation, was clearly demonstrated.

The process operates at 1188-1218K which decreases the CH_4 slip (one of the main problems in syngas production) to 2.7 mol%. When CO_2/CH_4 reforming is used to produce CO for polycarbonate synthesis, the impurities in the CO (mainly H_2 and CH_4) cause inferior mechanical properties of polycarbonates made *via* the phosgene route [31]. Therefore an as low as possible methane slip in the reforming step is required.

Under the reaction conditions applied in the SPARG process, higher hydrocarbons (C_2^+) in the feed will be thermally cracked to form pyrolytic carbon. The C_2^+ species in the feed were quantitatively removed by a pre-reforming step. Although the problems related to catalyst deactivation are minimized the SPARG process operates in the presence of sulfur. Thus, traces of sulfur might be present in the syngas produced. When a pure syngas is required an additional cleaning step will be necessary which involves an additional investment. Therefore, a catalyst which operates carbon free without the addition of sulfur is preferred.

1.3.4 Chemical energy transmission

Highly endothermic reactions such as steam reforming and CO_2 reforming are candidates for chemical energy transmission systems [36-43]. When energy is available (e.g. sunlight during the day), an endothermic reaction is carried out. The products of the reaction can be stored or transported to another location where energy is required. Then the reversed reaction, now exothermic, is carried out and the energy is released again (Figure 3). An example of energy transmission in this way is the ADAM-EVA process [40]. In the EVA plant, steam reforming is carried out using a nuclear power source to supply the required energy. The resulting syngas is transported to the ADAM plant where methanation of the syngas is performed to release energy.

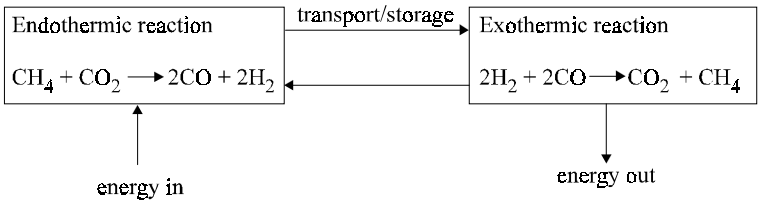

Figure 3 *The chemical energy transmission system*

When CO_2/CH_4 reforming is used for the energy storage (in CO/H_2) two possibilities to regain the energy exist [33, 41-43]. In the so called closed loop thermochemical heat pipe the CO/H_2 mixture is converted back to CO_2/CH_4 and the process can start again. In the open loop thermochemical heat pipe the resulting CO/H_2 mixture is combusted to CO_2 and H_2O when energy is needed.

1.3.5 CO_2 reforming and the environment

Generally, CO_2 is considered to be responsible for the global warming due to the greenhouse effect. At first glance CO_2/CH_4 reforming seems a possibility to decrease the amount of CO_2 in the atmosphere. However, CO_2 reforming is an endothermic reaction, thus, energy is required to run the reaction. Edwards [33] showed that when methane is combusted to (H_2O and CO_2) for the energy production (assuming 80% efficiency of the burner) about 0.35 moles of CO_2 are produced by the combustion per mol of CO_2 converted in the reforming reaction. It was further assumed that the syngas produced was used for the production of methanol ($2H_2 + CO \rightleftharpoons CH_3OH$). Thus a H_2/CO ratio of at least

2 is needed. When CO_2/CH_4 reforming is used to produce syngas ($H_2/CO=1$) part of the CO needs to be removed. This can occur *via* the water-gas shift reaction ($CO + H_2O \rightleftharpoons H_2 + CO_2$) which means that another 0.67 moles of CO_2 are produced per mol of CO_2 converted in the reforming reaction. Thus in total more than 1 mol of CO_2 (0.35 moles during combustion of methane, 0.67 moles from the watergas shift reaction) is produced per mol of CO_2 converted. In other words, when CO_2/CH_4 reforming is used for methanol synthesis it does not contribute to a CO_2 removal from the environment unless a non-fossil energy source is used for the production of the required energy.

Moreover, some debate exists about whether CO_2 is the main contributor to the greenhouse effect [44] or not. The i.r. radiation from sunlight reflected on the earth is absorbed by gases in the atmosphere; this causes the greenhouse effect. Because most of the reflected i.r. radiation, matching that of CO_2, is already absorbed by the current CO_2 concentration in the atmosphere it is highly doubtful if more CO_2 in the atmosphere will increase the greenhouse effect. It is more likely that other gases such as N_2O, CH_4, O_3 and CFC's will increase the greenhouse effect.

The CO_2 output of a 2500kW power plant (which is average size) is enough to satisfy the worlds' demand for methanol, when it is produced *via* CO_2/CH_4 reforming [32]. Thus all the power plants in the world produce far more CO_2 than can be used for methanol synthesis. Moreover, the production of methanol is only a temporary storage of CO_2. At the end most of the products produced from methanol end up as CO_2 by combustion, thus the 'stored' CO_2 is released again into the atmosphere. On basis of the considerations described above it must be concluded that CO_2/CH_4 reforming is not a feasible way to decrease the greenhouse effect.

1.4 State of the art

1.4.1 Catalysts used for CO_2/CH_4 reforming

As early as 1928, Fischer and Tropsch showed that most group VIII metals show appreciable activity for CO_2/CH_4 reforming [45]. Since then, many authors have investigated metals such as Ni, Ru, Rh, Pt, Ir and Pd [46-50] for the reaction. Although there is some debate about the order of activity of these metals, Rh was preferred by most authors due to its good activity and stability. Ni catalysts, however, are commercially more interesting compared to noble metals but their main draw back is the high rate of coke formation [39, 49, 51, 52]. From an economic point of view (relatively low price and good availability) Pt is a reasonable compromise.

The most commonly used support for CO_2/CH_4 reforming is γ-Al_2O_3 [39, 45, 53-55]. However also other supports like MgO [49, 51], TiO_2 [50], SiO_2 [50] and Eu_2O_3 [52] were used. Modifications of γ-Al_2O_3 [45, 50, 56] by addition of basic promoters such as MgO and CaO to enhance catalyst stability were sometimes realized. This indicates the importance of the support for the stability of the catalyst.

1.4.2 Mechanism of CO_2/CH_4 reforming

In principal two mechanisms for CO_2/CH_4 reforming are discussed in the literature. Mark *et al.* [54, 57] and Erdöhelyi *et al.* [58] suggest an Eley Rideal type mechanism in which methane is adsorbed and decomposed on the metal (Rh) to H_2 and adsorbed carbon. The carbon on the catalyst reacts directly with CO_2 from the gas phase to yield CO.

In the alternative mechanism [39, 47, 49, 51, 59-62] methane is decomposed on the metal to yield a surface CH_x species and hydrogen. Upon sorption, carbon dioxide dissociates to CO and adsorbed oxygen. That oxygen reacts with the CH_x species to give CO and hydrogen. While it is agreed that the CH_x species are formed on the metal, the nature of carbon dioxide activation is unclear. Qin *et al.* suggest that CO_2 dissociates on

the metal (Rh) to form Rh-CO and Rh-O [49]. This is also supported by Bodrov *et al*. for CO_2/CH_4 reforming over a Ni foil [61]. Vannice *et al*. [59], in contrast, suggest that adsorbed hydrogen reacts with CO_2 to form CO and an OH group (retained on the surface). However, it is not clear whether CO_2 is activated on the support or if the metal is involved. The OH groups are thought to react at the metal-support interface with CH_x, (resulting from methane decomposition) to form a CH_xO species which subsequently decomposes to CO and H_2.

With respect to the involvement of the support in the reaction mechanism it is important to mention that Nakamura *et al.* [50] observed an increase in the activity for Rh/SiO_2 when γ-Al_2O_3, TiO_2 or MgO was added to the support. This was attributed to enhanced CO_2 activation on the support. Zhang *et al*. [63] attributed the remarkable stability of Ni/La_2O_3 compared to Ni/γ-Al_2O_3 or Ni/CaO to the fact that La_2O_3 activated CO_2 in the form of $La_2O_2CO_3$.

1.4.3 Deactivation of reforming catalysts

The deactivation of CO_2-reforming catalysts is thought to be due to the loss of metal surface area [3, 39, 46, 51, 53, 64]. This can either be the result of sintering of the metal particles or by blocking of the metal surface sites by carbonaceous deposits. Compared to steam reforming, the risk of coke formation during CO_2/CH_4 reforming is higher [3]. The CO_2/CH_4 reforming reaction is thought to consist of similar elementary reaction steps as in steam reforming ($H_2O + CH_4 \rightleftharpoons CO + 3H_2$) [61], (although an alternative mechanism exists [54, 57, 58]) but the absence of water and the high C/H ratio in the reactant feed favours extensive coke formation during CO_2/CH_4 reforming [3]. Minimization of coking rates is, thus, one of the key aspects for designing a stable catalyst for the reaction. Coke forms readily *via* methane decomposition ($CH_4 \rightleftharpoons C + 2H_2$) and CO disproportionation ($2CO \rightleftharpoons C + CO_2$). However, Rostrup-Nielsen *et al*. showed for Ni, Ru, Rh, Pd, Ir and Pt supported on MgO [51], and Richardson *et al.* for Rh/γ-Al_2O_3 [39] that under dry reforming conditions coke originates mainly from methane. In

contrast Tsipouriari *et al.* [53] claim that coke is formed out of carbon dioxide over Rh/γ-Al_2O_3. This is in conflict with observations from other authors who showed that an excess of CO_2 in the feed stream suppresses coke formation [3, 30, 31, 46, 64].

Minimizing the risk of coke formation can be achieved by increasing the H/C or O/C content of the feed by i.e., (i) the addition of water (coupling with steam reforming) [3, 49, 65, 66], (ii) the addition of oxygen (coupling with partial oxidation) [3, 67], or (iii) the use of catalysts which minimize the rate of coking.

Besides coke formation, sintering of the metal particles can also account for the loss of catalytic activity. Sintering was observed by Tsipouriari *et al*. for Rh/γ-Al_2O_3 [53] and Swaan *et al*. [68] for Ni/SiO_2. Tsipouriari *et al*. observed for Rh/γ-Al_2O_3 a fast coke build up on the catalyst during the first 10 minutes time on stream. After this period the amount of coke on the catalyst remained constant while the Rh particle size and the deactivation were still increasing. Thus, they explained the deactivation of the Rh/γ-Al_2O_3 catalyst by the loss of metal area due to sintering. Swaan *et al*. observed an increase in the Ni particle size during use of the catalyst. However, these authors observed also two types of coke on their catalyst of which one could be correlated to the activity loss of the catalyst. They concluded that the sintering had only a limited effect on the deactivation of the catalyst.

1.5 Scope and structure of the thesis

The major drawback of CO_2/CH_4 reforming is catalyst deactivation due to coke formation. As discussed above, the stability of reforming catalysts can be enhanced by adding steam or O_2 to the reactants. A more elegant way to overcome the coking problem is the development of a catalyst on which coke formation is kinetically suppressed. The research described in this thesis aims at the development of such a catalyst. Moreover, the mechanism and the factors influencing the stability of the catalysts will be discussed.

In Chapter 2 the experimental details of the experiments described in this thesis will be given. Chapter 3 shows a comparison of Pt and Rh catalysts on different supports. It will be shown that Pt supported on ZrO_2 is an excellently suited catalyst for CO_2/CH_4 reforming. Some physico-chemical properties of this catalyst will be described. In Chapter 4 parameters influencing the activity of Pt/ZrO_2 are described. It will be shown that the activity of Pt/ZrO_2 is determined by the length of the $Pt\text{-}ZrO_2$ perimeter rather than by the availability of Pt. This indicates that a support related species is involved in the reaction mechanism. This concept is further substantiated in Chapter 5. Based on steady state and transient kinetic measurements as well as spectroscopic studies a mechanism for CO_2/CH_4 reforming over Pt catalysts is proposed. Using this mechanism and the physico-chemical properties of different Pt catalysts, requirements to obtain a stable catalyst for CO_2/CH_4 reforming are discussed in Chapter 6.

1.6 References

1. Kirk Othmer Encyclopedia of Chemical Technology, 4th edition, John Wiley & Sons, NewYork, 13 (1993) 744.
2. P.F. van der Oosterkamp, Q. Chen, J.A.S. Overwater, J.R.H. Ross, A.N.J. van Keulen, 9th International Symposium on Large Chemical Plants, Antwerp, October 1995.
3. N.R. Udengaard, J.B. Hansen, D.C. Hanson, J.A. Stal, Oil & Gas Journal, 62 (March 1992) 9.
4. S. Yarchak, Stud. Surf. Sci. Catal., 36 (1988) 251.
5. A.N.J. van Keulen, PhD thesis, University of Twente, Enschede, The Netherlands (1996).
6. Energy in Profile, Shell Briefing Service, Shell International Petroleum Compagny Ltd., annual publication (1987-1995).
7. Ullman's Encyclopedia of Industrial Chemistry, 5th Edition, VCH Weinheim, Germany (1989).
8. The Shell Review, Shell International Petroleum Compagny Limited (1994).
9. Liquified Natural Gas, Shell Briefing Service, no 4, Shell International Petroleum Compagny Limited (1992).
10. A.M. Maitra, Appl. Catal. A: General, 104 (1993) 11.
11. G. Renesme, J. Saint-Just, Y. Muller, Catal. Today, 13 (1992) 371.
12. G.C. Hoogendam, PhD thesis, University of Twente, Enschede, The Netherlands (1996).
13. N.R. Foster, Appl. Catal., 19 (1985) 1.
14. H.D. Gesser, N.R. Hunter, C.B. Prakash, Chem. Rev., 85 (1985) 235.

15. M.J. Brown, N.D. Parkyns, Catal. Today, 8 (1991) 305.
16. J.R. Rostrup-Nielsen, Catal. & Sci. Tech. (J.R. Anderson, M. Boudart eds.), 5 (1984) 3.
17. G.W. Bridger, C.C. Chinchen, Catalyst Handbook (W.V. Twigg ed.) Wolfe Scientific Books, London (1970) 64.
18. J.P. van Hook, Catal. Rev. Sci. Eng., 21 (1981) 1.
19. Gas Process Handbook '92, Hydroc. Proc. (April 1992) 140.
20. D.J. Borgars, Advances in ammonia plant technology, Chapter 10 in Synthesis of ammonia (V.A. Vancini, Macnillan eds.), London (1971) 261.
21. M.A. Peña, J.P. Gómez, J.L.G. Fierro, Appl. Catal. A: General, 144 (1996) 7.
22. J.R. Rostrup-Nielsen, Catal. Today, 18 (1993) 305.
23. J.R. Rostrup-Nielsen, Catal. Today, 21 (1994) 257.
24. D.A. Hickman, L.D. Smidt, J. Catal., 138 (1992) 267.
25. V.R. Choudary, A.M. Rajput, R.V. Rane, Catal. Lett., 15 (1992) 363.
26. A.G. Steghuis, J.G. van Ommen, K. Seshan, J.A. Lercher, Stud. Surf. Sci. Catal., 107 (1997) 403.
27. F. van Looij, PhD Thesis, University of Utrecht, Utrecht, The Netherlands (1994).
28. M.J. v.d. Burgt, C.J. van Leeuwen, J.J. delÁmico, S.T. Sie, Stud. Surf. Sci. Catal., 36 (1988) 473.
29. Gas Process Handbook '88, Hydroc. Proc. (April 1988) 77.
30. S. Teuner, Hydroc. Proc., 64 (1985) 106.
31. G. Kurz, S. Teuner, Erdol. Kohle, 43(5) (1990) 171.
32. K. Seshan, J.A. Lercher, Carbon Dioxide Chemistry: Environmental Issues (J. Paul, C.-M. Pradier eds.), the Royal Society of Chemistry, Cambridge U.K., (1994) 16.
33. J.H. Edwards, A.M. Maitra, Fuel. Proc. Technol., 41 (1995) 269.
34. S. Michel, Hydroc. Proc., (April 1989) 37.
35. Gas Process Handbook 1992, Hydroc. Proc., 90 (1992).
36. K. Kugher, H.F. Niessen, M. Roth-Kamal, D. Bocher, B. Ruter, K.A. Theis, Nucl. Eng. Design, 34 (1975) 65.
37. T.A. Chubb, Chem. Tech., 6 (1976) 654.
38. G. DeMaria, L. Dálessio, E. Coffari, M. Paolucci, C.A. Tiberio, Solar Energy, 35 (1985) 409.
39. J.T. Richardson, S.A. Paripatyadar, Appl. Catal., 61 (1990) 293.
40. B. Höhlein, R. Menzer, J. Range, Appl. Catal., 1 (1981) 125.
41. D. Fraenkel, R. Levitan, M. Levy, Int. J. Hydrogen Energy, 11 (1986) 267
42. M. Levy, R. Rosin, R. Rubin, Solar Energy, 50 (1993) 179.
43. J.H. Edwards, Catal. Today, 23 (1995) 59.
44. C.J.F. Böttcher, De ingenieur, 10 (1994) 6.
45. F. Fischer, H. Tropsch, Brennst. Chem. (1928) 39
46. A.T. Ashcroft, A.K. Cheetham, M.L.H. Green, P.D.F. Vernon, Nature, 225 (1991) 352.
47. F. Solymosi, Gy. Kutsan, A. Erdöhelyi, Catal. Lett., 11 (1991) 149.
48. P.D.F. Vernon, M.L.H. Green, A.K. Cheetham, A.T. Ascroft, Catal. Today, 13 (1992) 417.
49. D. Qin, J. Lapszewicz, Catal. Today, 21 (1994) 551.
50. J. Nakamura, K. Aikawa, K. Sato, T. Uchijima, Catal. Lett., 25 (1994) 265.
51. J. R. Rostrup-Nielsen, J.-H. Bak Hansen, J. Catal., 144 (1993) 38.

52. J.S. Perera, J.W. Sankar, J.M. Thomas, Catal. Lett., 11 (1991) 219.
53. V.A. Tsipouriari, A.M. Efstathiou, Z.L. Zhang, X.E. Verykios, Catal. Today, 21 (1994) 579.
54. M.F. Mark, W.F. Maier, Angew.Chem. Int. Ed. Engl., 15-16 (1994) 33.
55. Y. Sakai, H. Saito, T. Sodesawa, F. Nozaki, React. Kinet. Catal. Lett., 24 (1984) 253.
56. A.M. Gadalla, M. E. Sommer, Chem. Eng. Sci., 44 (1989) 2825.
57. M.F. Mark, W.F. Maier, J. Catal., 164 (1996) 122.
58. A. Erdöhelyi, J. Cerenyi, F. Solymosi, J. Catal., 141 (1993) 287.
59. M.C.J. Bradford, M.A. Vannice, Appl. Catal. A: general, 142 (1996) 97.
60. D. Qin, J. Lapszewicz, X. Jiang, J. Catal., 159 (1996) 140.
61. I.M. Bodrov, L.O. Apel'baum, Kinet. Katal., 8 (1967) 379.
62. I.M. Bodrov, L.O. Apel'baum, M.I. Temin, Kinet. Katal., 8 (1967) 821.
63. Z. Zhang, X.E. Verykios, S.M. MacDonald, S. Affrossman, J. Phys. Chem., 100 (1996) 744.
64. K. Seshan, H.W. ten Barge, W. Hally, A.N.J. van Keulen, J.R.H. Ross, Stud. Surf. Catal., 81 (1994) 285.
65. D. Qin, J. Lapszeicz, Catal. Today., 21 (1994) 551.
66. E. Riensche, H. Fedder, Stud. Surf. Catal., 77 (1993) 541.
67. T.S. Christensen, I.I. Primdahl, Hydroc. Proc., (March 1994) 29.
68. H.M. Swaan, V.C.H. Kroll, G.A. Martin, C. Mirodatos, Catal. Today, 21 (1994) 571.

2

Experimental

2.1 Catalyst preparation

2.1.1 Preparation of impregnated catalysts

Catalysts consisting of Pt (Rh) supported on inorganic carriers were prepared by the wet impregnation technique. For this purpose a solution of $H_2PtCl_6.6H_2O$ ($RhCl_3.3H_2O$) in water (0.01g Pt (Rh) per ml) was used. The supports (Table 1) which were in powder form were isostatically pressed into pellets at 4000 bars for 5 minutes. The pellets were crushed and sieved to obtain grains with diameters between 0.3 and 0.6 mm. γ-Al_2O_3 was obtained as extrudates, these were only crushed and sieved to yield grains with 0.3-0.6mm diameter. The grains were first calcined for 15 hours at 1125K (heating rate 3K/min) in flowing air (30ml/min (NTP)) and subsequently impregnated with the H_2PtCl_6 ($RhCl_3$) solution to yield a catalyst with the desired Pt (Rh) loading. The catalyst was dried at 365K for 2 hours in a rotating evaporator followed by drying over night at 395K in static air. The impregnated grains were calcined at the desired temperature for 15 hours (heating rate 3K/min). The Pt (Rh) content of the catalyst was determined by atomic absorption spectroscopy.

Table 4 *Supports used in this study*

Support	Supplier	Supplier code	BET surface area (m^2/g)
γ-Al_2O_3	AKZO	000-3AQ	110
TiO_2	Degussa	P-25	7
SiO_2	AKZO	F7	220
ZrO_2 (monoclinic)	Gimex	RC-100	17

2.1.2 Preparation of unsupported Pt

Unsupported Pt was prepared as described by Paal *et al.* [1] however, we used Pt-metal in stead of H_2PtCl_6 as the starting material. 5 grams of Pt-metal were dissolved in 100ml aqua regia. To remove the excess of nitric acid, the solution was concentrated to

a syrup. Subsequently, concentrated HCl was added and the solution was concentrated again. This procedure was repeated 3 times [2]. The resulting orange syrup was dissolved in 50ml of water and cooled to 273K. 100ml of hydrazine (in 400ml of water) were slowly added which resulted in the formation of a grey precipitate. After stirring overnight at room temperature the precipitate was filtered and washed thoroughly with water. The grey solid was dried at 393K for several hours in air and subsequently reduced at 1025K in 5%H_2/N_2. The BET surface area of the resulting metal was 0.25m^2/g and its hydrogen chemisorption capacity (H/Pt) was 0.001.

2.1.3 Unsupported Rh

Unsupported Rh sponge was used as obtained. Prior to testing, the metal was reduced *in situ* at 1025K. The hydrogen chemisorption capacity of the metal after reduction was H/Rh=0.0008.

2.2 Catalyst testing

Typically 300mg of catalyst were loaded into a tubular quartz reactor (inner diameter 5 mm) which was placed in an oven (Figure 1). The catalyst grains were kept in place by quartz wool plugs. A thermocouple was placed on top of the catalyst bed to measure the catalyst temperature. The oven temperature was controlled by an Eurotherm temperature controller. The catalysts were reduced *in situ* with 5% H_2 in N_2 for 1 hour at 1125K. After reduction, the temperature was lowered in Ar to the (initial) reaction temperature and the feed gas mixture (25% CH_4 (vol), 25% CO_2, 5% N_2 and 45% Ar with a total flow of 170ml.min^{-1}) was switched to the reactor. The reaction products were analyzed in a gas chromatograph (Varian 3300), equipped with two 3m carbosieve columns and a TCD.

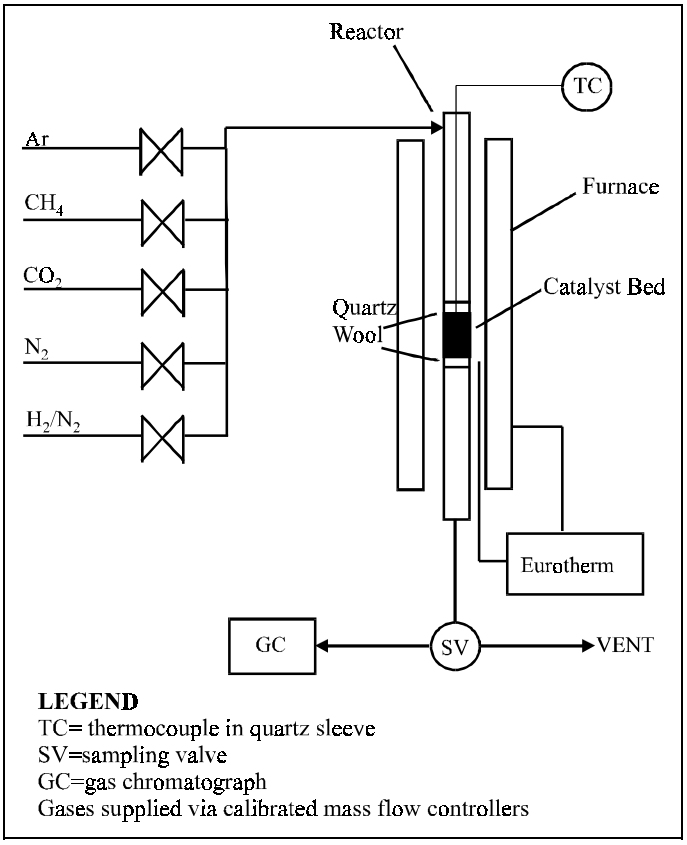

Figure 4 *Setup for catalyst testing*

The conversions and yields of the different components were calculated from the concentration measured by GC in the following way:

$$\textit{Methane conversion: } X_{CH_4} = \frac{CH_{4(in)} - CH_{4(out)} \cdot \theta}{CH_{4(in)}} .100\%$$

$$\textit{Carbon dioxide conversion: } X_{CO_2} = \frac{CO_{2(in)} - CO_{2(out)} \cdot \theta}{CO_{2(in)}} .100\%$$

$$\textit{Carbon monoxide yield: } Y_{CO} = \frac{CO_{(out)} \cdot \theta}{CH_{4(in)} + CO_{2(in)}} .100\%$$

$$\textit{Water yield: } Y_{H_2O} = \frac{H_2O_{(out)} \cdot \theta}{2CH_{4(in)}} .100\% \qquad \textit{Hydrogen yield: } Y_{H_2} = \frac{H_{2(out)} \cdot \theta}{2CH_{4(in)}} .100\%$$

$$\textit{Dilution factor: } \theta = \frac{N_{2(in)}}{N_{2(out)}}$$

The dilution factor is included in order to correct for the volume change during conversion. During dry reforming 2 moles of gas are overall converted to 4 moles of gas ($CO_2 + CH_4 \rightleftharpoons 2CO + 2H_2$). N_2 was added to the feedstream to determine this dilution factor.

2.3 Pulse experiments and coke determination

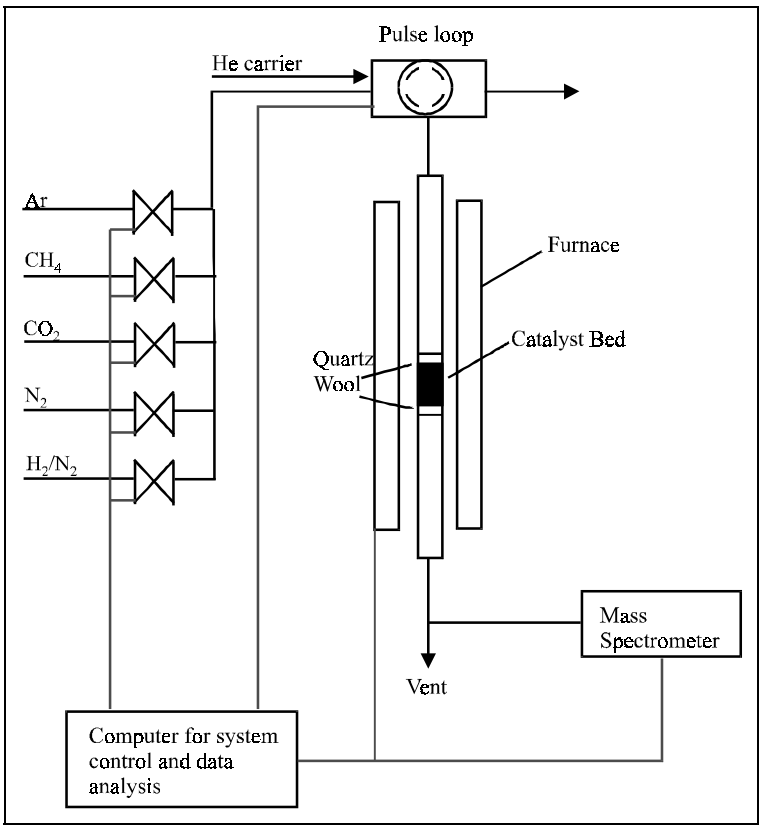

Figure 5 *Schematic representation of the experimental setup for transient kinetic measurements*

Pulse experiments were performed in an Altamira AMI-2000 apparatus (Figure 2). The Pt/ZrO_2 catalyst (0.5wt%, 500mg) was reduced at 1125K in a flow of 30ml.min^{-1} $5\%H_2/N_2$. Subsequently the temperature was lowered to the desired temperature while flushing in He to remove any adsorbed hydrogen. The sample was continuously exposed to a flow of 30ml.min^{-1} He. The desired gas was pulsed into this He stream (pulse size $2.1*10^{-5}$ moles). The reaction products were quantified with a mass spectrometer.

The same setup was used for the determination of the amount of carbonaceous deposits on used catalysts. The used catalyst (usually 150mg) was heated to 1125K in He to remove adsorbed water and CO_2. Subsequently O_2 was pulsed and the CO (m/e=28)

and CO_2 (m/e=44) signals were measured with the mass spectrometer and quantified.

2.4 Temperature Programmed Desorption (TPD) of pyridine

The acidities of the catalysts were examined by means of Temperature Programmed Desorption (TPD) of pyridine. For this purpose the same apparatus as decribed for the pulse experiments (see §2.3) was used. Prior to adsorption the catalysts were reduced in 5%H_2/N_2 at 1125K. Subsequently the sample was degassed in He and cooled to 475K. At this temperature pyridine (0.6µl.min^{-1}) was injected with a syringe into the He carrier (30ml.min^{-1}). After degassing at 475K, the sample was cooled to 425K and the desorption was started (He flow 30 ml.min^{-1}, heating rate 20K/min). The desorption was followed by means of a mass spectrometer.

2.5 Temperature Programmed Reduction (TPR)

The apparatus used for TPR experiments is schematically given in Figure 3. Generally 400mg of the catalyst was loaded into the reactor and flushed with He for 1 hour at 473K. Subsequently the temperature was lowered to 353K and the He was replaced by 5%H_2/Ar. After 1 hour flushing the temperature was raised to 1073K (heating rate 10K.min^{-1}). In case of a TPR-

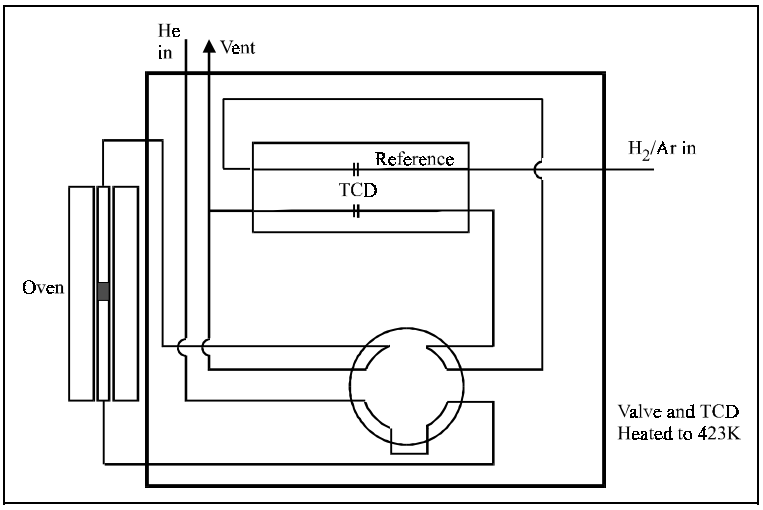

Figure 6 *Schematic representation of the TPR setup*

TPO cycle, after performing a TPR the H_2/Ar mixture was switched to He and the reactor was flushed with He for 30 minutes. Then the sample was cooled to 353K in air. The second TPR was performed as described above.

2.6 Hydrogen chemisorption measurements

Hydrogen chemisorption was carried out in a volumetric system (Figure 4). The

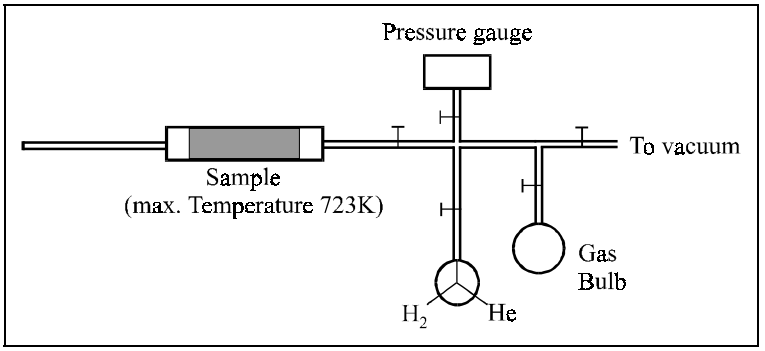

Figure 7 *Setup used for hydrogen chemisorption measurements*

sample (usually 1.5g) was reduced for 2 hours at 673K in H_2 (when a higher reduction temperature was required, the sample was previously reduced *ex situ* at the higher temperature). After reduction the sample was degassed at 673K for 1 hour in high vacuum (10^{-6} mbar). The sample was cooled to room temperature (295K) and the H_2 desorption isotherm was measured by dosing decreasing amounts of H_2 (in the range 500-0mbar) to the sample. The hydrogen chemisorption capacity was calculated by extrapolation of the hydrogen uptake to zero pressure.

The length of the Pt-ZrO_2 perimeter was calculated from hydrogen chemisorption values. The H/Pt ratio was converted to a Pt coordination number using values from Kip *et al.* [3] and Vaarkamp *et al*. [4]. These coordination numbers were related to particle sizes (in atoms) as described by the same authors. From these particle sizes the amount

of Pt atoms on the perimeter was calculated using the tables in references [3, 4] assuming that the particles were hemispheres.

2.7 XAS measurements

XAS measurements were performed at the SRS (Daresbury, UK), beamline 9.2, equipped with a Si (220) monochromator detuned to 50% to remove higher harmonics; or at the NSLS (Brookhaven, Upton New York), beamline X23A-2, equipped with a Si (311) monochromator which did not need to be detuned.

The catalyst was grained and pressed into a self supporting wafer, 110mg for 1wt% Pt/ZrO_2, 80mg for 1wt% Pt/TiO_2, and 200mg for 1wt% $Pt/\gamma\text{-}Al_2O_3$ to assure a total absorption of approximately 2.5 absorption units ($\mu x<2.5$, μ=absorption coefficient, x=sample thickness [5]). The catalysts were reduced *ex situ* at the desired temperature. Prior to the EXAFS experiments catalysts were rereduced *in situ* at 775K. EXAFS measurements were carried out at liquid nitrogen temperature. To isolate the EXAFS from the X-ray absorption edge, a polynomial function characteristic of the background was subtracted. The oscillations were normalized by the mass areal loading of Pt. The oscillations were k^2-weighted and Fourier transformed within the limits k=3 to k=18 to isolate the contributions of the different coordination shells. The contribution of Pt-Pt in the first shell was fitted using phase shift and amplitude functions obtained from a Pt foil measured under the same conditions. From the fitting procedure the Pt-Pt coordination number, the Pt-Pt distance and the Debye-Waller factor were obtained.

2.8 IR spectroscopic measurements of CO_2 adsorption on Pt/ZrO_2

The catalyst powder was pressed into a self supporting wafer. This wafer was

analyzed *in situ* during the reaction by means of transmission absorption IR spectroscopy using a Bruker IFS 88 FTIR spectrometer (resolution 4 cm^{-1}). The IR cell was constructed as a continuously stirred tank reactor (volume 1.5 cm^3) equipped with 1/16-in. gas in- and outlet tubings and CaF_2 windows. The partial pressure of each of the reactants was 250mbar, the difference to 1 bar being He and N_2.

2.9 X-ray Photoelectron Spectroscopy (XPS)

To investigate to oxidation state of Pt in Pt/ZrO_2 catalysts XPS was used. The catalyst sample was grinded and placed on a sticking tape. Subsequently the sample was evacuated and the XPS spectra were recorded. The instrument used was a Kratos XSAM 800 which utilised (15kV, 15mA) Mg Kα x-rays. The carbon signal of the sample was used to calibrate the peak position of the Pt-$4f_{7/2}$ band.

2.10 Acknowledgements

The XAFS measurements were carried out at SRS, Daresbury, UK (beamline 9.2) and the National Synchrotron Light Source (beamline X23A2), Brookhaven National Laboratory, which is supported by the US Department of Energy, Division of Material Sciences and Division of Chemical Sciences.

2.11 References

68. Z. Paal, Z. Zhan, E. Fulop, B. Tesche, J. Catal., 156 (1995) 19.
69. Vogel's Quantitative inorganic analysis, 3th ed., revised by J. Bassett, R.C. Denney, G.H. Jeffery, J. Mendham, The Chaucer Press Ltd. (1978) 474.

3. B.J. Kip, F.B.M. Duivenvoorden, D.C. Koningsberger, R. Prins, J. Catal., 105 (1987) 26.
4. M. Vaarkamp, J.V. Grondelle, J.T. Miller, D.J. Sajkowski, F.S. Modica, G.S. Lane, B.C. Gates, D.C. Koningsberger, Catal. Lett., 6 (1990) 369.
5. S.M. Heald, X-ray Absorption, Principles, Applications, Techniques of EXAFS, SEXAFS and XANES (D.C. Koningsberger, R. Prins eds.), John Wiley & Sons, New York (1988) 87.

3

Design, preparation and characterization of a Pt based catalyst for CO_2/CH_4 reforming

Abstract

The activity and stability of noble metal catalysts for CO_2/CH_4 reforming depend crucially on both the support and the metal. Pt/ZrO_2, Rh/ZrO_2 and $Rh/\gamma\text{-}Al_2O_3$ are active and stable catalysts. However, Pt was preferred for further investigations. ZrO_2 is an appropriate support due to the excellent performance of Pt/ZrO_2 compared to $Pt/\gamma\text{-}Al_2O_3$, Pt/TiO_2 and Pt/SiO_2. Not all accessible Pt atoms contribute equally to the activity of Pt/ZrO_2. The fraction less active Pt increases above 0.5wt% Pt, thus, 0.5wt% is the optimal weight loading. For Rh catalysts all accessible Rh atoms seem to contribute equally to the activity of the catalyst. When all Pt is reduced (i.e., above 475K) the reduction temperature had no influence on the activity of Pt/ZrO_2 although ZrO_2 (in the vicinity of Pt) might be partially reduced above a reduction temperature of 632K. During dry methane reforming water was observed as reaction product due to the reverse water gas shift reaction ($H_2 + CO_2 \rightleftharpoons CO + H_2O$) which is not in thermodynamic equilibrium.

This causes the H_2/CO ratio in the product stream to decrease to lower values than one. At higher temperatures and conversions the formed water might react with the methane left in the feed ($H_2O + CH_4 \rightleftharpoons CO + 3H_2$) which increases the H_2/CO ratio to a value of one.

3.1 Introduction

Methane reforming with carbon dioxide is thought to consist of similar elementary reaction steps as in methane reforming with steam [1], but the absence of water and the high C/H ratio in the reactant feed favours, thermodynamically, coke formation during CO_2/CH_4 reforming [2]. The effect of coke formation varies with`1 the metal catalyst used. For Ni catalysts coke is formed as whiskers with the Ni particle on top of it [3-5]. Whisker formation causes a significant expansion of the catalyst bed resulting in severe operational problems. Moreover, since the Ni particle is located on top of the filament the contact between metal and support is lost which makes it difficult to regenerate the catalyst.

Noble metals are known to form less coke under CO_2-reforming conditions [6] and the coke formed differs in nature from that found with Ni catalysts. On noble metals coke is thought to block the metal [6, 7] inducing deactivation due to the loss of available surface metal atoms. Options to reduce the coke build up include the increase of the H/C or O/C content of the feed by (i) the addition of water (CO_2 plus steam reforming) [2, 8, 9], (ii) the addition of oxygen (CO_2 reforming plus partial oxidation) [2, 9], or (iii) the use of catalysts which minimize the rate of coking.

As early as 1928, Fischer and Tropsch showed that most group VIII metals are active for CO_2/CH_4 reforming [10]. Since then, many authors have investigated metals such as Ni, Ru, Rh, Pt, Ir, and Pd [6, 9, 11-13]. Although there is some debate about the ranking on basis of activity for these metals, Rh was preferred by most authors due to its good activity and stability. Ni catalysts, however, are commercially more interesting compared to noble metals, but their main draw back is the high rate of coke formation [7, 9, 14, 15]. From an economic point of view (relatively low price and good availability) Pt might be seen as a reasonable compromise.

The most commonly used support for CO_2/CH_4 reforming is Al_2O_3 [8, 10, 14, 16-18]. Modifications to the support were sometimes made [10, 18, 19] by addition of basic

promoters such as MgO and CaO which enhance the catalyst stability. This underlines the importance of the chemical nature of the support to achieve a stable catalyst. Suitable supports have to be resistant to the high temperatures used during CO_2/CH_4 reforming and they have to maintain the metal dispersion of the catalyst during operation. Therefore, different supports (γ-Al_2O_3, TiO_2, SiO_2 and ZrO_2) were choosen for investigation of their behavior during CO_2/CH_4 reforming.

On basis of the consideration described above the design, preparation and characterization of Pt based catalysts is described in this chapter. For comparison Rh based catalysts were included in the study.

3.2 Experimental

All experimental details involving catalyst preparation, testing and characterization are given in Chapter 2.

3.3 Results

3.3.1 Activity and stability

The physico-chemical properties of the catalysts tested are summarized in Table 1. This table shows that both Rh and Pt can be very well dispersed over ZrO_2 and γ-Al_2O_3. On SiO_2, Rh could be reasonably dispersed (H/Rh=0.58), whereas Pt was poorly dispersed on this support (H/Pt=0.19). The Pt dispersion on TiO_2 is also low (H/Pt=0.25). For Pt/ZrO_2 the hydrogen chemisorption capacities of catalysts with different metal concentrations are also summarized in the table. As can be seen the fraction of exposed Pt of Pt/ZrO_2 decreased with increasing metal loading.

Table 1 *Some physico-chemical properties of various Pt and Rh catalysts*

Catalyst	Specific surface area (BET) (m^2/g)	Metal loading (wt%)	Hydrogen chemisorption capacity (H/Metal)
Pt/ZrO_2	17	0.5	1.10
Pt/ZrO_2	18	1	0.82
Pt/ZrO_2	17	3	0.19
Pt/TiO_2	7	0.5	0.25
$Pt/\gamma\text{-}Al_2O_3$	112	0.5	0.80
Pt/SiO_2	220	0.5	0.19
$Rh/\gamma\text{-}Al_2O_3$	110	0.5	0.79
Rh/SiO_2	216	0.5	0.58
Rh/ZrO_2	18	0.5	1.50

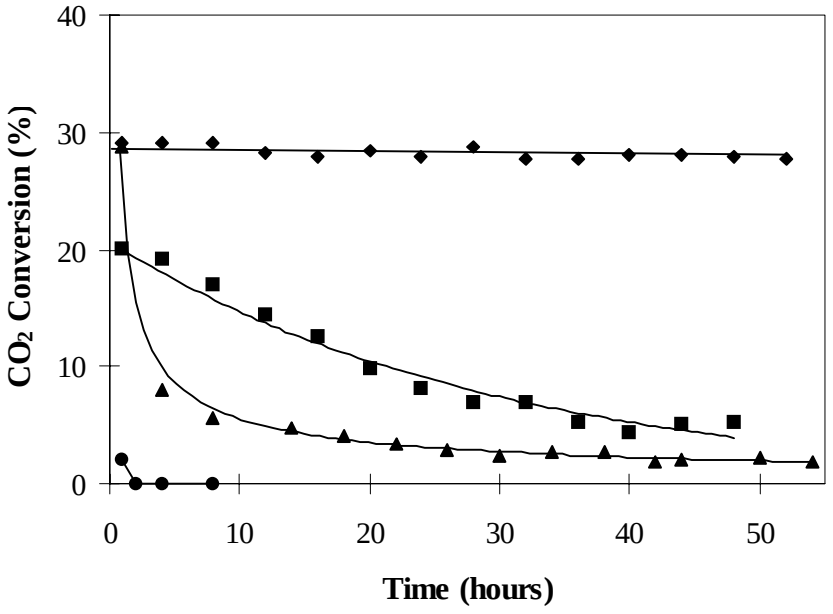

Figure 8 *Stability of different 0.5wt% Pt catalysts at 875K, 300mg catalyst, total flow=170ml.min^{-1}, CO_2/CH_4 /Ar+N_2 =1/1/2, ◆=Pt/ZrO_2, ■=Pt/TiO_2, ▲=$Pt/\gamma\text{-}Al_2O_3$, ●=Pt/SiO_2, thermodynamic conversion=55%*

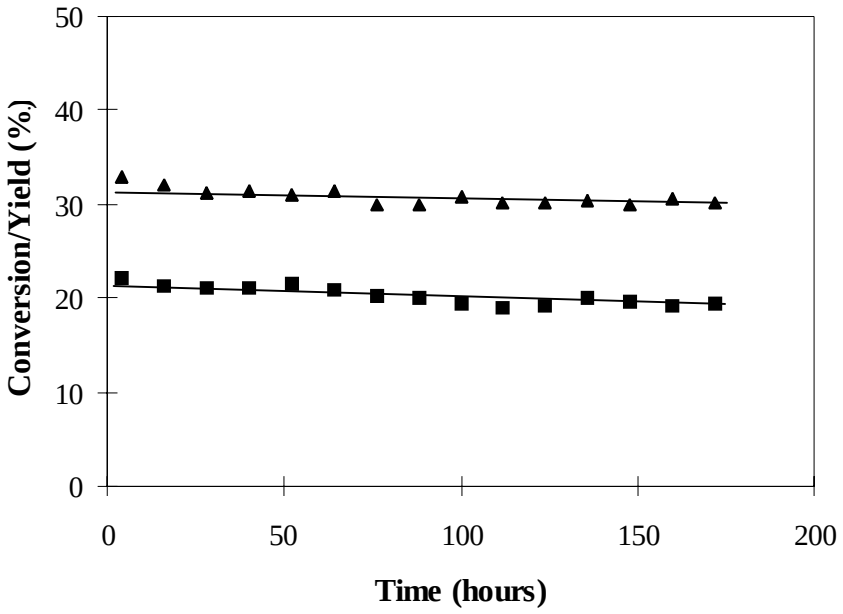

Figure 2 *Long term stability test of 0.5wt% Pt/ZrO_2 at 855K, 300mg catalysts, total flow=170ml.min-1, $CO_2/CH_4/Ar/N_2$ =1/1/2, ◢= CO_2 convn., ◼=CH_4, thermodynamic CO2 conversion=55%*

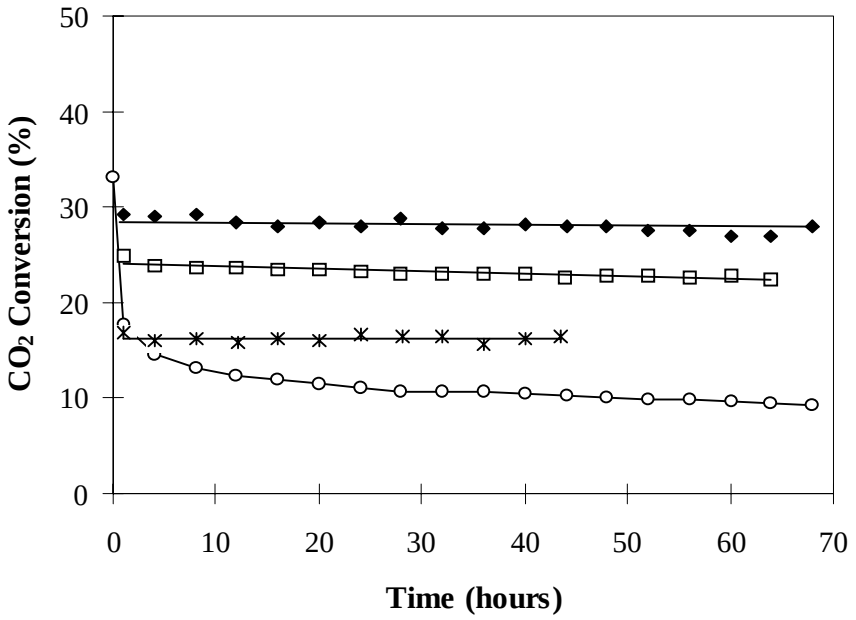

Figure 3 *Stability of Pt and Rh catalysts (0.5wt% metal) for CO_2/CH_4 reforming at 875K, total flow 170ml.min^{-1}, $CO_2/CH_4/Ar+N_2$=1/1/2, ◆=300mg Pt/ZrO_2, ❑=50mg $Rh/\gamma\text{-}Al_2O_3$, *=50mg Rh/ZrO_2, ○=300mg Rh/SiO_2, thermodynamic conversion=55%*

In Figure 1, the activities of Pt catalysts (0.5wt% Pt) based on different supports are compared for CO_2/CH_4 reforming at 875K. In this figure only the CO_2 conversion is plotted. In none of the experiments the conversions reached thermodynamic limits (i.e., 55% CO_2 conversion). Under the conditions chosen the initial activities of all catalysts except Pt/SiO_2 were in the same range (around 30% CO_2 conversion, compared on catalyst weight basis). However, the stability of the catalysts is strikingly different. Pt/γ-Al_2O_3 and Pt/TiO_2 deactivated strongly whereas Pt/ZrO_2 was stable, the latter one showed only minor deactivation, even after 180 hours deactivation was hardly observed (Figure 2). In Figure 2 both the CO_2 and CH_4 conversions are plotted. The CO_2 conversion is higher than the CH_4 conversion which can be explained by the occurance of the reverse water gas shift reaction ($CO_2 + H_2 \rightleftharpoons CO + H_2O$, this will be explained in more detail later in this chapter). Pt/SiO_2 showed only a very low activity (<2% CO_2 conversion) and

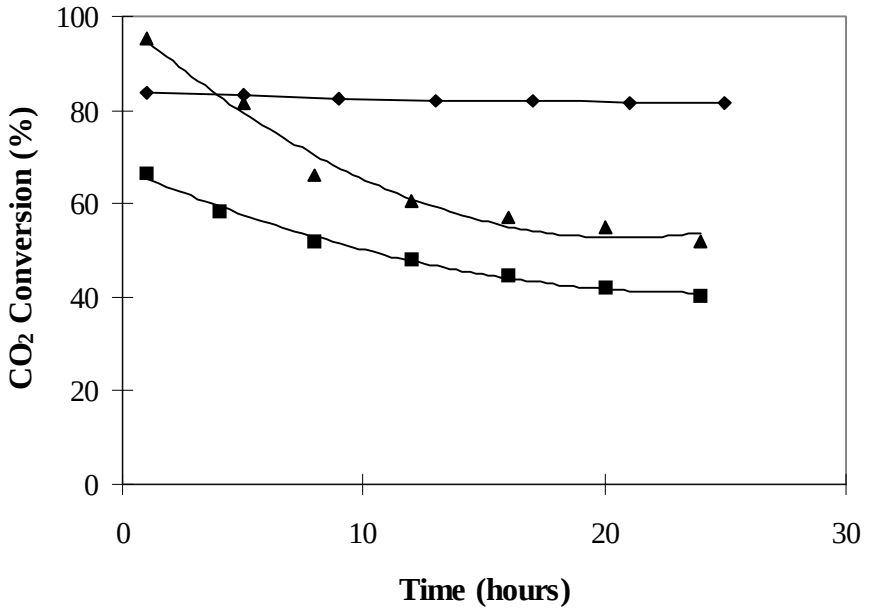

Figure 11 *Stability test of Pt catalysts at 1125K, total flow=170ml.min^{-1}, $CO_2/CH_4/Ar+N_2$ =1/1/2, ◆=200mg Pt/ZrO_2, ◢=300mg Pt/γ-Al_2O_3, ■=300mg Pt/TiO_2, thermodynamic conversion=97%*

deactivated within a few minutes time on stream. In Figure 3 the most stable Pt based catalyst (Pt/ZrO_2 (Figure 1)) is compared with different supported Rh catalysts. It can be

seen from this figure that the stabilities of $Rh/\gamma\text{-}Al_2O_3$, Rh/ZrO_2 and Pt/ZrO_2 are comparable. However, the Rh based catalysts are more active (on a weigth basis) compared to Pt/ZrO_2 (note that for $Rh/\gamma\text{-}Al_2O_3$ and Rh/ZrO_2 only 50mg of catalyst was used whereas this was 300mg for Pt/ZrO_2). In contrast to Pt/SiO_2, Rh/SiO_2 has initially a good activity. However, this catalyst deactivated quickly and lost about 60% of its initial activity during the first 10 hours time on stream. After this period the catalyst showed a stable, but low activity.

Table 2 *Comparison of deactivation rates over 0.5wt% Pt catalysts at 875K and 1125K*

Catalyst	Relative activity loss during 25 hours at 875K* (%)	Relative activity loss during 25 hours at 1125K* (%)
Pt/ZrO_2	1	2
Pt/TiO_2	60	35
$Pt/\gamma\text{-}Al_2O_3$	85	40

* relative activity loss=activity after 25hours/initial activity*100%

The stability of the different Pt catalysts at a higher temperature (1125K) is shown in Figure 4. A comparison of the relative deactivation (i.e., CO_2 conversion after 25hours/ initial CO_2 conversion) at

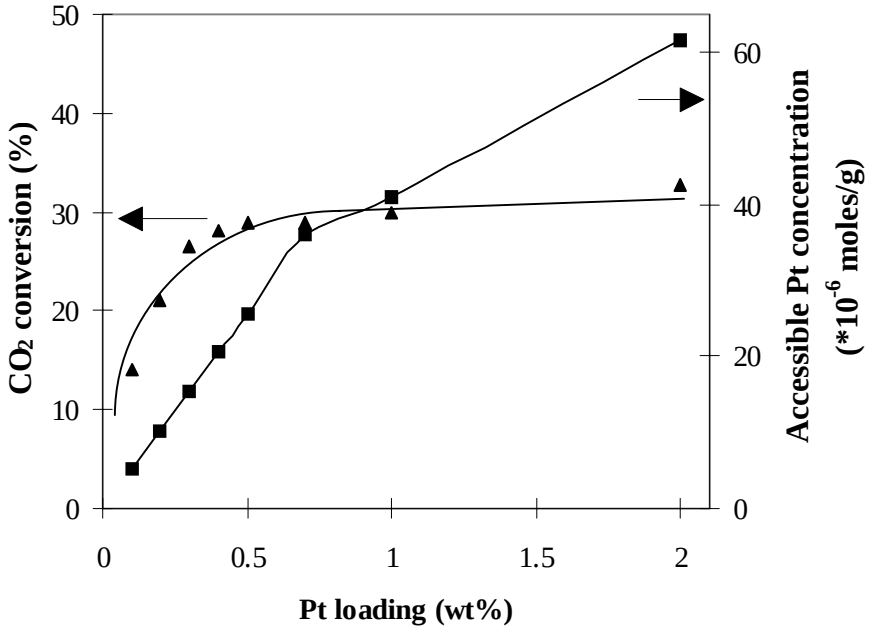

Figure 12 *Influence of the Pt loading on the amount of accessible Pt and the activity of Pt/ZrO_2 catalysts for CO_2/CH_4 reforming at 875K, 300mg catalyst, total flow=170ml.min^{-1}, $CO_2/CH_4/Ar+N_2=1/1/2$*

875K and 1125K is summarized in Table 2. Clearly, the stability of the catalysts is increased by increasing the reaction temperature. At 875K Pt/γ-Al_2O_3 lost 85% of its activity after 5 hours reaction, whereas it lost only 40% of the initial activity after 25 hours time on stream at 1125K. Pt/TiO_2 deactivates with 60% at 875K, during 25 hours of reaction, while this was only 40% at 1125K.

The influence of the metal loading on the activity of Pt/ZrO_2 is plotted in Figure 5. From this figure it can be seen that up to 0.5wt% Pt the activity of the catalyst, compared on a weight of catalyst basis, increased significantly with increasing metal loading (i.e., with the metal content in the reactor). Above 0.5wt% the conversion leveled off, while the amount of accessible Pt still increased. This aspect will be discussed in more detail in Chapter 4. From the results described above, it was decided to use 0.5wt% Pt for further characterization, testing and optimization.

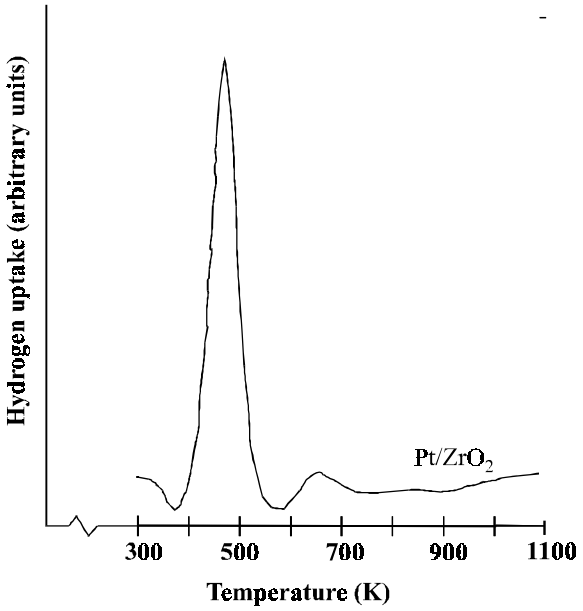

Figure 13 *TPR trace of 0.5wt% Pt/ZrO_2 in 5% H_2/Ar, flow=30ml.min^{-1}, temperature ramp=10K.min^{-1}*

3.3.2 Characterization of Pt/ZrO_2

To investigate the reduction behavior of Pt/ZrO_2 TPR (Temperature Programmed Reduction) was carried out. The resulting TPR trace is plotted in Figure 6. Two regions of hydrogen uptake with maxima at 472K and at 632K were observed. The reduction of Pt was also followed with XANES. In Figure 7 the temperature resolved XANES spectra of 1 wt% Pt/ZrO_2 in 5% H_2/N_2 are shown. As the temperature increased, the intensity of the white line decreased. Above a temperature of 480K the intensity of the white line remained constant.

The influence of the reduction temperature on the activity of Pt/ZrO_2 is

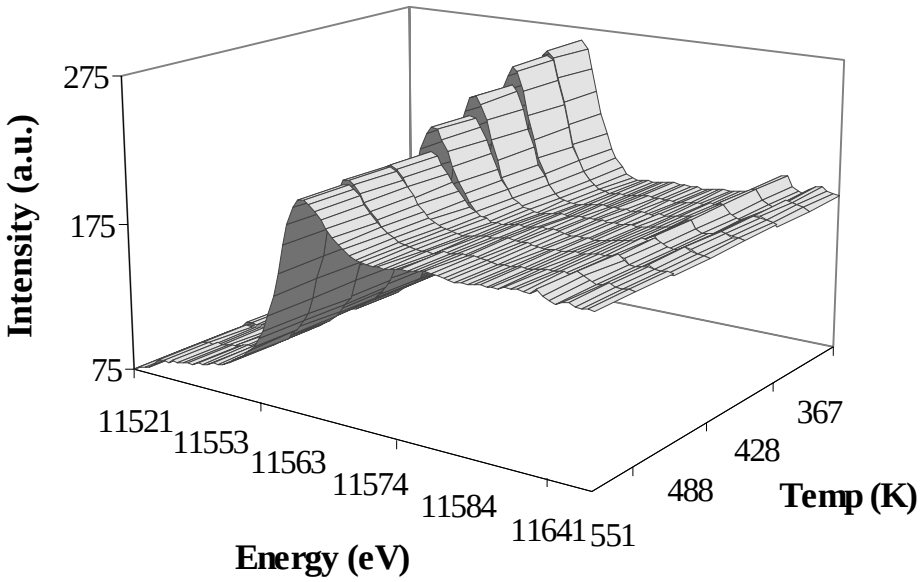

Figure 7 *XANES spectra of 0.5wt% Pt/ZrO_2 during reduction in 5%H_2 in N_2*

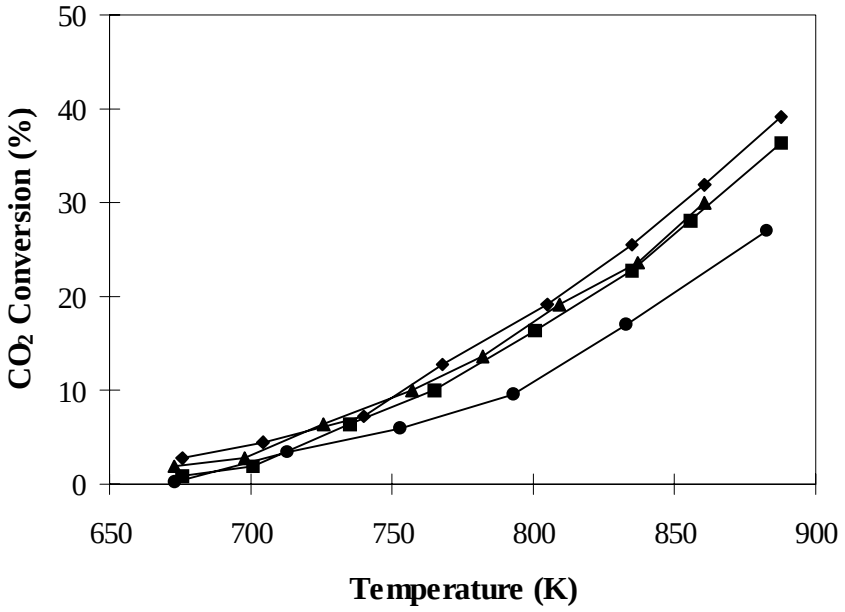

Figure 8 *Influence of the reduction temperature on the activity of 0.5wt% Pt/ZrO_2, ◆ T_{red}=1125K, ▲ T_{red}=875K, ■ T_{red}=475K; ●=unreduced, $CO_2/CH_4/Ar/N_2$ =42/42/75/10 ml.min^{-1}, 300mg catalyst*

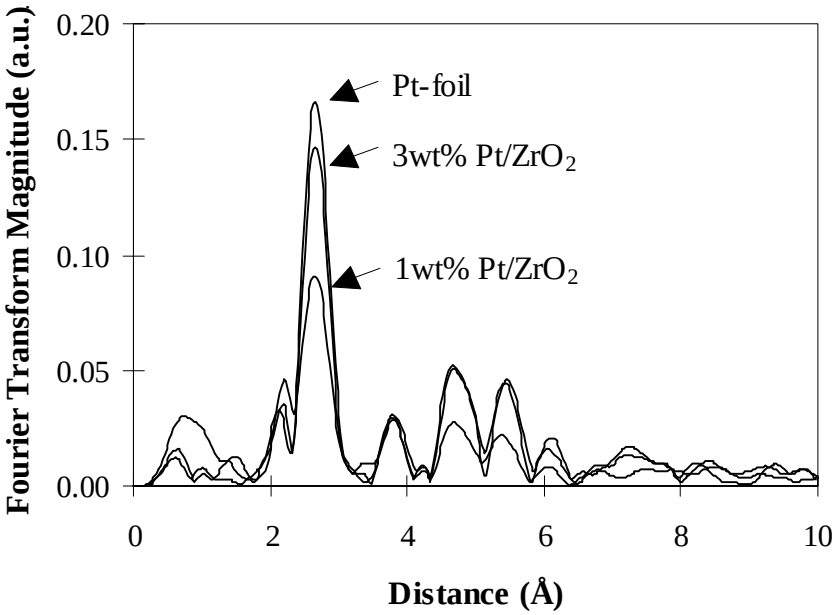

Figure 16 *k^2-weighted Fourier Transformed EXAFS spectra of Pt-foil and Pt/ZrO_2 having different Pt loadings*

summarized in Figure 8. Above a reduction temperature of 475K its influence on the activity of the catalyst was insignificant. However, an unreduced catalyst was less active than the reduced ones.

The fractions of accessible Pt shown in Figure 5 were calculated on basis of hydrogen chemisorption. The fractions of accessible Pt calculated from hydrogen chemisorption were compared with those calculated from EXAFS. In Figure 9 the Fourier Transformed EXAFS spectra of 1wt% and 3wt% Pt/ZrO_2 are shown. For comparison the Pt foil (reference) is also included. The peak at 2.8Å represents the Pt-Pt contribution.

Table 3 *Comparison of EXAFS results with H_2-chemisorption obtained on Pt/ZrO_2*

Weight loading (%)	H/Pt[1]	Coordination number[1]	r_{Pt-Pt} (Å)	$\Delta\sigma^2$ ($*10^{-3}$ Å^2)
1	0.82 (80)	6.5 (86)	2.773	1.44
3	0.19 (19)	11.2 (15)	2.776	0.07

[1] The value in brackets denotes the Pt dispersion (%) calculated according to Kip *et al.* [20]

The intensity of this peak, which is correlated to the average number of Pt neighbours in the first coordination shell, increased with increasing Pt-concentration. In Table 3 the results of the EXAFS experiments and hydrogen-chemisorption are compiled. It is seen that excellent agreement between the values for the fraction of accessible Pt obtained by EXAFS and chemisorption exists.

3.3.3 Activity of 0.5wt% Pt/ZrO_2

The catalytic activity of 0.5wt% Pt/ZrO_2 as function of the temperature is shown in Figure 10. The maximum conversions/yields as calculated from thermodynamics are shown in Figure 11. For calculation of the thermodynamic equilibrium, carbon formation was not taken into account. The thermodynamic equilibrium constant was calculated on basis of a gas mixture with the composition $CO_2/CH_4/He/H_2/CO/H_2O$ =1/1/2/0/0/0. By comparing Figures 10 and 11 we note that under reaction conditions thermodynamic limitations are not reached. Increasing the temperature increased the CO_2 and CH_4

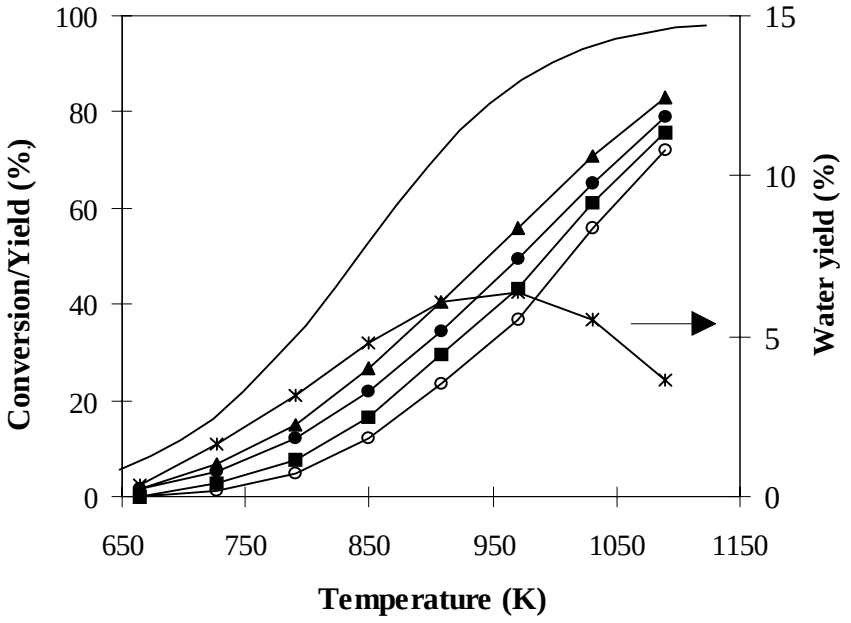

Figure 10 *Activity of 300mg Pt/ZrO_2, total flow=170ml.min^{-1}, $CO_2/CH_4/Ar+N_2$ =1/1/2, ▲=CO_2, ●=CO, ■=CH_4, ○=H_2,*=H_2O , solid line=CO_2 conversion calculated from thermodynamics*

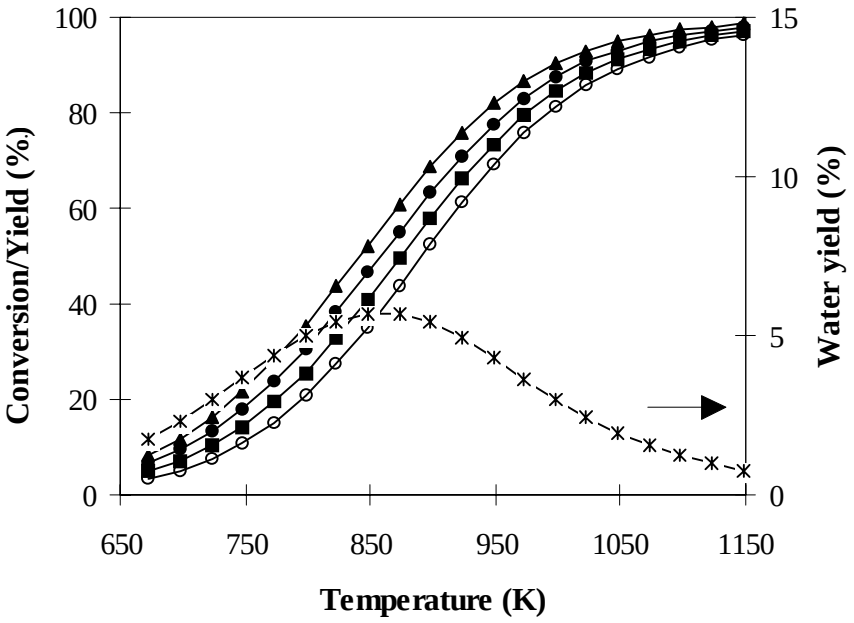

Figure 18 *Conversions calculated from thermodynamics, $CO_2/CH_4/He/H_2/CO/H_2O=1/1/2/0/0/0$, ▲=$CO_2$, ●=CO, ■=$CH_4$, ○=$H_2$, *=$H_2O$*

conversions and also the H_2 and CO yields increased. In addition to H_2 and CO, water was observed as a reaction product. The water yield reached a maximum at 950K. Above this temperature the amount of water in the product stream decreased. The CO_2 conversion always exceeded the CH_4 conversion and the CO yield was always higher than the H_2 yield.

3.4 Discussion

In Figure 12 the product distribution as calculated from thermodynamics [21] is shown. For this calculation the feed consisted of CO_2/CH_4/He with a ratio 1:1:2 and as products CO, H_2, H_2O and C (graphite) were allowed. It can be seen from this figure that the formation of coke is predicted over the whole range of temperatures, but it decreases with increasing reaction temperature. When coke formation is taken into account in the

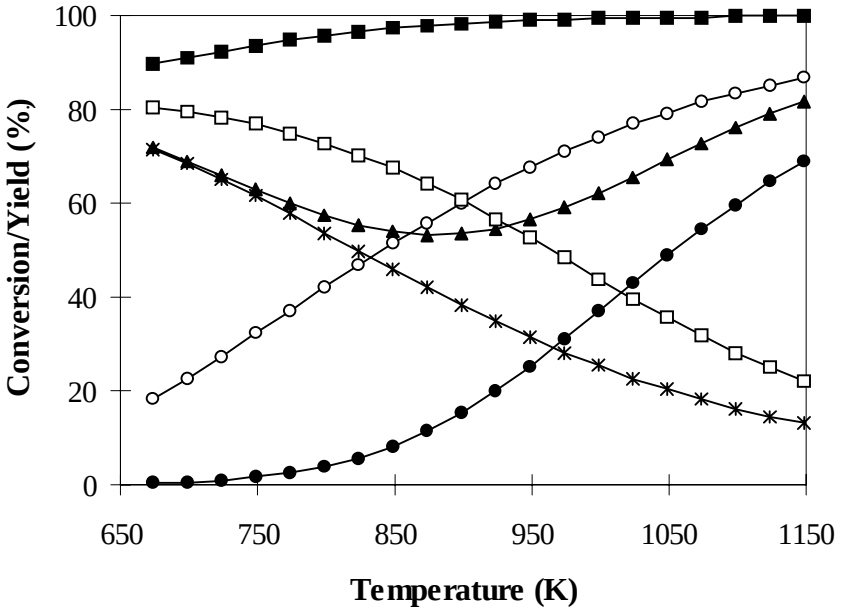

Figure 19 *Product distribution calculated from thermodynamics, $CO_2/CH_4/He/H_2O/CO/H_2/C=1/1/2/0/0/0/0$, ▲=$CO_2$, ●=CO, ■=$CH_4$, ○=$H_2$, *=$H_2O$, □=C*

thermodynamics calculation, already at low temperatures (675K) very high CO_2 and CH_4 conversions can be obtained with a high selectivity to C and CO. This is in agreement with thermodynamic calculations of Udengaard *et al.* [2] who showed a high thermodynamic driving force to form coke under the conditions of dry methane reforming. However, the catalysts described in the present study form orders of magnitude less carbon than predicted by thermodynamics (Chapter 6), thus, coke formation was excluded from further thermodynamic calculations (Figure 11).

The activity of different Pt catalysts is compared in Figure 1. It can be seen that all catalysts (Pt/γ-Al_2O_3, Pt/TiO_2 and Pt/ZrO_2) except Pt/SiO_2 showed initially a good activity for CO_2/CH_4 reforming. However, Pt/ZrO_2 was the only stable Pt catalyst and is, thus, preferred. Remarkably, Pt/SiO_2 had only a very low activity for CO_2/CH_4 reforming. This is attributed to the incapability of this catalyst to activate CO_2 (see Chapter 4). Rh/SiO_2 on the other hand showed initially a good activity (Figure 3). This indicates that Rh is more active for CO_2/CH_4 reforming than Pt. Indeed, all Rh based catalysts were

more active than the Pt-based catalysts (Figure 3) which is consistent with the measured activity of the unsupported metals (Table 4), Pt metal is less active than Rh metal. This is also confirmed by different authors who preferred Rh based catalysts [6, 9, 11-13] due to their high activity. Although Rh based catalysts are active and stable catalysts for CO_2/CH_4 reforming, it was decided to investigate Pt-based catalysts in more detail due to the better availability of Pt.

It was shown in Figure 1 that Pt/ZrO_2 is the only stable Pt catalyst, thus, it was decided to investigate this catalyst in more detail. An investigation of the influence of the Pt content in Pt/ZrO_2 on the activity of the catalyst showed that up to 0.5wt% the activity increased with increasing metal loading (Figure 5). Above 0.5wt% the activity levels off while the accessible Pt content still increased. Thus, it must be concluded that at higher Pt concentration not all accessible Pt atoms contribute equally to the activity of the catalyst (see Chapter 4). The fraction 'less active Pt' increased with increasing Pt concentration (>0.5wt%, this will be studied in detail in Chapter 4). Therefore, further investigations in this chapter were carried out with 0.5wt% Pt/ZrO_2. The fact that the activity loss of Rh/SiO_2 (70% of the initial activity was lost after 25 hours, see Figure 3) was accompanied by a decrease of 74% of the Rh surface area suggested to us that the activity of the Rh catalyst was determined by the accessibility of Rh. This is also supported by the fact that the influence of the support on the activity of Rh catalysts was

Table 4 *Activity of Pt and Rh for CO_2/CH_4 reforming, CO_2/CH_4/He/Ar =50/50/170/30 ml.min^{-1}, 1g catalyst for Pt and 50mg catalysts for Rh, T=925K*

Metal	amount of accessible metal (moles/g)[1]	CO_2 conversion (%)	TOF (s^{-1})
Pt	$5.3*10^{-6}$	1.5	0.1
Rh	$7.8*10^{-6}$	10	9.6

[1] based on hydrogen chemisorption, using the models of Kip *et al*. [20]

only minor (see Figure 1 and 3 and Table 4). For Pt based catalysts the support has a significant influence on the activity and stability of the catalysts. This might indicate that the accessible Pt atoms located on the Pt-support perimeter have special catalytic properties (see Chapter 4). This in contrast to Rh catalysts in which all accessible Rh atoms are equally active being in good agreement with results from Mark *et al*. [17, 22].

Because the catalysts used for CO_2/CH_4 reforming need to be resistant to high temperatures the catalysts were reduced at high temperature. Therefore, it is mandatory to understand the influence of the reduction temperature on the state of the Pt and the activity of the catalyst. During temperature programmed reduction (TPR) of 0.5wt% Pt/ZrO_2 reduction peaks (see Figure 6) were observed at 475K and at 632K. When the hydrogen uptake during TPR is compared with the intensity of the Pt L_{III}-white line (Figure 13), it can be seen that the hydrogen uptake at 475K was accompanied by a decrease in the white line. As the intensity of the white line is proportional to the charge at the Pt [23, 24] (a higher oxidation state op Pt is represented by a higher intensity of the white line) this indicates that Pt is reduced at this temperature. This agrees well with TPR results of Hoang *et al*. [25] (on Pt/ZrO_2), the reduction peak (attributed to the reduction of Pt^{4+} to Pt^0) being in their case at 553K.

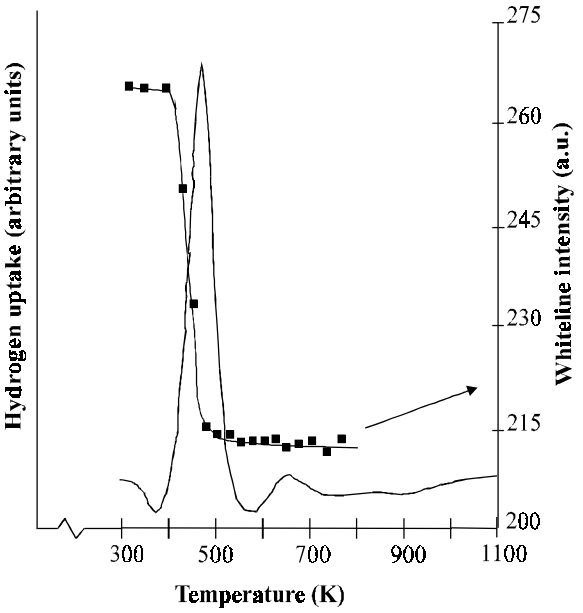

Figure 13 *Comparison of the TPR trace with the intensity of the Pt-whiteline during reduction*

The second hydrogen uptake during TPR at 632K was not accompanied by a decrease of the Pt-white line. This indicates that this hydrogen consumption is not affiliated with the reduction of Pt. Therefore, we assign it to the (partially) reduction of ZrO_2 which was also suggested previously [25-30]. For blank ZrO_2 hydrogen consumption

was detected at 925K and ascribed to reduction of ZrO_2 [25]. The lower maximum of reduction in our case is tentatively attributed to the reduction of ZrO_2 in the vicinity of Pt. We speculate that hydrogen is activated on Pt and partially reduces the ZrO_2 in the direct vicinity of the Pt particle. Evidence for the existence of Zr^{3+} was given by Morterra *et al*. [27] based on ESR experiments. Others concluded the existence of Zr^{3+} from indirect measurements like CO adsorption, followed by TPD or IR [26, 28, 29]. Also a SMSI state, i.e. the decoration of the metal by the partially reduced support [31, 32], was suggested for Rh/ZrO_2 [28] and Ni/ZrO_2 [30].

When the influence of the reduction temperature on the activity of Pt/ZrO_2 is compared to its reduction state, it can be seen that when all Pt is reduced (reduction above 475K, see Figure 6) further increase in the reduction temperature and, hence, the partial reduction of the support does not influence the activity of the catalyst. As reforming catalysts are used at high temperatures (T>1100K) we employed a reduction temperature (1125K) in the same range.

During CO_2/CH_4 reforming over Pt/ZrO_2 not only H_2 and CO were observed as

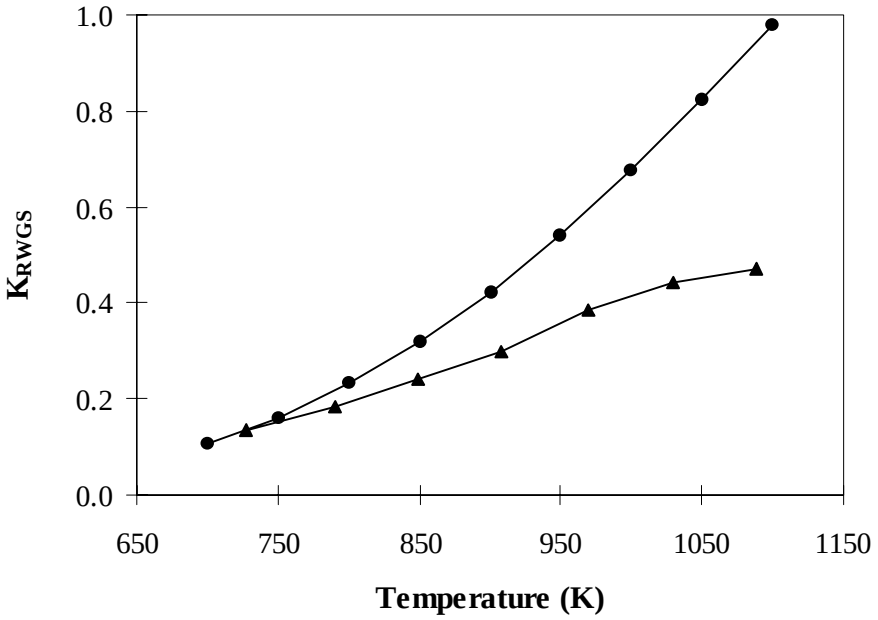

Figure 14 *K-values for the RWGS reaction ($H_2 + CO_2 \rightarrow CO + H_2O$) obtained over Pt/ZrO_2 (▲) and as calculated from thermodynamics (●)*

reaction products but also a significant amount of water (Figure 5). This clearly indicates that at least one side reaction occurs. The most likely reaction is the reverse watergas shift reaction (RWGS; $CO_2 + H_2 \rightleftharpoons CO + H_2O$). This explains, why the CO_2 conversion is higher than the CH_4 conversion. CO_2 is converted in a second reaction whereas CH_4 is not. The occurance of RWGS also explains the higher CO yield compared to the H_2 yield as CO is formed in this reaction and hydrogen consumed.

In Figure 14 the equilibrium constant calculated from thermodynamics (K_{RWGS}) for the RWGS reaction and as obtained over Pt/ZrO_2 are shown. The figure shows that the RWGS reaction is not at thermodynamic equilibrium under the reaction conditions. At high temperatures, the thermodynamic equilibrium constant for steam reforming (($K_{steam\ reforming}$, $CH_4 + H_2O \rightleftharpoons 3H_2 + CO$) increases strongly (Figure 15). Thus, at higher

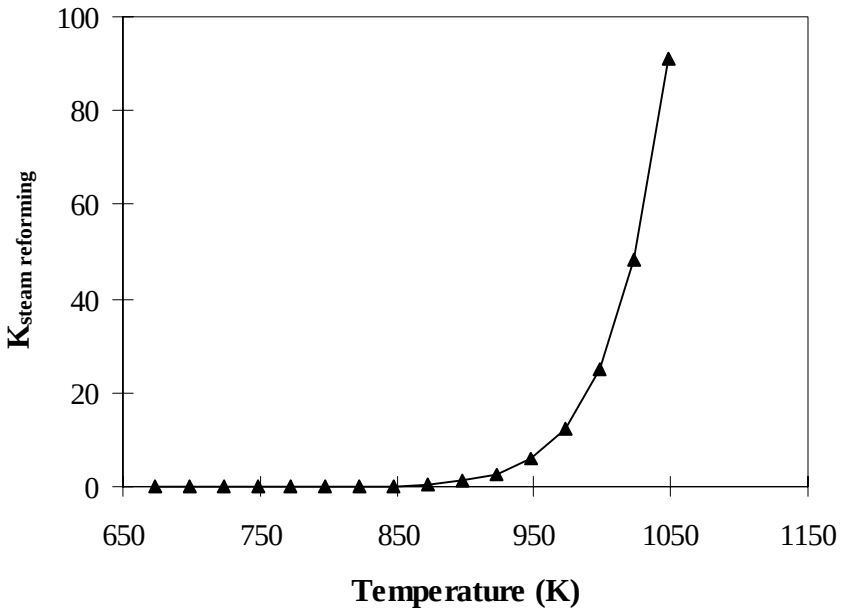

Figure 15 *K-values for steam reforming calculated from thermodynamics*

temperatures the thermodynamic driving force for the steam reforming reaction increases. Moreover, from the results published by Qin *et al.* [8] an activation energy of 108kJ.mol^{-1} (over Pt/MgO) could be calculated while for the reverse water gas shift reaction activation energies, over Pt catalysts, in the range 50-75kJ.mol^{-1} are reported [33]. This indicates that

the steam reforming becomes more significant at higher temperatures compared to the reverse water gas shift reaction. Thus the water formed is converted with methane to $3H_2$ and CO which increases the H_2/CO ratio to one at higher temperatures.

3.5 Conclusions

Pt/ZrO_2 having 0.5wt% Pt (calcined at 875K and reduced at 1125K) is an excellently suited catalyst for dry CO_2/CH_4 reforming. It can operate for 180 hours without significant deactivation. The stability of noble metal catalysts for CO_2/CH_4 reforming does not only depend on the metal ($Rh/\gamma\text{-}Al_2O_3$ is stable whereas $Pt/\gamma\text{-}Al_2O_3$ deactivates) but also on the support ($Pt/\gamma\text{-}Al_2O_3$ deactivates whereas Pt/ZrO_2 is stable). Above 0.5wt% not all accessible Pt contributes equally to the activity of the catalyst. In contrast to this, the activity of Rh catalysts is determined by the availability of Rh. When Pt was completely reduced (above 475K) the reduction temperature did not further influence the activity of the catalyst indicating that sintering does not occur in H_2. The support might be partially reduced when the reduction temperature is higher than 632K, however, this had no influence on the activity of the catalyst. The reforming reaction is accompanied by the reverse water gas shift reaction. This decreased the H_2/CO ratio to values lower than 1. At higher temperatures (>900K) steam reforming becomes more significant which increases the H_2/CO ratio.

3.6 References

6. I.M. Bodrov, L.O. Apel'baum, Kinet. Katal., 8 (1967) 379.
2. N.R. Udengaard, J.H. Bak Hansen, D.C. Hanson, J.A. Stal, Oil Gas J., 90 (1992) 62.
3. W. Hally, J.H. Bitter, K. Seshan, J.A. Lercher, J.R.H. Ross, Stud. Surf. Sci. Catal., 88 (1994) 167.
4. D.L. Trimm, Catal. Rev.-Sci. Eng., 16 (1977) 155.
5. E. Boellard, P.K. de Bokx, A.J.H.M. Kock, J.W. Geus, J. Catal., 96 (1985) 481.
6. A.T. Ashcroft, A.K. Cheetham, M.L.H. Green, P.D.F. Vernon, Nature, 225 (1991) 352.

7. J. R. Rostrup Nielsen, J. Catal., 144 (1993) 38.
8. D. Qin, J. Lapszewicz, Catal. Today, 21 (1994) 551.
9. E. Riensche, H. Fedder, Stud. Surf. Catal., 21 (1994) 551.
10. F. Fischer, H. Tropsch, Brennst. Chem., (1928) 39.
11. F. Solymosi, Gy. Kutsan, A. Erdohelyi, Catal. Lett., 11 (1991) 149.
12. P.D.F. Vernon, M.L.H. Green, A.K. Cheetham, A.T. Ascroft, Catal. Today, 13 (1992) 417.
13. J. Nakamura, K. Aikawa, K. Sato, T. Uchijima, Catal. Lett., 25 (1994) 265.
14. J.T. Richardson, S.A. Paripatyadar, Appl. Catal., 61 (1990) 293.
15. J.S. Perera, J.W. Sankar, J.M. Thomas, Catal. Lett., 11 (1991) 219.
16. V.A. Tsipouriari, A.M. Efstathiou, Z.L. Zhang, X.E. Verykios, Catal. Today, 21 (1994) 579.
17. M.F. Mark, W.F. Maier, Angew. Chem. Int. Ed. Engl., 33 15/16 (1994) 1657
18. Y. Sakai, H. Saito, T. Sodesawa, F. Nozaki, React. Kinet. Catal. Lett., 24 (1984) 253.
19. A.M. Gadalla, M. E. Sommer, Chem. Eng. Sci., 44 (1989) 2825.
20. B.J. Kip, F.B.M. Duivenvoorden, D.C. Koningsberger, R. Prins, J. Catal., 105 (1987) 26.
21. Thermodynamic calculations were carried out with help of the computer program HSC Chemistry for Windows 2.0, Outokumpu Research Oy, Finland.
22. M.F. Mark, W.F. Maier, J. Catal., 164 (1996) 122.
23. Y. Iwasawa (ed.), X-ray absorption fine structure for catalysts and surfaces, World Scientific Singapore (1996).
24. A. Jentys, G.L. Haller, J.A. Lercher, J. Phys. Chem., 97(2) (1993) 484.
25. D.-L. Hoang, H. Lieske, Catal. Lett., 27 (1994) 33.
26. C. Dall'Agnol, A. Gervasini, F. Morazzoni, F. Pinna, G. Strukul, L. Zanderighi, J. Catal., 96 (1985) 106.
27. C. Morterra, E. Giamello, L. Orio, M. Volante, J. Phys. Chem., 94 (1990) 3111.
28. A. Trunschke, D.L. Hoang, H. Lieske, J. Chem. Soc. Faraday Trans., 91(24) (1995) 4441.
29. M.-Y. He, J.G. Ekerdt, J. Catal., 87 (1984) 238.
30. P. Turlier, G.A. Martin, React. Kinet. Catal. Lett., 21 (1982) 287.
31. S.J. Tauster, S.C. Fung, R.L. Garten, J. Am. Chem. Soc., 100 (1978) 170.
32. S.J. Tauster, Acc. Chem. Res., 20 (1987) 389.
33. M.S. Spencer, Catal. Lett., 32 (1995) 9.

4

Active sites and the influence of the pretreatment on Pt/ZrO_2 catalysts for CO_2/CH_4 reforming

Abstract

Active Pt-catalysts for CO_2-reforming are able to form carbonate species from CO_2 on the support of the catalyst. This suggests that the mechanism for CO_2/CH_4 reforming involves the activation of CO_2 on the support. Methane is activated on the metal. Because not all accessible Pt atoms contribute equally to the activity of the catalyst it is concluded that the most active sites for CO_2/CH_4 reforming on these catalysts are located on the Pt-ZrO_2 perimeter. The perimeter concentration of Pt in these catalysts can be changed either by varying the metal loading or by sintering of the Pt particles by increasing the calcination temperature (in the range 925-1125K). Increasing the reduction temperature of the catalyst did not influence the activity of the catalyst indicating that sintering does not occur in hydrogen. This was supported by the fact that the Pt-Pt coordination number calculated from EXAFS did not increase. However, the hydrogen chemisorption capacity was markedly decreased by increasing the reduction temperature. This is explained by the presence of a strong metal support interaction state (SMSI) after high temperature reduction. Under reaction conditions this state does not persist.

4.1 Introduction

In the previous chapter it was shown that Pt/ZrO_2 is an excellent catalyst for CO_2/CH_4 reforming. In this chapter the results of the experiments performed in order to optimize the metal loading and the pretreatment conditions of this catalyst will be discussed.

First the influence of the metal loading on the activity of Pt/ZrO_2 will be described. While using the catalyst with the optimal metal loading the influence of the calcination and reduction temperature on the activity of the catalyst is investigated. The catalysts are characterized by means of XPS, XAFS, TPR and hydrogen chemisorption in order to correlate the state of the catalyst and its activity for CO_2/CH_4 reforming.

4.2 Experimental

Experimental details are given in Chapter 2.

4.3 Results

4.3.1 Influence of the metal loading on the activity

In Chapter 3 it was shown that 0.5wt% Pt/ZrO_2 is an excellent catalyst for CO_2/CH_4 reforming. It was also shown that not all accessible Pt contributed equally to the activity of the catalysts. By increasing the metal concentration (>0.5 wt%) the activity per accessible Pt atom decreased (see Figure 1). This will be investigated in more detail in this chapter. The physico-chemical properties of the catalysts used for this study are summarized in Table 1. Up to 0.5wt% of Pt all catalysts had a Pt dispersion of 100% while at higher metal loadings the dispersion decreased (to 58% for 2wt% Pt/ZrO_2).

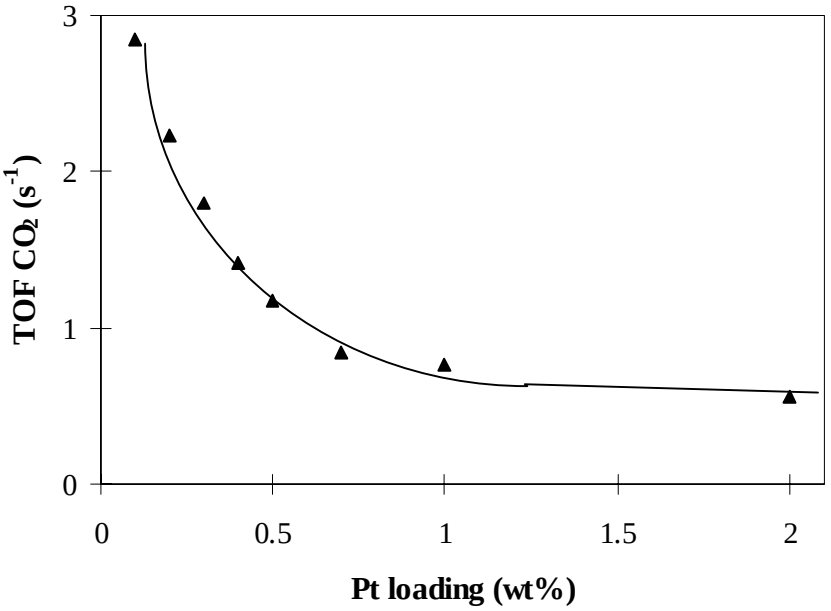

Figure 1 *Influence of the metal loading on the activity of the accessible Pt for Pt/ZrO_2 catalysts, $CO_2/CH_4/Ar/N_2$ =42/42/75/10 ml.min^{-1}, 300mg catalyst, T=875K*

Table 9 *Dispersions of Pt/ZrO_2 catalysts having different metal loadings*

Metal loading (wt%)	Dispersion from hydrogen chemisorption* (%)	Dispersion from EXAFS* (%)
0.2	100	-
0.3	100	-
0.4	100	-
0.5	100	-
0.7	97	-
1.0	80	80
2.0	58	-

* Calculated using the models of Kip *et al*. [2].

Figure 2 displays the variation of the catalytic activity at 875K nd the accessible Pt concentration for the series of Pt/ZrO_2 catalysts with different Pt loadings. With increasing metal loading the concentration of accessible Pt increased. However, while at a low Pt content (<0.5wt%) the activity increased with increasing metal loading, the increase in activity stagnated at higher metal loading (>0.5wt%). This could not be due to blocking of the pores by Pt because

adsorption/desorption studies showed that the

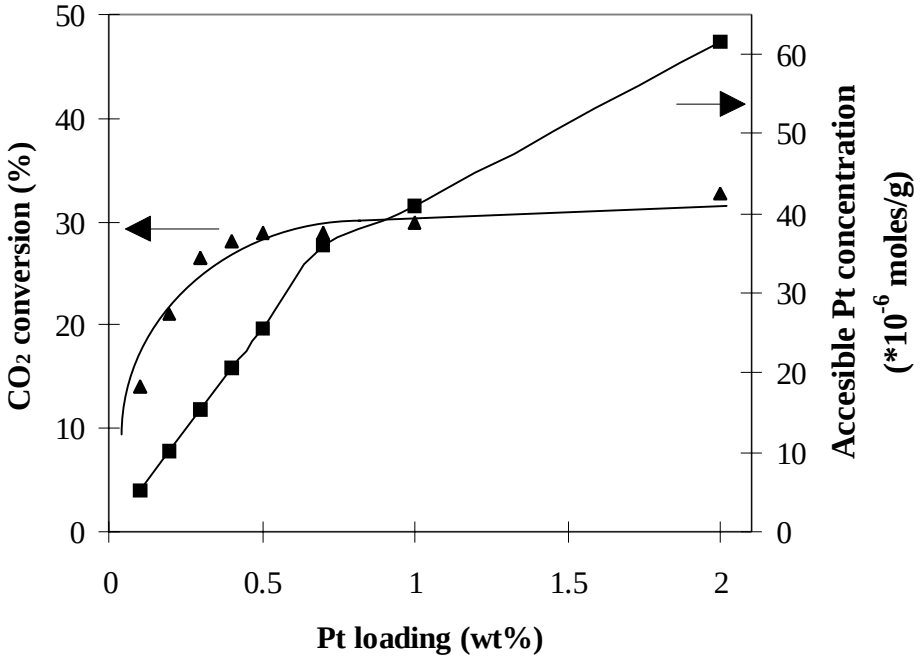

Figure 2 *Influence of the Pt loading on the amount of accessible Pt and the activity of Pt/ZrO_2 catalysts for CO_2/CH_4 reforming at 875K, $CO_2/CH_4/Ar/N_2$ =42/42/75/10 ml.min^{-1} 300mg catalyst*

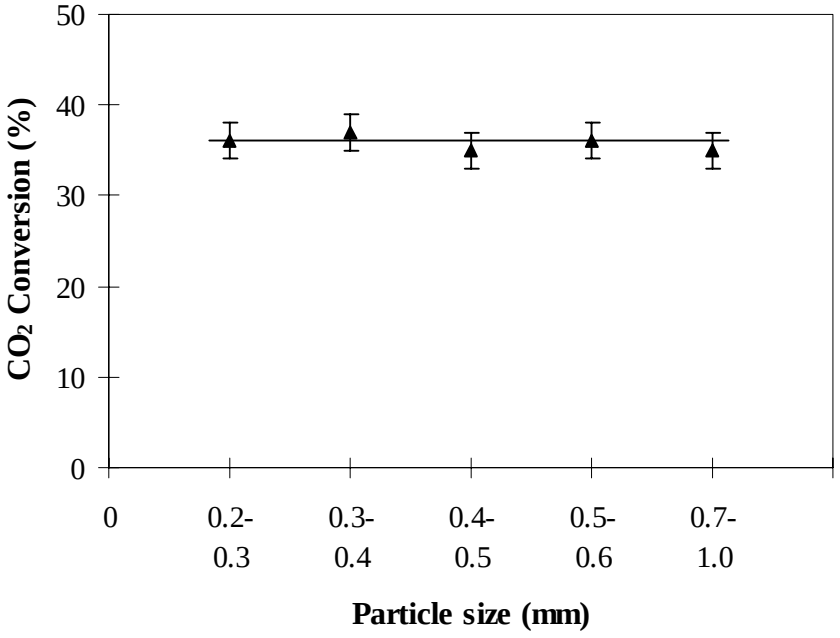

Figure 3 *Influence of the catalyst particle size on the activity of 0.5wt% Pt/ZrO_2 at 900K, $CO_2/CH_4/Ar/N_2$ =42/42/75/10 ml.min^{-1}, 300mg catalyst*

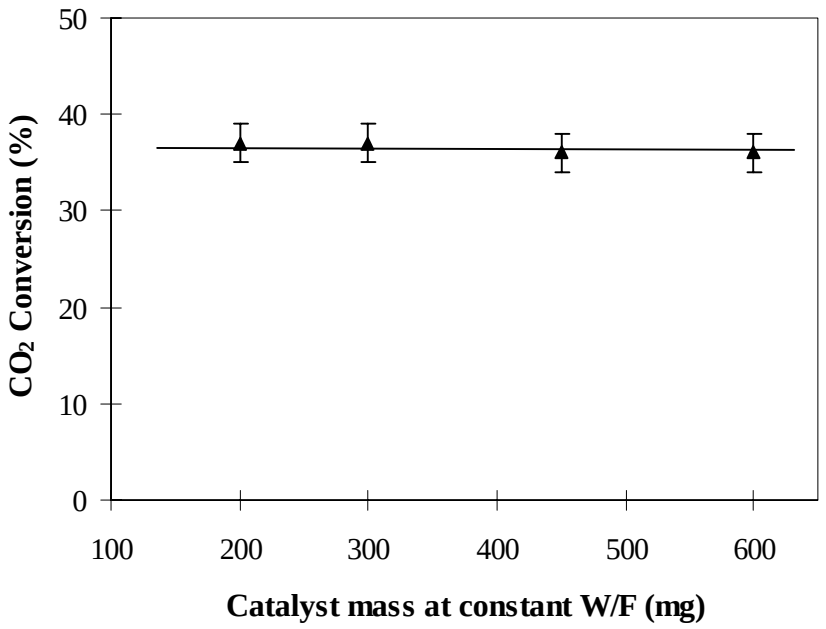

Figure 4 *Influence of the gasfilm thickness on the activity of 0.5wt% Pt/ZrO_2 (W/F=180g.s/l) at 900K*

average pore size is 28nm and cylindrical in shape, whereas the Pt particle size is 2-3nm. To check whether the conversions of the optimal catalyst (0.5wt% Pt/ZrO_2) are influenced by internal mass transfer limitations, the conversions obtained with catalysts having different particle sizes (0.1-1.0 mm) are compared in Figure 3. Such comparison showed clearly that the conversion is not influenced by the particle size (note that 0.3-0.6mm is normally used). Thus, the presence of internal mass transfer limitations could be excluded. To investigate the influence of external diffusion limitations, the activity was measured as a function of the catalyst loading at constant W/F (W=catalyst weight, F=total flow of feed gas, see Figure 4). The conversion is not affected by changing the amount of catalyst and the flow, i.e., at constant contact time. Thus, external mass transfer limitations do not occur under the conditions applied. Thermodynamic limitations were also ruled out since the carbon dioxide conversion calculated from thermodynamics is 55% at 875K whereas the maximum conversion observed under the experimental conditions is 33% (Figure 2). It is therefore concluded that the non-linear dependence of the activity of Pt/ZrO_2 as a function of the accessible Pt area is a result of a change in the

catalytic properties at higher metal concentrations.

4.3.2 Influence of the support on the activity

The activity of Pt catalysts for CO_2/CH_4 reforming per accessible Pt atom is compiled in Table 2. The unsupported Pt black catalyst was prepared as described by Paal *et al.* [1] using the 'hydrazine method'. After reduction of the catalyst at 975K its surface area was $0.25 m^2/g$ (measured by the BET method and calculated from hydrogen

Table 10 *Comparison of the activities of different Pt-catalysts (0.5wt% Pt/support), T=925K, $CO_2/CH_4/He+N_2$=50/50/100 ml/min^{-1}*

Catalyst	Pt surface area (m^2/g)	CO_2 convn ($*10^{-6}$moles/g.s)	TOF of CO_2 (s^{-1})
Pt/ZrO_2	1.2	520	20
$Pt/\gamma\text{-}Al_2O_3$	0.96	632	25
Pt/TiO_2	0.31	338	52
Pt/SiO_2	0.15	0.1	0.2
Pt-black	0.25	0.7	0.1
Pt-black/ZrO_2	0.24	3.7	1.1

chemisorption). From Table 2 it can be seen that the catalytic activity of Pt-black (TOF) is two orders of magnitude lower compared to Pt/ZrO_2, Pt/TiO_2 and $Pt/\gamma\text{-}Al_2O_3$. The activity of Pt-black compares however well with the low activity of Pt/SiO_2. This leads to the conclusion that the use of a suitable support can strongly increase the activity of the Pt metal. The positive involvement of the support for the reaction was shown by the use of Pt-black impregnated with a solution of $ZrOCl_2$ (and subsequently calcined and reduced at 875K). The activity per accessible Pt atom of this catalyst was increased by an order of magnitude compared to the untreated Pt-black sample. The increase in activity of Pt-black after impregnation with $ZrOCl_2$ indicates clearly that ZrO_2 contributes to the activity of Pt/ZrO_2 for the reforming reaction.

The results compiled in Table 2 indicate that the activity of the Pt catalysts for CO_2/CH_4 reforming depends crucially on the support. This indicates that a support related species is involved in the reaction mechanism. Because the supports themselves were inactive for the reforming reaction it is concluded that also the metal is indispensable. Thus, a combination of species formed on the support and species formed on the metal are a prerequisite for the reaction to proceed, thus, stressing the importance of the Pt-support perimeter for the reaction. Therefore, Pt/ZrO_2 catalysts having different particle sizes (thus different perimeter concentrations) were prepared by changing the preparation procedure of the catalysts.

4.3.3 Influence of the pretreatment procedure on activity and particle morphology

Influence of the calcination on the particle size and the activity

The preparation of the catalysts involved calcination of the support grains, followed by impregnation of the grains with a H_2PtCl_6 solution (see Chapter 2). This

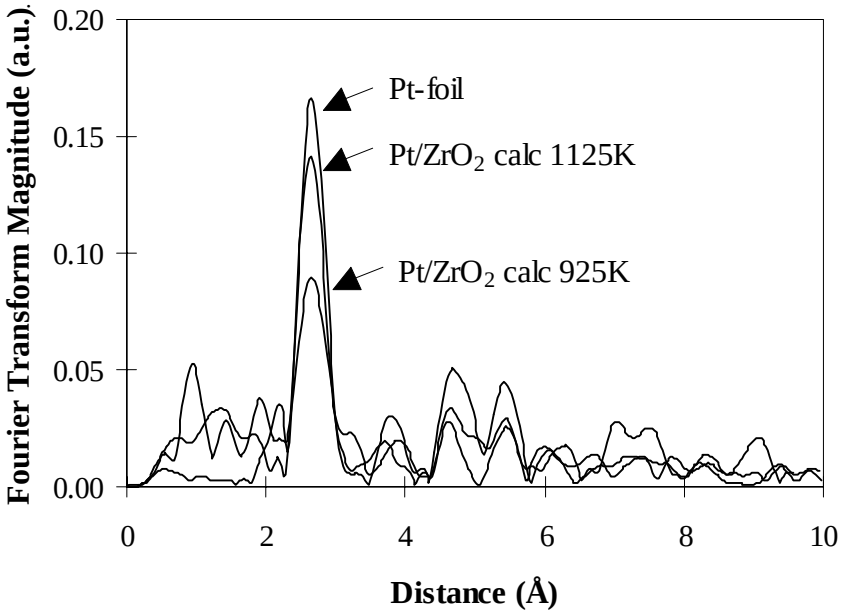

Figure 5 *k^2-weighted Fourier Transformed EXAFS spectra of Pt-foil and 1wt% Pt/ZrO_2 calcined at different temperatures*

Table 3 *Influence of the calcination temperature on the activity of 0.5 and 1wt% Pt/ZrO_2 (reduction temperature 775K)*

Metal loading (wt%)	Calcination temperature (K)	Coordination number from EXAFS*	Hydrogen chemisorption capacity (H/Pt)*	CO_2 conversion at 875K (%)
1	925	6.5 (86)	0.82 (80)	30
1	1125	10.7 (20)	0.33 (30)	8
0.5	925	-	1.10 (100)	29
0.5	1025	-	0.50 (48)	24
0.5	1125	-	0.35 (33)	7

* The value in brackets denotes the Pt dispersion calculated from EXAFS or hydrogen chemisorption according to Kip *et al.* [2]

catalyst precursor was calcined prior to *in situ* reduction and testing. The temperature of calcination of the blank support did not influence the activity of the final catalyst although the surface area (BET) decreased from $33m^2/g$ to $18m^2/g$ when the calcination temperature of the support was increased from 925K to 1125K. On the other hand, increasing the calcination temperature after impregnation (from 925K to 1125K) resulted in a significant increase in the Pt-Pt coordination number from 6.5 to 10.7 (see Figure 5 and Tables 3 and 4) indicating an increase in the Pt particle size. The fraction of available Pt calculated from EXAFS agreed well with that calculated from hydrogen chemisorption

Table 4 *Influence of the calcination temperature on the EXAFS of 1wt% Pt/ZrO_2 (reduction temperature: 775K)*

Calcination temperature (K)	Coordination number from EXAFS	$\Delta\sigma^2$ ($*10^{-3}Å^2$)	r (Å)
925	6.5	1.44	2.772
1125	10.7	0.01	2.770

measurements which showed a decrease of the H/Pt ratio from 0.82 to 0.33 as the calcination temperature was increased. The decrease in the fraction of accessible Pt was accompanied by a drop in activity.

Influence of the calcination temperature on the state of Pt

Calcining Pt/ZrO_2 at a higher temperature did not only change the Pt particle size but it also changed the appearance of the catalyst. After calcination at 1125K the color of the catalyst was black whereas it was brown after calcination at 875K. This indicates that Pt was present in the zero valent state after calcination at 1125K. XPS was used to investigate the oxidation state of Pt in the two samples. The resulting XPS spectra are shown in Figure 6. The binding energies of the Pt-4f electrons are shown in this figure. Clearly, by increasing the calcination temperature the binding energy of the Pt-$4f_{7/2}$ electrons shifted to lower values (72.8 eV for the sample calcined at 925K and 71.1 eV for the sample calcined at 1125K) indicating that Pt was in a lower oxidation state after high temperature calcination. The state of Pt was also investigated by means of TPR. The

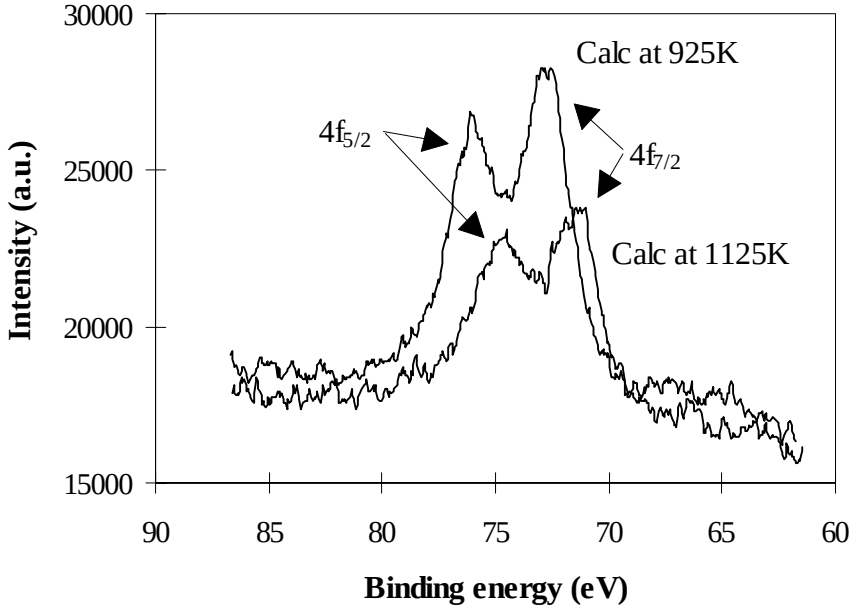

Figure 6 *XPS spectra of the Pt-4f band of 0.5wt% Pt/ZrO_2 calcined at different temperatures*

reduction behavior of the two samples (having different calcination temperatures) and bare ZrO_2 is compared in Figure 7. The sample calcined at 925K showed two reduction peaks as was already described in Chapter 3. For the sample calcined at 1125K no significant hydrogen uptake was observed.

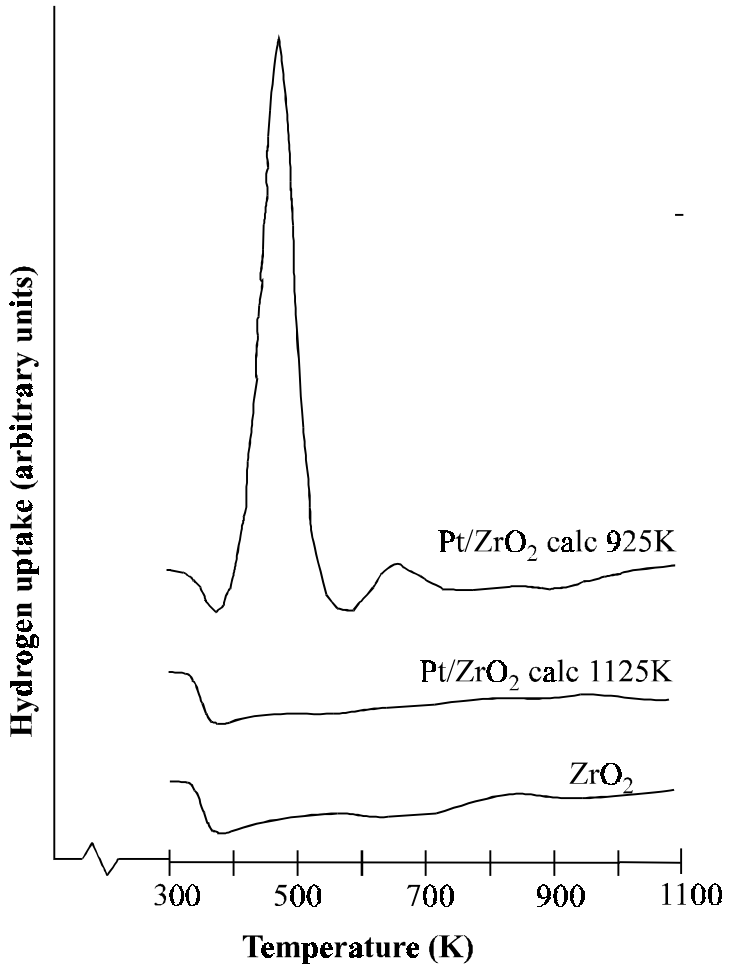

Figure 29 *Influence of the calcination temperature on the reducebility of 0.5wt% Pt/ZrO_2, flow=30ml.min, 5%H_2/Ar, heating ramp=10K.min^{-1}*

Influence of the reduction temperature on activity and particle morphology

Prior to testing, all catalysts were reduced *in situ*. Although it was shown in Chapter 3 that the reduction temperature (above 475K) did not have an influence on the activity of Pt/ZrO_2, increasing the reduction temperature (from 775K to 1125K) decreased

the hydrogen chemisorption capacity of the catalysts significantly. The H/Pt ratio

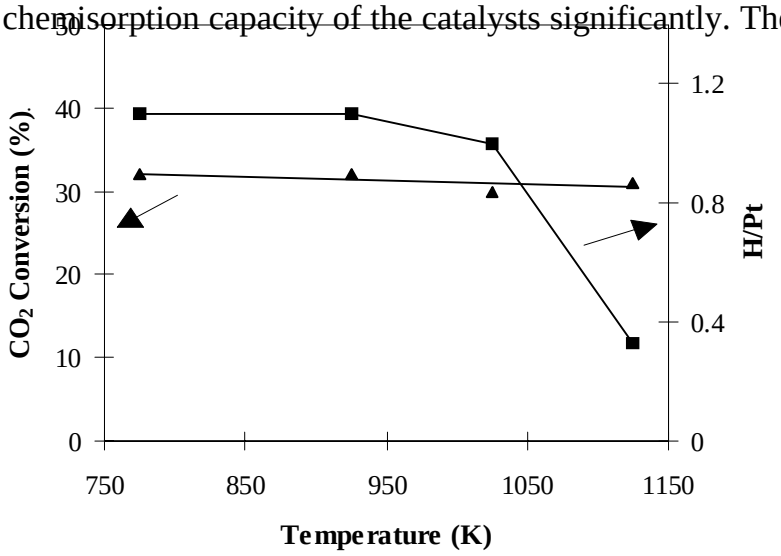

Figure 8 *Influence of the reduction temperature of Pt/ZrO_2 on the hydrogen chemisorption capacity and activity of the catalyst*

Table 5 *Influence of the reduction temperature on activity, hydrogen chemisorption capacity and Pt coordination number of Pt/ZrO_2*

Catalyst	Reduction temperature (K)	CO_2 conversion at 875K (%)	Hydrogen chemisorption capacity (H/Pt)*	Coordination number from EXAFS*
1wt% Pt/ZrO_2	775	30	0.82 (78)	6.5 (86)
1 wt% Pt/ZrO_2	1125	29	0.33 (30)	7.0 (81)
0.5wt% Pt/ZrO_2	775	29	1.1 (100)	-
0.5wt% Pt/ZrO_2	1125	28	0.35 (33)	-
0.5wt% Pt/ZrO_2	1125/875/ 675#	28	0.70 (67)	-

* The value in brackets denotes the Pt dispersion calculated from EXAFS or hydrogen chemisorption according to Kip *et al*. [2]

first temperature (1125K) is the initial reduction temperature; second temperature is the oxidation temperature; third temperature is the reduction temperature before the chemisorption measurement

decreased from 1.1 to 0.33 (see Figure 8) by increasing the reduction temperature from 775K to 1125K. EXAFS measurements on the other hand showed that the average Pt-Pt coordination number and, thus, the Pt particle size did not increase (Table 5). It should be emphasized that the values for the percentage of metal exposed obtained by hydrogen chemisorption for samples reduced at low temperature (775K) and by EXAFS are in good agreement. However, after a high temperature reduction (1125K) the fraction of Pt exposed calculated from EXAFS is higher than the value calculated from hydrogen chemisorption (Table 5). When a Pt/ZrO_2 catalyst with an apparent low dispersion (H/Pt=0.33, reduction temperature 1125K) was treated with 0.1% O_2 or air and subsequently reduced at a low temperature (675K), a higher dispersion (H/Pt=0.7) was obtained (Table 5).

4.4 Discussion

As can be seen in Figure 2 there is no straightforward relation between the concentration of accessible Pt and the activity of Pt/ZrO_2. For catalysts with Pt concentrations above 0.5wt% the amount of accessible Pt still increases, whereas the activity of the catalyst remains almost the same. It was already shown in §4.3.1 that this could not be explained by blocking of the pores, mass transfer or thermodynamic limitations. Thus it must be concluded that not all available Pt contributes equally to the activity of the catalyst and that the catalytic properties of Pt/ZrO_2 changed at higher metal loading. It is shown in Table 2 that the support has a significant influence on the activity of the different Pt catalysts. Therefore, it is concluded that the Pt atoms in the vicinity of the support might have special catalytic properties. When the activity and the perimeter concentration of the Pt/ZrO_2 catalysts is plotted as function of the metal loading (Figure 9) it can be seen that both the conversion and the concentration of Pt on the $Pt\text{-}ZrO_2$

perimeter show a similar dependence upon the metal loading. Thus, we related the activity

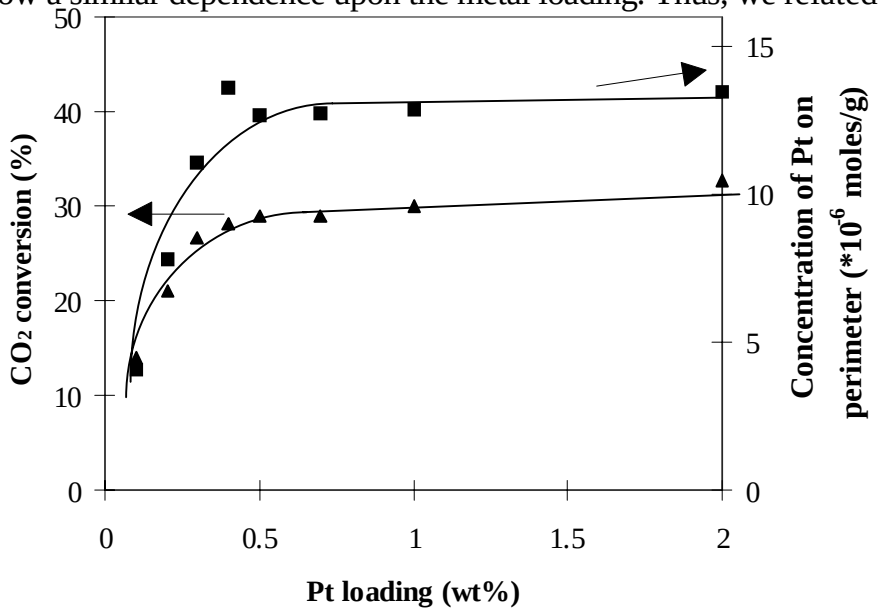

Figure 9 *Influence of the Pt-loading on the concentration of Pt on the perimeter and the activity of Pt/ZrO_2 catalysts for CO_2/CH_4 reforming at 875K, total flow=170ml.min^{-1}, CO_2/CH_4 /Ar+N_2 =1/1/2*

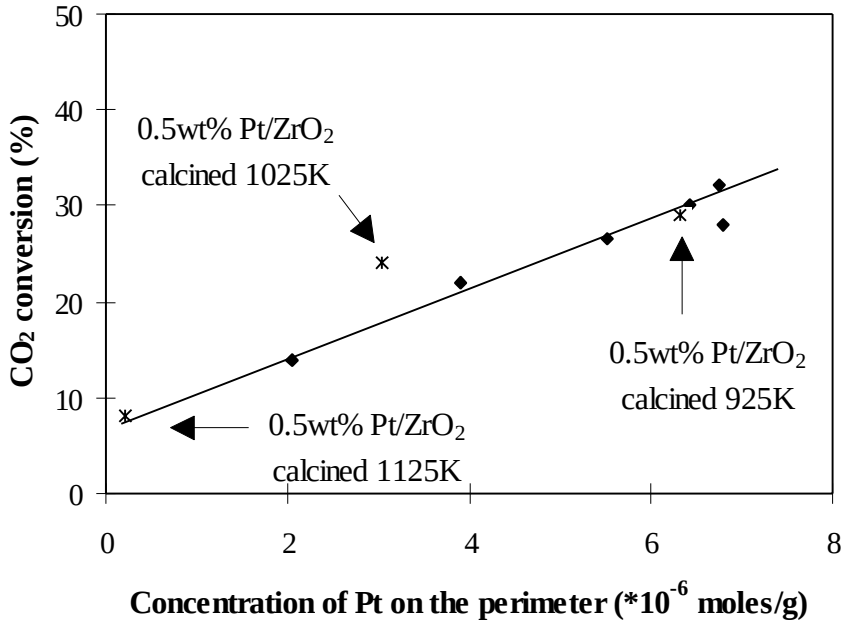

Figure 10 *Influence of the amount of accesible Pt on the activity of Pt/ZrO_2 catalysts for CO_2/CH_4 reforming at 875K, *=Pt/ZrO_2 calcined at 925, 1025 and 1125K*

of Pt/ZrO_2 to the perimeter length of the $Pt\text{-}ZrO_2$ boundary (see Figure 10). The lengths of the different perimeters obtained for Pt/ZrO_2 catalysts with different metal loadings are represented by the diamonds (◆). Alternatively, the perimeter length was varied by changing the calcination temperature of the 0.5wt% Pt/ZrO_2 catalyst. Tables 3 and 4 show that increasing the calcination temperature (925K, 1025K, 1125K) decreased the dispersion of this catalyst due to sintering. The activities of these catalysts are also shown in Figure 10 (represented by the asterisks). These points fit the line in the figure describing the linear relationship between the Pt perimeter and the activity of the catalyst. This indicates that the higher calcination temperature changed the length of the perimeter, but did not change its nature.

The importance of the support for the reforming reaction is also substantiated by the use of Pt-black and Pt/SiO_2 which were at least two orders of magnitude less active compared to Pt/ZrO_2 (Table 2). When ZrO_2 was impregnated on Pt-black the activity of Pt-black was increased by an order of magnitude. This clearly shows that although Pt alone is active for CO_2/CH_4 reforming the activity can be significantly enhanced by the presence of a support. The enhancement of catalyst activity by the support was also shown for different other reactions. Levin *et al.* [3, 4] observed for CO_2/CO methanation an increase in the activity of Rh when it was decorated by partially reduced titania. Similar observations were made by Boffa *et al.* using oxides like NbO_x, TaO_x and ZrO_x [5]. Koerts *et al.* observed a decrease of the activation energy for CO methanation over Rh/SiO_2 when the catalyst was doped with vanadium indicating the significance of the support for this reaction [6]. The involvement of the support in the reaction mechanism was also shown for the watergas-shift reaction ($CO + H_2O \rightleftharpoons H_2 + CO_2$). A mechanism involving the formation of formates on the support, their migration to the metal followed by decomposition on the metal was discussed [7]. A similar mechanism was proposed for the hydrogenation of CO [8-10].

Having established that the perimeter is decisive for dry methane reforming, the remaining question to be addressed is the role of the support on a molecular level.

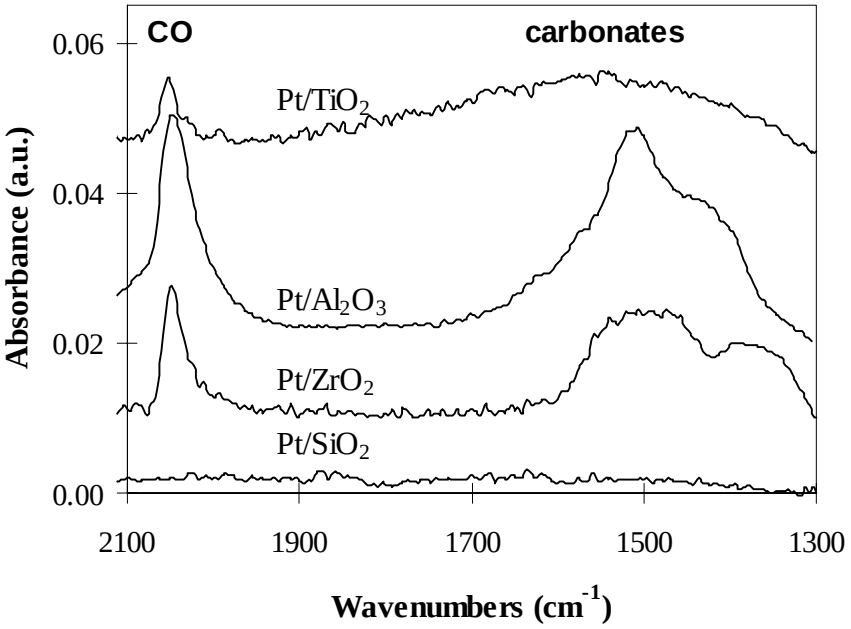

Figure 11 *Infrared spectra of CO_2 adsorption on different Pt catalysts, T=775K, pCO_2=0.25, total flow=30ml.min^{-1}*

Infrared spectroscopic studies of CO_2 adsorption on Pt-catalysts showed the formation of linearly bound CO on Pt, and carbonate type species on the support for Pt/γ-Al_2O_3, Pt/TiO_2 and Pt/ZrO_2 (Figure 11), although the type of carbonate species seems to be different for the various supports. Pt/SiO_2 did not show the formation of carbonate type species on the support while it proved to be active for methane decomposition. On Pt-black no carbonates could be formed on the support because this catalyst is unsupported. In general, it can be concluded that the catalysts which could form carbonates on the support (Pt/γ-Al_2O_3, Pt/TiO_2, Pt/ZrO_2 and Pt-black/ZrO_2, see Table 2) showed a much higher activity compared to the catalysts which could not form carbonates on the support (Pt-black, Pt/SiO_2). Note in this context that the importance of carbonate, for CO_2/CH_4 reforming, was previously suggested by Nakamura *et al.* [11]. They reported that the activity of a Rh/SiO_2 catalyst which did not form carbonates was enhanced by adding MgO, Al_2O_3 or TiO_2 i.e., compounds which facilitate carbonate formation.

Based on the above described results we propose a bifunctional mechanism for dry methane reforming in which CO_2 is activated on the support, while methane is activated

on the metal. The two activated species may react with each other on the Pt-ZrO_2 boundary. A similar mechanism was proposed by Zhang *et al.* [12] for reforming over Ni/La_2O_3. This catalyst was remarkably stable compared to other Ni catalysts for CO_2/CH_4 reforming [13-16]. This was attributed to the ability of the La_2O_3 support to facilitate CO_2 activation in the form of LaO_2CO_3. Reaction of the LaO_2CO_3 species with the activated methane on the metal yields syngas.

Increasing the calcination temperature caused sintering of the Pt particles, which decreased the activity of the catalyst due to a decrease in the perimeter concentration. Moreover, the binding energy of the Pt-$4f_{7/2}$ electrons shifted from 72.8 eV for the sample calcined at 925K to 71.1eV for the sample calcined at 1125K. This indicates that the sample calcined at 1125K contained Pt in the zero valent state [17] which is also supported by the TPR experiments. For the sample calcined at 1125K no hydrogen uptake was observed indicating that Pt was already in the zero valent state. The existence of Pt in the more oxidized state after calcination at 925K can be explained in two ways. Thermodynamic calculations showed that PtO_2 decomposes easily (even in air) at higher

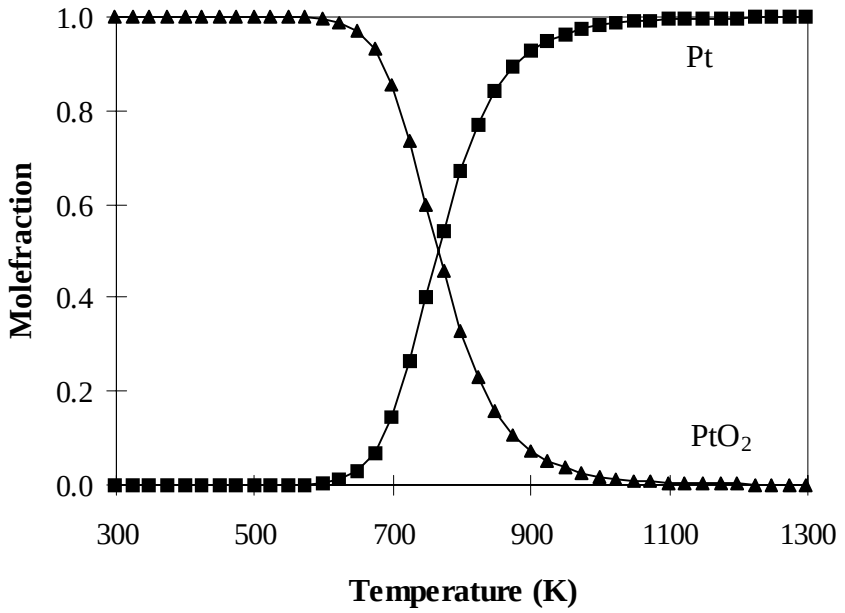

Figure 34 *Decomposition of PtO_2 in 10 folds excess of O_2 according to thermodynamics*

temperatures (Figure 12). This might explain the more reduced state of Pt in the sample calcined at 1125K although the differences on basis of thermodynamics between 925K and 1125K are small (see Figure 12). Alternatively, the Pt particles in the sample calcined at 925K are smaller than in the sample calcined at 1125K (see Table 4). It was shown by different authors that smaller metal particles are easier oxidized than large particles [18-20]. Since the above mentioned XPS and TPR experiments were carried out *ex situ* the samples might have been oxidized in air which proceeds faster for the sample calcined at 925K due to the smaller Pt-particle size of this sample.

In contrast to the calcination temperature, the reduction temperature did not affect the activity of Pt/ZrO_2. However, the hydrogen chemisorption capacity markedly decreased (Figure 8, Table 5) after high temperature reduction indicating an increase in the Pt particle size. EXAFS measurements did not show an increase in the Pt-Pt coordination number indicating that the Pt particle size remains unaffected by the reduction temperature (Table 5). Thus we conclude that these Pt/ZrO_2 catalysts have a

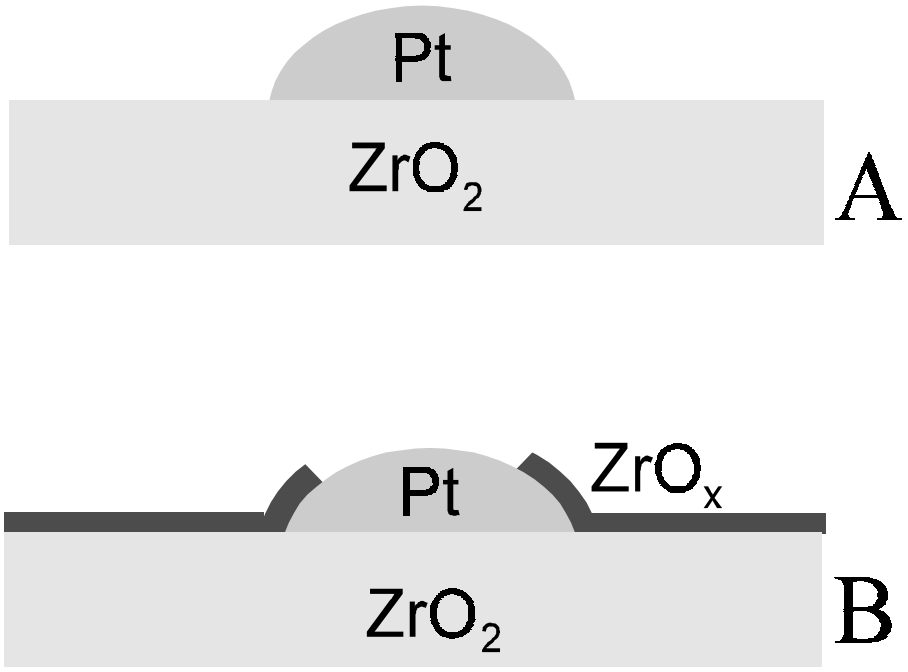

Figure 13 *State of Pt/ZrO_2 (SMSI) during reduction, A=low temperature reduction, B=high temperature reduction*

'strong metal support interaction' which has been previously identified for Pt/TiO_2

catalysts [21, 22] and is also reported to occur on ZrO_2 containing catalysts [23, 24]. In the SMSI state Pt is decorated by the partially reduced oxide (Figure 13) suppressing the hydrogen chemisorption capacity, but leaving the particle size unaffected. This process can be reversed by O_2 or water. Our results showed that the SMSI state could be reverted by oxygen treatment of the sample (Table 5). During reaction conditions this SMSI state is absent, since it is possible to dissociate CO_2 on the catalyst to CO and O_{ads} as shown by IR spectroscopy (Figure 11). The O_{ads} might be responsible for oxidizing the ZrO_x species on the Pt and, thus, minimizing the extent of decoration with oxide islands. Because the SMSI state is not present under reaction conditions, the fraction of metal exposed after low temperature reduction is representative for the Pt availability under reaction conditions.

4.5 Conclusions

In supported Pt catalysts not all the exposed Pt atoms contribute equally to the activity of the catalyst for CO_2/CH_4 reforming. Pt atoms on the support-metal perimeter determine the activity. This is explained in terms of the CO_2 activation *via* carbonate species on the support that must be in the proximity of the Pt particles to react with the methane which is activated on the Pt. The perimeter concentration can be changed by either changing the metal loading or by changing the calcination temperature. The significance of the support is also manifested in the low activity of Pt black and Pt/SiO_2 which were incapable of forming carbonates on the support and showed a low activity for reforming. During high temperature reduction SMSI states evolve on Pt/ZrO_2 catalysts. However, this state does not influence the activity of the catalyst, because adsorbed oxygen (from CO_2 dissociation) destroys it under reaction conditions.

4.6 References

34. Z. Paal, Z. Zhan, E. Fulop, B. Tesche, J. Catal., 156 (1995) 19.
2. B.J. Kip, F.B.M. Duivenvoorden, D.C. Koningsberger, R. Prins, J. Catal., 105 (1987) 26.
3. M.E. Levin, M. Salmeron, A.T. Bell, G.A. Somorjai, J. Chem. Soc., Faraday Trans 1, 83 (1987) 2061.
4. M.E. Levin, M. Salmeron, A.T. Bell, G.A. Somorjai, J. Catal., 106 (1987) 401.
5. A.B. Boffa, C. Lin, A.T. Bell, G.A. Somorjai, Catal. Lett., 27 (1994) 243.
6. T. Koerts, W.J.J. Welters, R.A. van Santen, J. Catal., 134 (1992) 1.
7. D.C. Grenoble, M.M. Edstadt, D.F. Ollis, J. Catal., 67 (1981) 90.
8. J.L. Robbins, E. Marucchi-Soos, J. Phys. Chem., 93 (1989) 2885.
9. P.G. Glugia, K.M. Bailey, J.L. Falconer, J. Phys. Chem., 92 (1988) 4474.
10. B. Sen, J.L. Falconer, J. Catal., 122 (1990) 68.
11. J. Nakamura, K. Aikawa, K. Sato, T. Uchijima, Catal. Lett., 25 (1994) 265.
12. Z. Zhang, X.E. Verykios, S.M. MacDonald, S. Affrossman, J. Phys. Chem., 100 (1996) 744.
13. J.R. Rostrup-Nielsen, J. Catal., 144 (1993) 38.
14. A.T. Ashcroft, A.K. Cheetham, M.L.H. Green, P.D.F. Vernon, Nature, 352 (1991) 225.
15. P.D.F. Vernon, M.L.H. Green, A.K. Cheetham, Catal. Today, 13 (1992) 417.
16. E. Ruckenstein, Y.H. Hu, Appl. Catal. A., 133 (1993) 149.
17. Handbook of X-ray Photoelectron Spectroscopy, Physical Electronics Division, Perkin Elmer Corporation, USA, (1979).
18. T. Frelink, PhD Thesis, University of Eindhoven, The Netherlands (1995).
19. J.C. Vis, F.J. van 't Blik, T. Huizinga, J. van Grondelle, R. Prins, J. Catal., 95 (1985) 333.
20. G.W. Busser, PhD Thesis, University of Twente, Enschede, The Netherlands (1997).
21. S.J. Tauster, S.C. Fung, R.L. Garten, J. Am. Chem. Soc., 100 (1978) 170.
22. S.J. Tauster, Acc. Chem. Res., 20 (1987) 389.
23. P. Turlier, G.A. Martin, React. Kinet. Catal. Lett., 21 (1982) 287.
24. C. Dall'Agnol, A. Gervasini, F. Morazzoni, F. Pinna, G. Stukul, L. Zanderighi, J. Catal., 96 (1985) 106.

5

Mechanistic aspects of CO_2/CH_4 reforming over Pt/ZrO_2

Abstract

As shown in the previous chapters, Pt/ZrO_2 is an active and stable catalyst for CO_2/CH_4 reforming of methane. The mechanism of CO_2/CH_4 reforming over Pt/ZrO_2 has been investigated using steady state and transient kinetic measurements and physico-chemical characterization techniques. Methane can be is decomposed on the metal to CH_x (average value of x=2) and H_2. The main route to CO_2 reduction occurs *via* initial formation of a carbonate species at the metal-support boundary. Reactive coke formed on the metal can react with the carbonate to a formate species and CO. The formate decomposes rapidly

to CO and a surface hydroxyl group.

5.1 Introduction

In principal two mechanisms for CO_2/CH_4 reforming are discussed in the literature. Mark *et al.* [1, 2] and Erdöhelyi *et al.* [3] suggest an Eley Rideal type mechanism in which methane is adsorbed and decomposed on the metal (Rh) to H_2 and adsorbed carbon. Subsequently, the carbon on the catalyst reacts directly with CO_2 from the gasphase to CO.

In the alternative mechanism [4-11] methane is decomposed on the metal to yield a surface CH_x species and hydrogen. Upon sorption, carbon dioxide dissociates to CO and adsorbed oxygen. That oxygen reacts with the CH_x species to CO and hydrogen. While it is agreed that the CH_x species are formed on the metal, the mechanism of carbon dioxide activation is unclear. Qin *et al.* suggest that CO_2 dissociates on the metal (Rh) to form Rh-CO and Rh-O [5]. This is also supported by Bodrov *et al*. for CO_2/CH_4 reforming over a Ni foil [10, 11]. Bradford *et al*. [8], in contrast, suggest that adsorbed hydrogen reacts with CO_2 to form CO and an OH group (retained on the support). However, it is not clear whether CO_2 is activated on the support or if the metal is involved. The OH groups were thought to react at the metal-support interface with CH_x (resulting from methane decomposition) to form a CH_xO species which subsequently decomposes to CO and H_2.

Experimental evidence for the involvement of the support in the reaction mechanism was reported by Nakamura *et al.* [12] who observed an increase in the activity for Rh/SiO_2 when γ-Al_2O_3, TiO_2 or MgO was added to the support. This was attributed to an enhanced CO_2 activation on the support in the form of carbonates. Zhang *et al*. [13] attributed the remarkable stability of Ni/La_2O_3 compared to Ni/γ-Al_2O_3 or Ni/CaO to the fact that La_2O_3 activates CO_2 in the form of $La_2O_2CO_3$.

In Chapter 4 it was shown that the support influences the activity of the Pt catalysts. Unsupported Pt-black and Pt/SiO_2 showed only a low activity, whereas Pt/γ-Al_2O_3, Pt/TiO_2 and Pt/ZrO_2 were active catalysts. The direct correlation of the activity of

Pt/ZrO_2 catalysts with the length of the Pt-ZrO_2 perimeter also indicated the significance of the support.

In this chapter we address the involvement of the individual phases Pt and ZrO_2 of Pt/ZrO_2 catalysts in the reaction mechanism, and discuss their influence on the elementary steps.

5.2 Experimental

All details involving catalyst preparation, testing and characterization are described in Chapter 2.

5.3 Results

5.3.1 Catalytic activity of Pt/ZrO_2

In Chapter 4 it was shown that the activity of Pt/ZrO_2 is determined by the concentration of the Pt-ZrO_2 perimeter rather than by the accessibility of Pt. This is again visualized in Figure 1 in which the linear dependence between the activity of Pt/ZrO_2 and the perimeter concentration is shown.

5.3.2 Interaction of methane with Pt/ZrO_2

The results of pulsing methane over a freshly reduced catalyst, bare ZrO_2 (treated in H_2) and in an empty reactor are shown in Figure 2. When methane was pulsed over a freshly reduced catalyst H_2 and CO were the only observed products in the gas phase. Over ZrO_2 only a very small fraction of methane was converted (<1%). In an empty reactor methane was not converted under the reaction conditions used. In Figure 3 the product distribution is shown as function of the amount of methane pulsed over the catalyst (pulse size

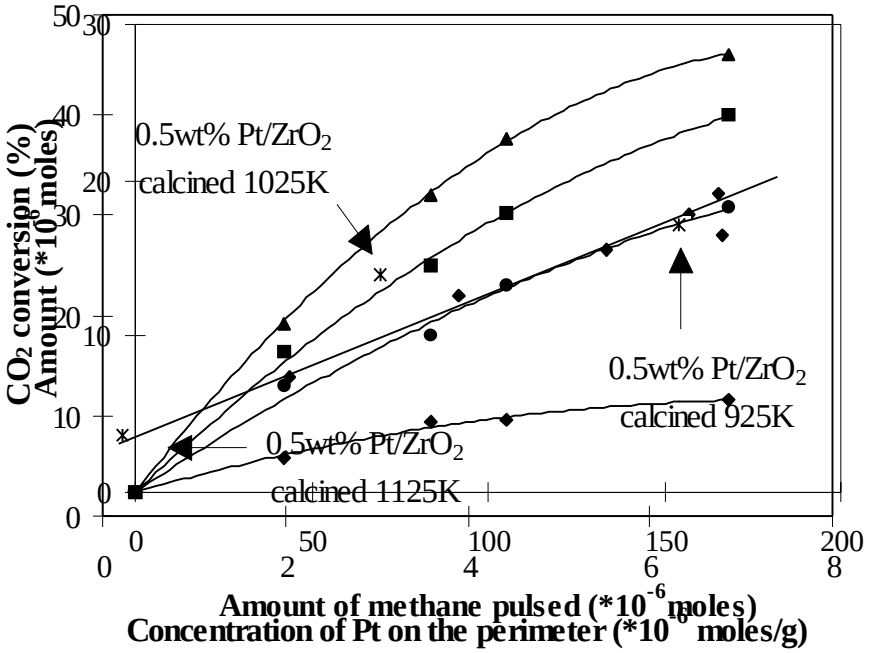

Figure 3 *Product distribution during methane pulsing over Pt/ZrO_2 at 875K (▲=H_2 yield, ■=CH_4 conversion, ●=C yield, ◆=CO yield)*

Figure 1 *Influence of the amount of accessible Pt on the activity of Pt/ZrO_2 catalysts for CO_2/CH_4 reforming, ◆=calcined at 925K*

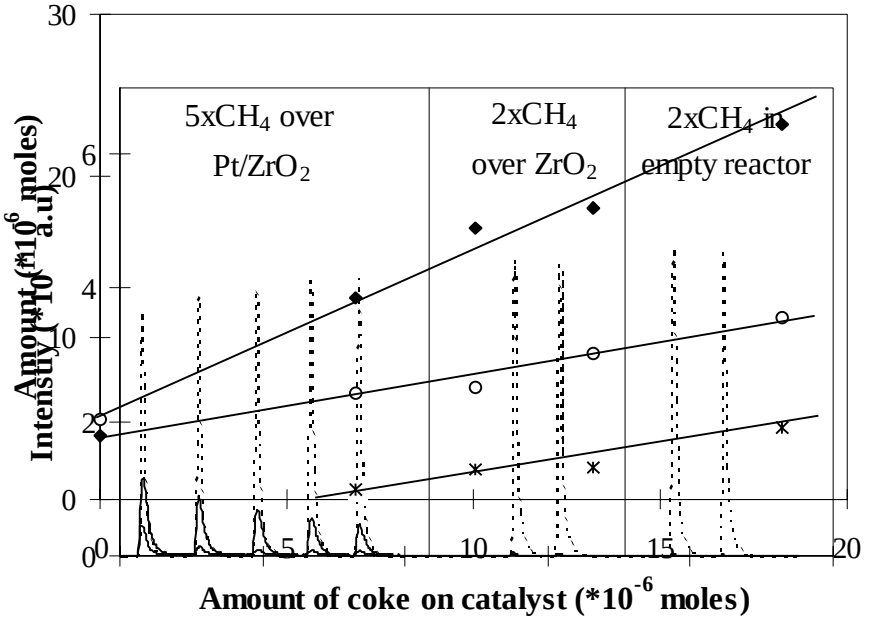

Figure 4 *Product distribution during CO_2 pulsing over coked Pt/ZrO_2 at 875K (○=CO_2 conversion, ◆=CO yield, *=CO_2 yield during subsequent O_2 pulses)*

Figure 2 *Methane pulsing over Pt/ZrO_2 at 875K (dashed line: m/e=15 (CH_4); higher solid line m/e=2(H_2); lower solid line: m/e=28(CO))*

Pulses

$2.1*10^{-5}$ moles CH_4). It can be seen that the rate of methane decomposition decreased with

increasing amount of pulsed methane. When methane is decomposed stoichiometrically, molar H_2 yields double the molar methane conversion ($CH_4 \rightleftharpoons 2H_2 + C$). The H_2 yield was only 1.2 times the methane conversion indicating that hydrogen containing species are retained on the surface of the catalyst. The CO yield is significantly lower than the amount of methane converted. Thus, coke must be deposited on the surface of the catalyst. After the methane pulses CO_2 was pulsed over this coke containing catalyst. The only product observed in this experiment was CO. In Figure 4 the CO_2 conversion and CO yield as function of the amount of coke on the catalyst is plotted. When the amount of coke on the catalyst increased, the CO_2 conversion and the CO yield increased. During all CO_2 pulse experiments 6 pulses of CO_2 ($12.6*10^{-5}$ moles) were given to the sample. Subsequently O_2 was pulsed over the catalyst to remove the remaining carbon.

Table 14 *Influence of the pretreatment on methane conversion over Pt/ZrO_2 at 875K*

Feed conditions		Conversion/Yield ($*10^{-5}$ moles)		
Pretreatment	Total amount of methane pulsed ($*10^{-5}$moles)	CH_4	CO	H_2
H_2	10.5	0.9	0.2	1.1
CO_2*	10.5	1.5	0.3	1.7

*2 pulses ($4.2*10^{-5}$ moles) CO_2

Table 1 shows the influence of the pretreatment of the catalyst with CO_2 on the methane conversion. The first row of this table compiles the product distribution during methane pulsing over a freshly reduced catalyst while the second row shows the results of methane pulsing over a reduced catalyst pretreated with 2 pulses ($4.2*10^{-5}$ mol) CO_2. By treating the catalyst in CO_2 the CH_4 conversion and the H_2 and CO yields increased. Both the $H_{2\ yield}/CH_{4\ converted}$ and CO/CH_4 ratio did not significantly increase by pretreating the catalyst in CO_2.

5.3.3 Interaction of carbon dioxide with Pt/ZrO_2

The transients observed during CO_2 pulsing over freshly reduced Pt/ZrO_2 are

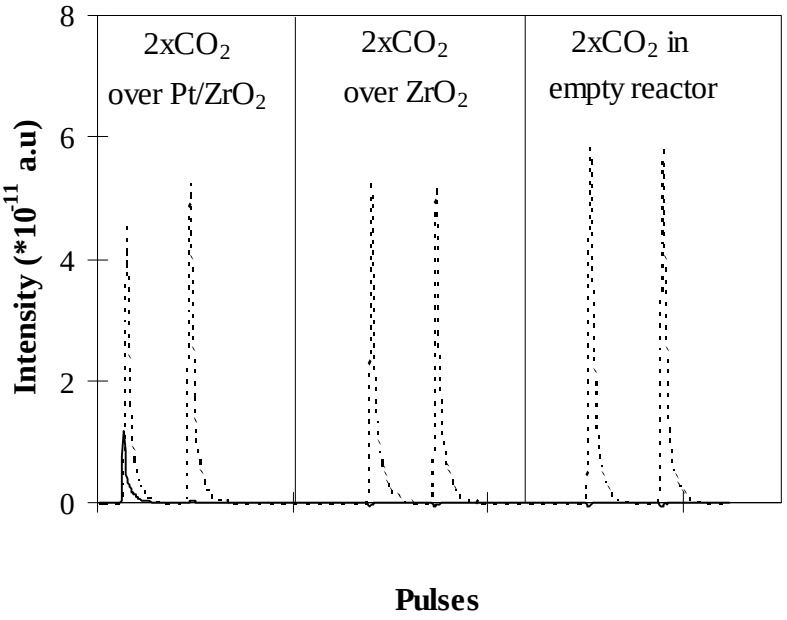

Figure 5 *Carbon dioxide pulsing over Pt/ZrO_2 at 875K (dashed line: m/e=44 (CO_2) ; solid line m/e=28 (CO)*)

shown in Figure 5. The results of pulsing CO_2 in an empty tube and over the bare ('reduced') support are included in the same figure. It can be seen in Figure 5 that CO_2 pulsing over freshly reduced Pt/ZrO_2 yields only CO ($CO_2 \rightleftharpoons CO + O$) in the gas phase. When CO_2 was pulsed over ZrO_2 or in an empty reactor CO formation was not observed. Some CO_2 uptake (10%) was observed over ZrO_2. Possibly, CO_2 is adsorbed on ZrO_2 and is subsequently slowly desorbed again but is not detectable in the background noise of the mass-spectrometer. The CO_2 conversions described in Figure 4 are corrected for the 'missing' 10% of CO_2.

The adsorption of CO_2 on Pt/ZrO_2 and ZrO_2 was also followed by means of time resolved i.r. spectroscopy at 775K. The results of these experiments are shown in Figures 6 and 7. When CO_2 was admitted to Pt/ZrO_2 i.r. bands were observed in two spectral regions. One band was characteristic for CO linearly adsorbed on Pt ($2053cm^{-1}$). The intensity of the CO band decreased with prolonged exposure to CO_2. After 15 minutes

time on stream the band of sorbed CO completely disappeared. Between 1300 and 1500

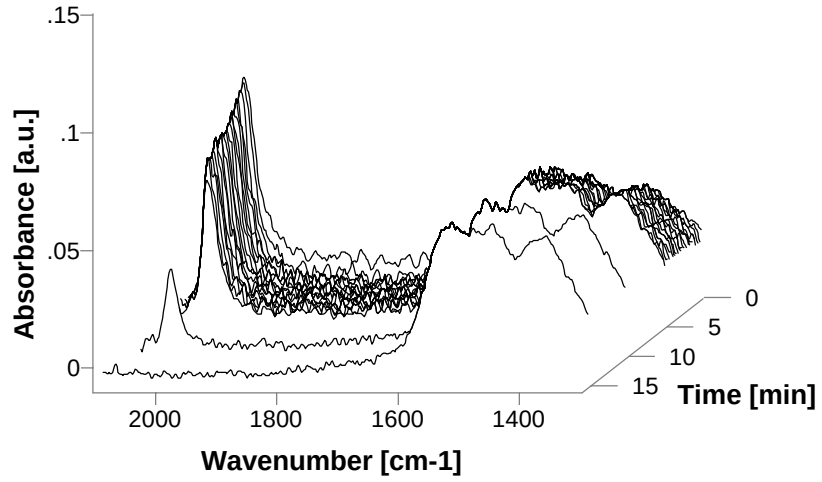

Figure 6 *Time resolved IR spectra during CO_2 adsorption on Pt/ZrO_2, $T=775K$, $pCO_2=0.25$, total flow 30ml/min^{-1}*

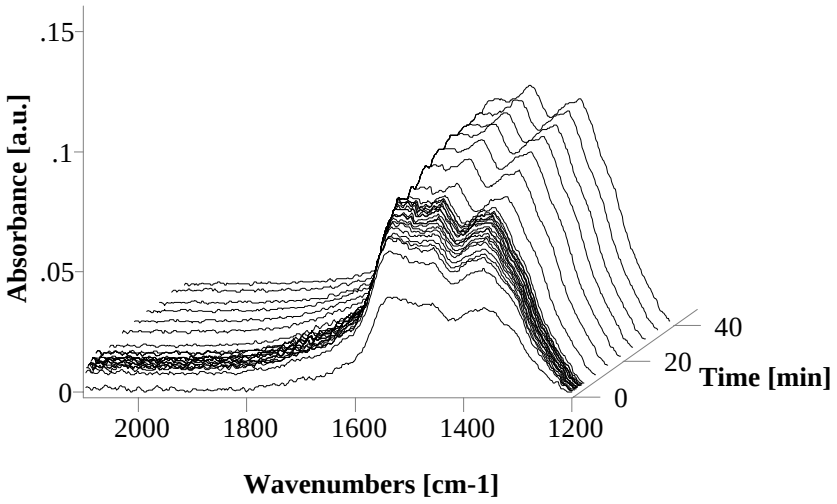

Figure 7 *Time resolved IR spectra during CO_2 adsorption on ZrO_2, $T=775K$, $pCO_2=0.25$, total flow 30ml/min^{-1}*

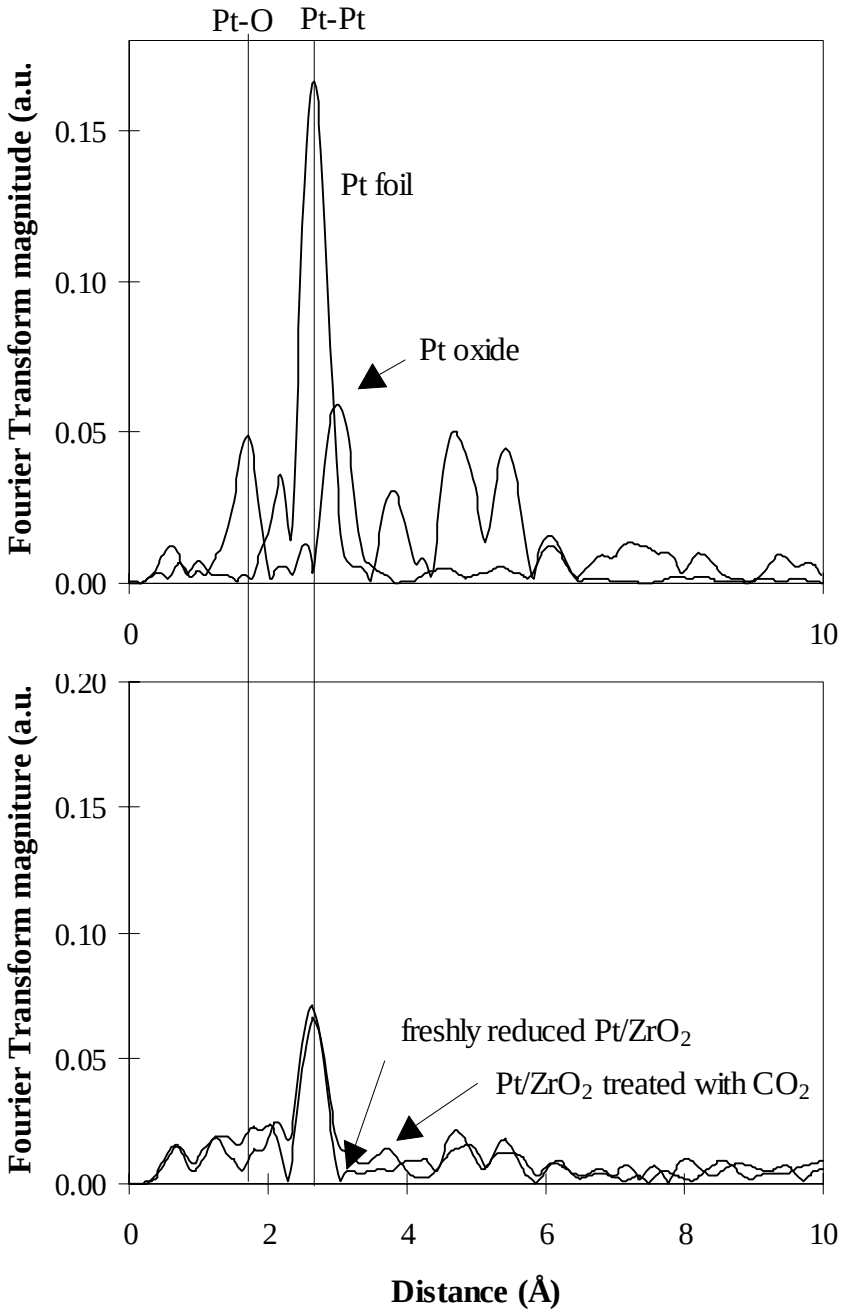

Figure 8 k^2 *weighted Fourier Transformed EXAFS spectra*
upper graph: references (Pt-foil and PtO_2
lower graph: Pt/ZrO_2*, freshly reduced and after 20 min* CO_2 *adsorption at 775K*

cm^{-1} three broad bands were observed and tentatively attributed to surface carbonates [14]. Similar bands were observed when CO_2 was passed over pure ZrO_2 (see Figure 7).

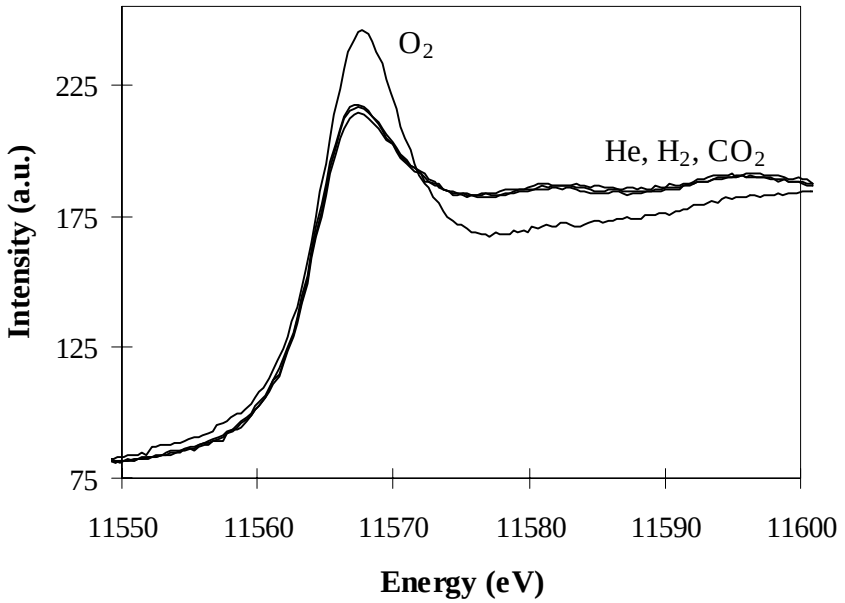

Figure 44 *XANES spectra of Pt/ZrO_2 in different atmospheres at 775K*

While this indicates that Pt/ZrO_2 (at least initially) can dissociate CO_2 to CO and oxygen, the location of the sorbed oxygen still needs to be addressed. Therefore, the catalysts were investigated by means of X-ray absorption spectroscopy in the presence of some of the reactants and products. Figure 8 shows the k^2-weighted Fourier transformed EXAFS spectra of freshly reduced Pt/ZrO_2, and Pt/ZrO_2 which was exposed to CO_2 at 775K for 20 minutes. For comparison, the spectra of the references, Pt and PtO_2, are also included. The radial distribution function of Pt/ZrO_2 did not show a peak at 1.8Å when exposed to CO_2 or when reduced in hydrogen indicating the absence of Pt-O bonds. In Figure 9 the L_{III}-XANES of Pt/ZrO_2 in different atmospheres are compiled. The intensity of the white line of Pt in H_2 is similar to that of Pt in CO_2 or He, while in oxygen a significant increase in intensity was observed.

5.4 Discussion

The linear relationship between the Pt-ZrO_2 perimeter concentration and the activity of the catalyst for reforming suggests that the metal/support interface is important for the activity of the catalyst. This is in line with previous suggestions by Nakamura *et al*. [12] and Zhang *et al*. [13].

Table 15 *Comparison of methane dissociation activity of Pt/ZrO_2 and Pt/γ-Al_2O_3 at 875K*

Feed conditions		Conversion/Yield ($*10^{-5}$ moles)		
Catalyst	Total amount of methane pulsed ($*10^{-5}$moles)	CH_4	CO	H_2
Pt/ZrO_2	4.2	0.9	0.2	1.1
Pt/γ-Al_2O_3	4.2	1.3	0.1	2.0

When methane is pulsed over freshly reduced Pt/ZrO_2, hydrogen and CO were observed as products in the gas phase (Figure 2). By increasing the amount of methane pulsed to the sample, the methane conversion decreased (Figure 3). This was attributed to an increase in the coverage of the metallic sites by coke. CO can be formed from the reaction of methane with oxygen from the catalyst. The importance of the support for CO formation during methane pulsing over Pt/ZrO_2 and Pt/γ-Al_2O_3 is shown in Table 2. Although both samples had the same pretreatment history, more CO was formed over Pt/ZrO_2 compared to Pt/γ-Al_2O_3. This indicates that the ability of the support to release oxygen might be important to form CO. Indeed, different authors observed that ZrO_2 is, at least, partially reducible [14-17] whereas γ-Al_2O_3 is considered to be not reducible [18]. However, prior to the methane pulsing the catalysts were reduced in H_2 which is a stronger reducing agent than methane. Thus it can be expected that the oxygen from the support was removed during reduction. The oxygen to yield CO might originate from traces of oxygen present in the carrier. Table 2 also shows that Pt/γ-Al_2O_3 is more active in methane decomposition compared to Pt/ZrO_2 and a higher coke build up on the former catalyst can be expected. However, it will be shown in Chapter 6 that this is not necessarily related to the higher deactivation rate of Pt/γ-Al_2O_3.

From the CO_2 pulse experiments described in Figure 5 we conclude that Pt/ZrO_2 is able to dissociate CO_2 to CO and adsorbed oxygen. When CO_2 was pulsed over ZrO_2 10% of the pulse was consumed without forming CO (Figure 5). I.r. experiments of CO_2 adsorption on Pt/ZrO_2 and ZrO_2 show that this might be attributed to the formation of carbonate species on the support (Figure 7) [19]. This also explains the CO_2 uptake observed during CO_2 pulsing over ZrO_2. The CO_2 is adsorbed on the support as a carbonate which is subsequently slowly released.

In summary, Pt/ZrO_2 is able to dissociate carbon dioxide to adsorbed CO and oxygen, and methane to adsorbed CH_x and H_2. As CH_4 did not decompose on ZrO_2, it is concluded that methane is dissociated on Pt. Also for CO_2 dissociation Pt seems to be indispensable. However, it appears that the CO_2 dissociation is facilitated when a proper support is available because a catalyst which did not form carbonates (Pt/SiO_2) did not show the formation of CO when exposed to CO_2. This leads to the conclusion that CO was not formed directly from CO_2 but from the decomposition of the carbonate.

The adsorbed coke from decomposed methane can be removed by pulsing carbon dioxide (see Figure 4). Twice the amount of CO was formed compared to the amount of CO_2 pulsed. This indicates that coke was removed by CO_2 ($CO_2 + CH_x \rightleftharpoons 2CO + x/2H_2$). Note that the removal of carbon with CO_2 was observed by Mark *et al*. who showed that carbon formed from methane on Rh/Al_2O_3, could be removed by CO_2 [1, 2]. Subsequent O_2 pulsing resulted in the formation of CO_2, this indicates that not all coke was removed by CO_2. The linearity of the CO_2 yield after O_2 pulsing with the coke content (Figure 4) indicates that a fraction of the coke could not be removed by CO_2. However, when the coke coverage is low, all coke seems to be removable with CO_2. Thus we speculate that methane pulsing leads to the formation of two types of coke. One type of coke can be removed with CO_2, while the other type could only be removed with O_2.

Although the coke formed could be removed by CO_2 and O_2, hydrogen which was still present at the surface is not removed (as discussed above the $H_{2,yield}/CH_{4\ ,converted}=1.2$ (during methane pulsing) whereas a ratio of 2 was expected). As neither hydrogen nor

water were observed during the CO_2 pulses, it is concluded that the hydrogen is retained on the catalyst surface. Note that it was shown in Chapters 3 and 4 that a SMSI like state can occur on Pt/ZrO_2. Thus, part of the hydrogen formed from methane decomposition can reduce part of the ZrO_2 to form water. Because water was not observed as a product during the methane pulse experiments it must be concluded that water remains on the surface of the catalyst most likely as OH-groups. Because the hydrogen balance is always 100% under steady state conditions, we conclude that the formation of OH groups on the catalyst is a transient effect during the pulse experiments. Under steady state conditions the OH groups might desorb as water or react further with methane to form hydrogen and CO (steam reforming).

From Figure 4 it is seen that precoking of the catalyst enhanced the CO_2 conversion and CO yield. On the other hand pretreating of the catalyst with CO_2 followed by methane pulsing showed an enhanced methane conversion compared to methane pulsing over a freshly reduced catalyst (Table 1). Similar observations were made by Solymosi *et al*. [3, 6]. This indicates that both components enhanced the activation of the other.

I.r. spectroscopy demonstrates that CO_2 can be dissociated to CO and, thus, O_{ads} (Figure 6). The decrease of the concentration of sorbed CO with time on stream is explained by blocking of the sites that decompose CO_2 with the oxygen that is concomitantly formed (self poisoning). However, the EXAFS experiments did not give evidence for the presence of Pt-O species so it is not likely that the oxygen is located on Pt. This is also confirmed by XANES experiments, because the intensity of the white line did not increase in the presence of CO_2 (Figure 9) which can be expected when Pt is oxidized [20]. Thus, we conclude that the oxygen is consumed by the support. This oxygen can be released again in the form of CO when methane is pulsed over the catalyst, as was described above.

In addition to CO formation, the i.r. spectra revealed the formation of carbonate type species [14, 18] on ZrO_2. In Chapter 4 it was shown that catalysts which did not

show the formation of carbonates, such as Pt/SiO_2 and Pt-black, had a very low activity for reforming. This clearly indicates that the ability to form carbonates is important for the activity of the catalyst. In order to form CO out of CO_2 at least one of the C-O bonds must be broken. For reactions in which C-O bond breaking was involved (CO/CO_2 methanation) it was shown that the presence of a support enhanced the activity of the catalysts compared to unsupported catalysts [12, 13, 21-25, Chapter 4]. Different authors [12, 13, 21-25] explained this by a weakening of the C-O bond when CO/CO_2 was adsorbed with the carbon on the support and the O-atom on the metal, i.e., at the metal-support perimeter. This facilitates the dissociation of the C-O bond and is in perfect agreement with our observation that Pt catalysts which were active for CO_2 refroming form carbonates on the support, i.e., CO_2 is easy to activate on these materials.

In summary, methane can be decomposed on Pt. The carbon left from this reaction can be removed by CO_2. CO_2 adsorbs on the support and forms carbonates. When carbonates could be formed the activity

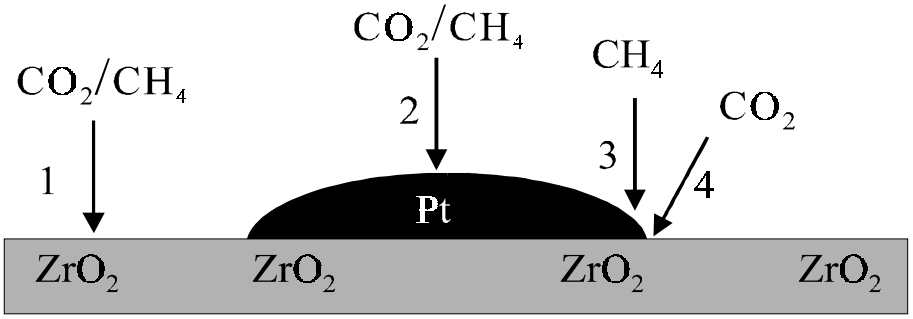

Figure 45 *Possible adsorption sites for CO_2 and CH_4 on Pt/ZrO_2*

of Pt/ZrO_2 has been shown to be linearly proportional to the concentration of the Pt-ZrO_2 perimeter. Based on these observations we propose a mechanism which involves the activation of methane on the Pt and activation of CO_2 on the support. At the Pt-ZrO_2 perimeter the activated species combine to form 2 CO molecules (Figure 10). The Figure shows the different possibilities of CO_2 and CH_4 to adsorb on Pt/ZrO_2. ***Pathway 1*** leads to the formation of carbonate species and coke on the support (see Chapter 6). ***Pathway***

2 leads to the formation of hydrogen and CO directly on the Pt. This pathway can be neglected on Pt catalysts as shown in Chapter 3 (Pt-black had a low activity). However on Rh catalysts this route contributes significantly to the overall activity of the catalysts [1,2, and Chapter 3]. In ***pathway 3 and 4*** methane is dissociated on the Pt particle in the vicinity of the Pt-ZrO_2 perimeter, generating CH_x type species on Pt and H_2 in the gas phase. Carbon dioxide is activated on the support in the vicinity of the Pt particle to form a carbonate. The carbonate might be reduced by the CH_x species to form formate and CO. The formate decomposes rapidly [25] to CO and an adsorbed OH group. OH groups can either recombine and desorb as water or react further with CH_x to form CO and hydrogen

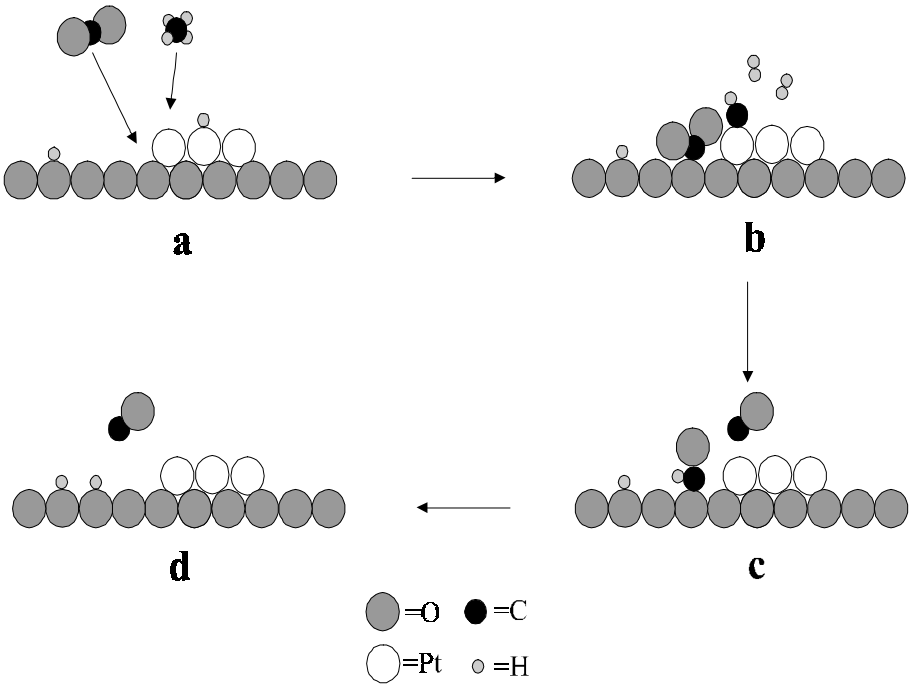

Figure 11 *Schematic representation of the proposed mechanism of CO_2/CH_4 reforming over Pt/ZrO_2.* ***a****: CO_2 adsorbs on the support as carbonate, methane decomposes on the metal.* ***b+c****: The coke species on the metal reduces the carbonate to a formate while CO is formed.* ***c****: The formate decomposes to OH and CO.*
Note that under steady state conditions OH groups and adsorbed hydrogen are presumed to be present.

(steam reforming). Note that also the reverse water gas shift reaction occurs on these catalysts thus an equilibrium between hydrogen and water (OH groups) exists. The

mechanism of CO_2/CH_4 reforming is schematically shown in Figure 11.

5.5 Conclusions

With pulse experiments, it is shown that methane is decomposed on the metal (Pt) to form CH_x and hydrogen. An i.r. spectroscopic study of CO_2 adsorption on the catalyst revealed the formation of carbonate species on the support and CO adsorbed on Pt. Catalysts which were incapable of forming the carbonates were almost inactive for reforming. It was shown (Chapter 4) that the activity of Pt/ZrO_2 depended linearly on the Pt-ZrO_2 perimeter concentration. On basis of these results a mechanism is proposed in which the carbonate on the Pt-ZrO_2 perimeter is reduced by the CH_x species on the metal to form CO and a formate species. In the next step the formate is decomposed to CO and an OH group which remaines on the surface. Under steady state conditions, the OH groups might either desorb as water or react with methane to form CO and hydrogen (steam reforming).

5.6 References

24. M.F. Mark, W.F. Maier, Angew. Chem. Int. Ed. Engl., 33 15/16 (1994) 1657.
2. M.F. Mark, W.F. Maier, J. Catal., 164 (1996) 122.
3. A. Erdöhelyi, J. Cerenyi, F. Solymosi, J. Catal., 141 (1993) 287.
4. J.T. Richardson, S.A. Paripatyadar, Appl. Catal., 61 (1990) 293.
5. D. Qin, J. Lapszewicz, Catal. Today, 21 (1994) 551.
6. F. Solymosi, Gy. Kutsan, A. Erdöhelyi, Catal. Lett., 11 (1991) 149.
7. J. R. Rostrup Nielsen, J.H. Bak Hansen, J. Catal., 144 (1993) 38.
8. M.C.J. Bradford, M.A. Vannice, Appl. Catal. A: general, 142 (1996) 97.
9. D. Qin, J. Lapszwewicz, X. Jiang, J. Catal., 159 (1996) 140.
10. I.M. Bodrov, L.O. Apel'baum, Kinet. Katal., 8 (1967) 379.
11. I.M. Bodrov, L.O. Apel'baum, M.I. Temin, Kinet. Katal., 8 (1967) 821.
12. J. Nakamura, K. Aikawa, K. Sato, T. Uchijima, Catal. Lett., 25 (1994) 265.

13. Z. Zhang, X.E. Verykios, S.M. MacDonald, S. Affrossman, J. Phys. Chem., 100 (1996) 744.
14. M. Bensitel, O. Saur, J.C. Lavalley, Mater. Chem. Phys., 17 (1987) 249.
15. A.L. Borer, C. Brönnimann, R. Prins, J. Catal., 145 (1994) 516.
16. C. Morterra, E. Giamell, L. Oria, M. Volante, J. Phys. Chem., 94 (1990) 311.
17. D.-L. Hoang, H. Lieske, Catal. Lett., 27 (1994) 33.
18. J.M. Rynkowsky, T. Paryjczak, M. Lenik, M. Farbotko, J. Goralski, J. Chem. Soc. Faraday Trans., 91 (1995) 3481.
19. L.H. Little, Infrared spectra of adsorbed species, Academic Press Londen (1966).
20. Y. Iwasawa (ed), X-ray absorption fine structure for catalysts and surfaces, World Scientific Singapore (1996).
21. A.B. Boffa, A.T. Bell, A. Somorjai, J. Catal., 139 (1993) 602.
22. W.M.H. Sachtler, D.F. Shriver, W.B. Hollenber, A.F. Lang, J. Catal., 92 (1985) 429.
23. R.A. Demmin, R.J. Gorte, J. Catal., 98 (1986) 577.
24. A. Fukuoka, T. Kimura, L-F. Rao, M. Ichikawa, Catal. Today, 6 (1989) 55.
25. C. Rhodes, G.J. Hutchings, A.M. Ward, Catal. Today, 23 (1995) 43.

Deactivation of Pt catalysts for CO_2/CH_4 reforming

Abstract

Oxide supported Pt catalysts have been shown to catalyze CO_2/CH_4 reforming through special ensembles of active sites at the metal support perimeter. Deactivation of Pt supported on γ-Al_2O_3, TiO_2 and ZrO_2 is mainly caused by carbon formation which depended markedly on the support. The rate of coke formation increased in the order Pt/γ-Al_2O_3>>Pt/TiO_2>Pt/ZrO_2. Coke was formed on the support and on the metal, for Pt/γ-Al_2O_3 it was estimated that 90% of the coke was located on the oxidic support. When the rate of coke formation on the support is high, the catalyst tends to deactivate strongly due to covering of the ensembles of active sites at the metal-support perimeter. For a catalyst with a support that does not form large amounts of coke on its own (such as ZrO_2) catalysts with larger Pt particles tend to deactivate more quickly than catalysts with smaller Pt-particles. This is attributed to an increasing imbalance in the formation of coke

on the metal and its removal by CO_2 on the perimeter.

6.1 Introduction

The deactivation of CO_2-reforming catalysts is explained by two independent processes, i.e., covering of the active sites by carbonaceous deposits [1-6] or sintering of the metal particles [4,7]. The activity of catalysts which deactivated due to coke formation could be restored by an oxidative treamtent [1-6] i.e., by the removal of coke. Although different authors [1-6] agreed that coke formation is the primary reason for catalyst deactivation, some debate exists on the source of the coke. In principal all three carbon containing species present during reforming (CH_4, CO and CO_2) can be the source of coke. Rostrup-Nielsen *et al*. showed for Ni, Ru, Rh, Pd, Ir and Pt supported on MgO [2], and Richardson *et al.* for Rh/γ-Al_2O_3 [3] that under CO_2-reforming conditions coke originates mainly from methane. Tsipouriari *et al.* [4] on the other hand claim that coke is formed from carbon dioxide. This is in contrast with many authors [1, 5, 6, 8, 9] who showed that an excess of CO_2 in the feed stream suppresses coke formation, which in principal is also the basis of the CALCOR process [8, 9], using dry CO_2-reforming in an excess of CO_2 to produce pure CO. Van Keulen [10] showed that over Pt/ZrO_2 coke was not formed *via* a secondary reaction of the CO formed. Eventhough the Boudouart reaction ($2CO \rightleftharpoons CO_2 + C$) is a well known reaction to form coke.

Deactivation due to sintering of the metal particles during CO_2 reforming is less pronounced. Although some authors observed an increase in the metal particle size during reforming, i.e., Tsipouriari *et al.* for Rh/γ-Al_2O_3 [4] and Swaan *et al*. [7] for Ni/SiO_2. Tsipouriari *et al*. observed a fast coke build up on the catalyst during the first 10 minutes time on stream. After this period the amount of coke on the catalyst remained constant, while the particle size of the Rh catalyst and the deactivation still increased. Thus, they explained the deactivation of the Rh/γ-Al_2O_3 catalyst by the loss of metal area due to sintering. Swaan *et al.* observed an increase in the Ni particle size of their catalysts however, they concluded that the contribution of sintering to deactivation was minimal.

From the above it can be concluded that supported metal catalysts used for CO_2/CH_4 reforming suffer mainly from deactivation caused by coke deposition of the active sites, but sintering of metal particles may also play some role. The results presented in this chapter relate the time on stream behavior of supported Pt-catalysts to the above discussed change in the surface state.

6.2 Experimental

All experimental details involving catalyst preparation, testing and characterization are given in Chapter 2.

6.3 Results

6.3.1 Stability of different Pt catalysts

In Figure 1 the activities of three Pt catalysts ($Pt/\gamma\text{-}Al_2O_3$, Pt/TiO_2 and Pt/ZrO_2) are shown as function of time on stream. The properties of these catalysts are compiled in Table 1. Figure 1 shows that $Pt/\gamma\text{-}Al_2O_3$ and Pt/TiO_2 deactivated significantly while Pt/ZrO_2 was stable during 50 hours of reaction. In Figure 2 the activity of each catalyst is normalized to its initial activity. $Pt/\gamma\text{-}Al_2O_3$ lost 95% of its initial activity during 50 hours of reaction. During the first 10 hours already 80% of the initial activity was lost. Compared to $Pt/\gamma\text{-}Al_2O_3$, the activity of Pt/TiO_2 decreased more gradually, but also with this material the catalytic activity dropped to 25% of its original value after 50 hours time on stream. Pt/ZrO_2 was very stable and lost less than 1% of its activity during this period. In Figure 3 the activities of 0.5wt% Pt/ZrO_2 catalysts that were calcined at 925, 1025 and 1125K are compiled. The catalytic activity decreased with increasing calcination temperature. Note, that also the stability of the catalysts decreased in the same sequence.

Surprisingly, the catalyst calcined at 1125K initially showed a slight increase in activity

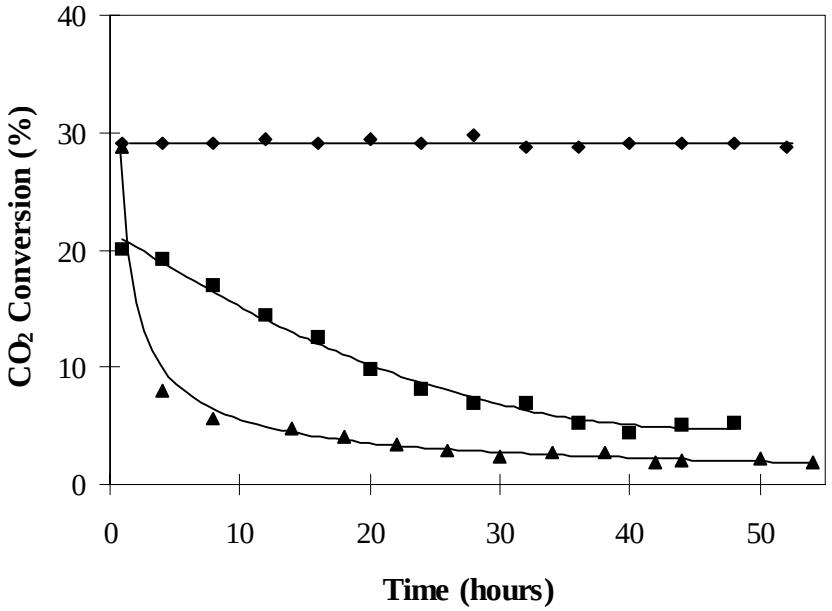

Figure 1 *Stability of different Pt catalysts at 875K, $CO_2/CH_4/Ar/N_2$ =42/42/75/10 ml.min^{-1}, 300mg catalyst, ◆=Pt/ZrO_2, ■=Pt/TiO_2, ▲=Pt/γ-Al_2O_3 (0.5wt%, other details are given in Chapter 2)*

Table 1 *Properties of different 0.5wt% Pt catalysts*

Catalyst	Supplier	Supplier code	BET area (m^2/g)	H/Pt*
Pt/γ-Al_2O_3	AKZO	000-3AQ	110	0.82
Pt/TiO_2	Degussa	P-25	7	0.25
Pt/ZrO_2 (monoclinic)	Gimex	RC-100	17	1.1

* hydrogen chemisorption capacity measured after reduction at 775K

which was followed, however, by a significant deactivation.

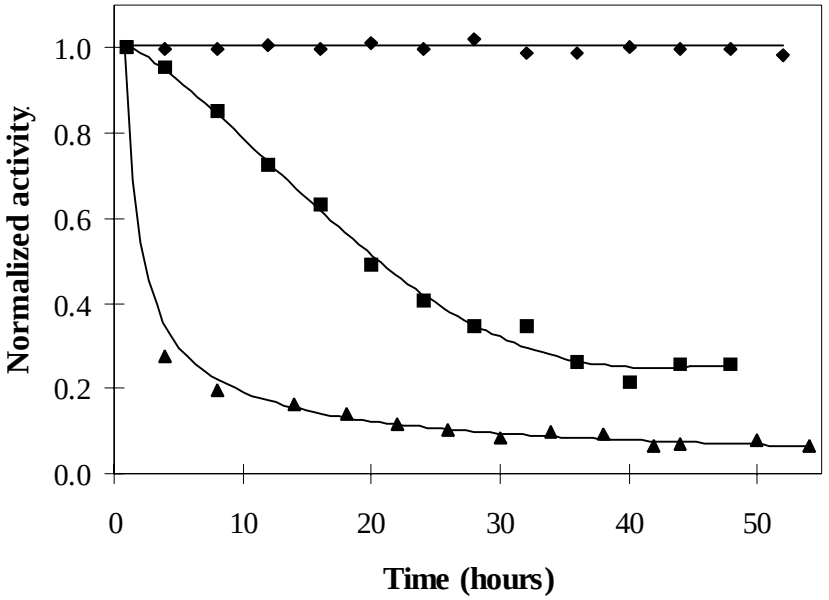

Figure 2 *Normalized activity of different Pt catalysts at 875K, $CO_2/CH_4/Ar/N_2$ =42/42/75/10 ml.min^{-1}, 300mg catalyst, ◆=Pt/ZrO_2, ■=Pt/TiO_2, ▲=Pt/γ-Al_2O_3*

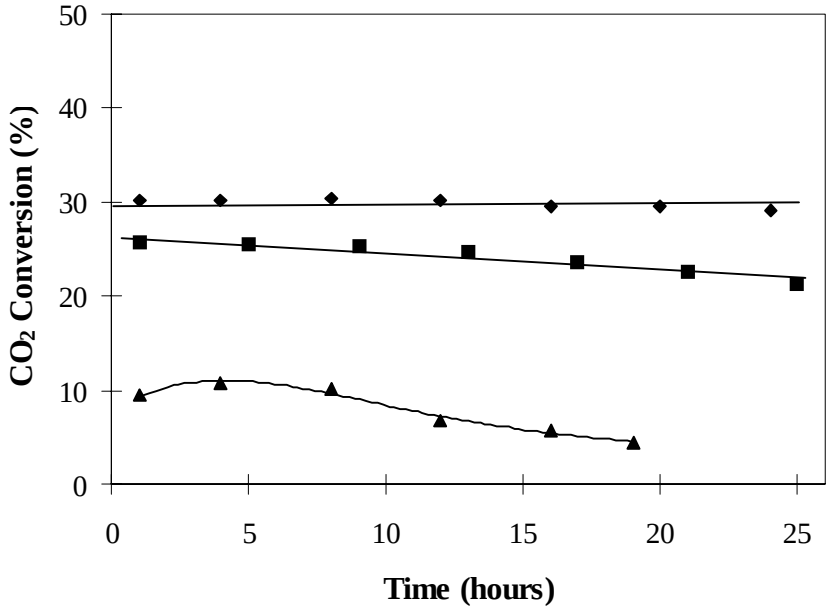

Figure 3 *Stability of Pt/ZrO_2 catalysts with different calcination temperatures, $CO_2/CH_4/Ar/N_2$ =42/42/75/10 ml.min^{-1}, 300mg catalyst, ◆=calcined at 925K, ■=1025K, ▲=1125K*

Table 17 *Influence of the reduction temperature on the Pt accessibility*

Catalyst	Reduction temperature 775K*		Reduction temperature 1125K*	
	H/Pt[1]	Pt-Pt coordination number[2]	H/Pt[1]	Pt-Pt coordination number[2]
0.5wt% Pt/ZrO_2	1.1	-	0.35	-
0.5wt% Pt/TiO_2	0.25	-	0.24	-
0.5wt% $Pt/\gamma\text{-}Al_2O_3$	0.85	-	0.79	-
1wt%Pt/ZrO_2	0.82 (80)	6.5 (86)	0.35 (32)	6.5 (86)
1wt% Pt/TiO_2	0.25# (24)	-	0.25 (24)	-
1wt% $Pt/\gamma\text{-}Al_2O_3$	0.82 (80)	-	0.77 (75)	8.0 (66)

* The values in brackets denote the Pt dispersion (%) calculated according to the models of Kip *et al.* [21]
# Reduction of Pt/TiO_2 at 475K did not change this value
[1] measured by volumetric H_2 chemisorption, [2] calculated from EXAFS

6.3.2 The fraction of available Pt; hydrogen chemisorption and EXAFS measurements

The hydrogen chemisorption capacities of Pt catalysts reduced at two different temperatures are shown in Table 2. In the same table the Pt-Pt coordination numbers as calculated from EXAFS (obtained on 1wt% Pt samples) are also compiled. It can be seen from the table that for Pt/ZrO_2 the hydrogen chemisorption capacity decreased (from H/Pt=1.1 to 0.35 for 0.5wt% Pt/ZrO_2 and from 0.82 to 0.35 for 1wt% Pt/ZrO_2) when the reduction temperature was raised from 775 to 1125K. The Pt-Pt coordination number of 1wt% Pt/ZrO_2 on the other hand did not change with the reduction temperature. In contrast, the reduction temperature did not influence the hydrogen chemisorption capacity

of 0.5 and 1wt% Pt/γ-Al_2O_3 which remained around 0.8. Also for Pt/TiO_2 the calculated fraction of Pt exposed (H/Pt=0.25) did not change with an increasing reduction temperature (475-1125K).

In Table 3 the hydrogen chemisorption capacity and the Pt-Pt coordination number

Table 3 *Influence of calcination temperature on Pt availability of Pt/ZrO_2*

Metal loading (wt%)	Calcination temperature[#] (K)	H/Pt[1*]	Pt-Pt coordination number[2*]
0.5	925	1.1 (100)	-
0.5	1075	0.78 (74)	-
0.5	1125	0.35 (34)	-
1	925	0.89 (84)	6.5 (91)
1	1075	0.70 (65)	-
1	1125	0.35 (34)	10.7 (20)

* The values in brackets denote the Pt dispersion (%) calculated according to Kip *et al.* [21]
[#] all catalysts were reduced at 775K
[1] measured by volumetric H_2 chemisorption, [2] calculated from EXAFS

for Pt/ZrO_2 calcined at different temperatures are compiled. The hydrogen chemisorption capacity and, thus, the fraction of Pt exposed decreased as the calcination temperature increased. This is accompanied by an increase of the Pt-Pt coordination number for 1wt% Pt/ZrO_2. The coordination number increased from 6.5 to 10.7 when the calcination temperature was varied from 925 to 1125K.

In Table 4 the hydrogen chemisorption capacities of three Pt-catalysts in different states (fresh, used (25 hours in CO_2/CH_4 at 875K) and regenerated (used catalyst oxidized in $5\%O_2$/He at 675K and subsequently reduced at 775K)) are compiled. The hydrogen chemisorption capacities of the used catalysts were at least an order of magnitude lower than those of the fresh catalysts. Despite the low hydrogen chemisorption capacity (H/Pt=0.07) of used Pt/ZrO_2 the catalyst was still active. Used $Pt/\gamma\text{-}Al_2O_3$ on the other hand showed a low hydrogen chemisorption capacity (H/Pt=0.09) and had lost about 90% of the initial activity. Similarly Pt/TiO_2 combined a low hydrogen chemisorption capacity (H/Pt=0.01) and a low catalytic activity. After oxidative regeneration the initial activity of all catalysts was restored. Note that Pt/ZrO_2 did not deactivate (under the reaction

Table 4 *Hydrogen chemisorption capacity and catalytic activity*

Catalyst	State	Hydrogen chemisorption capacity (H/Pt)	Pt Dispersion* (%)	CO_2 conversion (%)
Pt/ZrO_2	fresh[1]	1.11	100	30
	used[2]	0.07	7	29
	regenerated[3]	0.90	85	30
Pt/TiO_2	fresh[1]	0.25	25	20
	used[2]	0.01	1	8
	regenerated[3]	0.25	25	
$Pt/\gamma\text{-}Al_2O_3$	fresh[1]	0.82	80	31
	used[2]	0.09	9	3
	regenerated[3]	0.77	75	31

[1]reduced at 775K, [2] after testing at 875K for 25hrs, [3] coke burned off in air at 675K followed by reduction at 775K

* calculated from H/Pt according to Kip *et al.*[21]

conditions applied), however, it was given the same oxidative treatment to investigate its influence on the activity of this catalyst. For $Pt/\gamma\text{-}Al_2O_3$ during 4.5 hours of reaction the catalytic activity is shown in detail in Figure 4. During this period the activity decreased significantly. After 4.5 hours the catalyst was reactivated and the reaction was started again. Figure 4 shows that the original activity of the catalyst is restored after the oxidative treatment but the deactivation was faster with the regenerated catalyst than with the fresh catalyst.

The EXAFS results shown in Table 5 show that the Pt-Pt coordination number of fresh and used Pt/ZrO_2 and $Pt/\gamma\text{-}Al_2O_3$ catalysts were similar within experimental error and, thus, not influenced by the reaction. This indicates that sintering is not the major cause for the deactivation of the Pt-catalysts used in this study. Therefore, coke

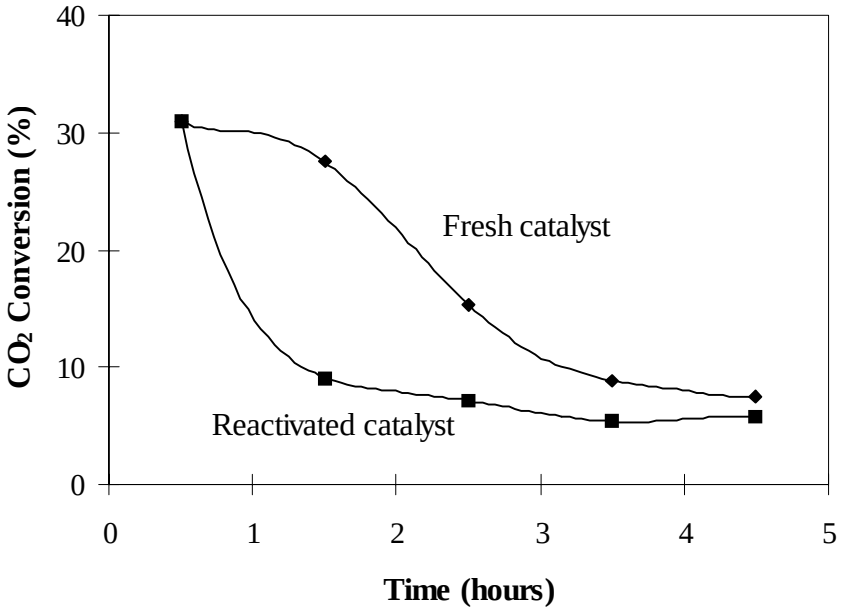

Figure 4 *Activity of Pt/γ-Al_2O_3 at 875K, $CO_2/CH_4/Ar/N_2$ =42/42/75/10 ml.min^{-1}, 300mg catalyst, ◆=freshly reduced catalyst, ■=reactivated by oxidation and subsequent reduction*

Table 5 *Structural parameters from EXAFS for fresh and used Pt catalysts*

Catalyst	State	Coordination number	Pt-Dispersion* (%)	Pt-Pt Distance (Å)	$\Delta\sigma^2$ ($*10^{-3}$Å^2)
Pt/ZrO_2	fresh[1]	6.5	91	2.770	1.44
	used[2]	7	85	2.762	1.20
Pt/TiO_2	fresh[1]	-	-	-	-
	used[2]	10.4	26	2.761	2.00
Pt/γ-Al_2O_3	fresh[1]	8.0	66	2.768	1.94
	used[2]	8.5	60	2.762	1.88

[1] reduced at 1125K, [2] used at 875K for 25h
* calculated according to Kip *et al.*[21]

formation on these catalysts is seen as the most important factor for catalyst deactivation and will, thus, be explored in detail in the next paragraph.

6.3.3 Coke formation on different Pt catalysts

To probe for the rate of coke formation during the reforming reaction, the reaction was stopped after various times on stream (i.e., after 0.5, 1, 2, 5, 10, 25 and 50 h for Pt/γ-Al_2O_3; 2, 5, 10, 25 and 50 h for Pt/TiO_2 and 25 and 180 h for Pt/ZrO_2) and the amount of coke on the catalyst was determined. In Figure 5 the amount of coke, formed per gram of catalyst as function of the total amount of CO_2+CH_4 converted, is shown (note that a double logarithmic scale is used in the figure). It can be seen that the slope of the lines in the figure increased in the order Pt/ZrO_2<Pt/TiO_2<Pt/γ-Al_2O_3, thus, the selectivity towards coke increased in the same order. In Figure 6 the amount of coke formed on the different catalysts normalized per unit surface area of the catalyst support is shown as function of the total amount of feed molecules converted. Compared on this basis, the amount of coke formed as function of the conversion on Pt/TiO_2 and Pt/γ-Al_2O_3 is similar although on Pt/TiO_2 slightly less coke is formed. On Pt/ZrO_2 the coke build up was much slower. In

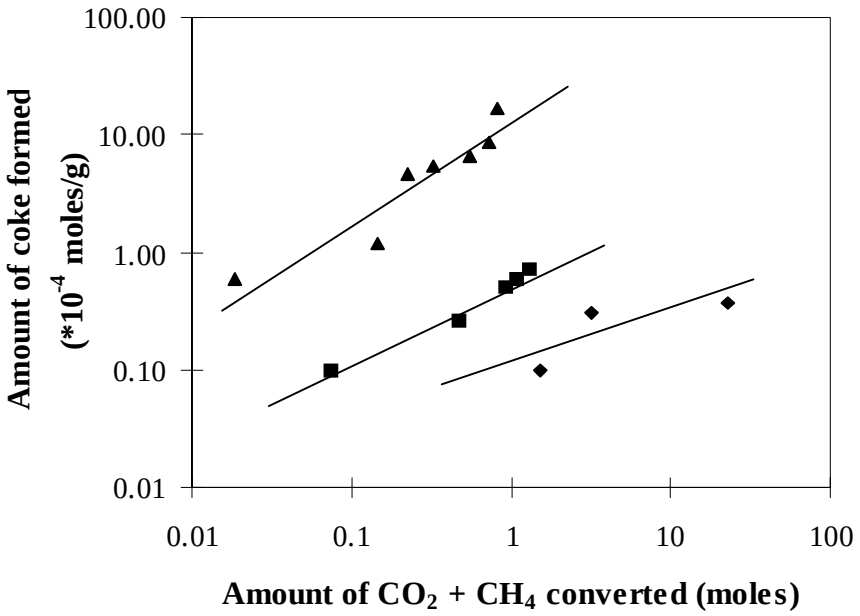

Figure 5 *Amounts of coke formed per gram of catalyst as function of the total amount of CO_2+CH_4 converted on different Pt catalysts at 875K, ◆=Pt/ZrO_2, ■=Pt/TiO_2, ▲=Pt/γ-Al_2O_3*

Figure 7 the activity per Pt atom at the Pt-support perimeter is plotted as function of the

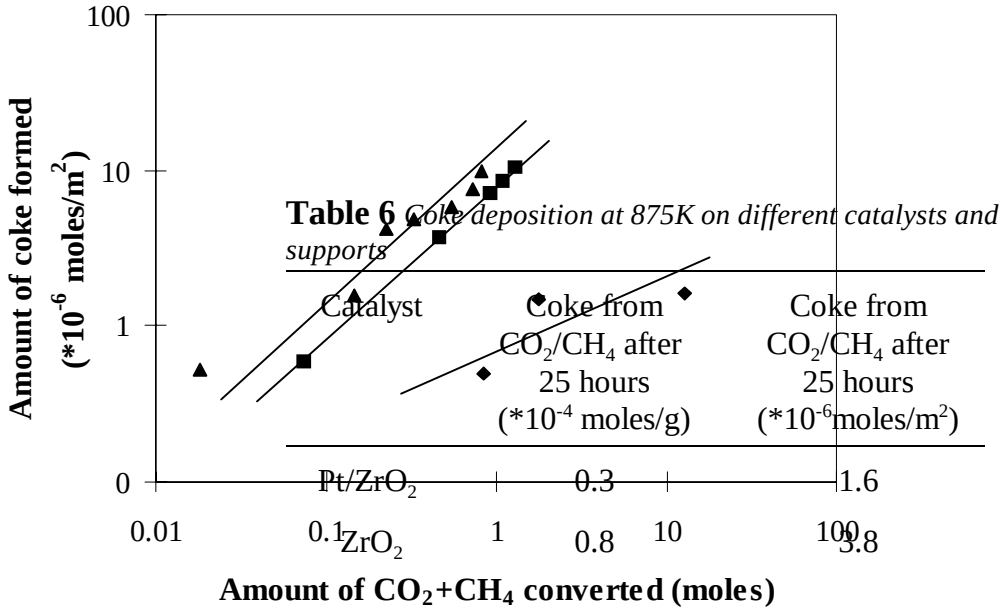

Table 6 *Coke deposition at 875K on different catalysts and supports*

Catalyst	Coke from CO_2/CH_4 after 25 hours ($*10^{-4}$ moles/g)	Coke from CO_2/CH_4 after 25 hours ($*10^{-6}$moles/m^2)
Pt/ZrO_2	0.3	1.6
ZrO_2	0.8	3.8
Pt/TiO_2	0.5	7.1
TiO_2	1.3	18.5
$Pt/\gamma\text{-}Al_2O_3$	8.9	8.0
$\gamma\text{-}Al_2O_3$	2.1	1.9

Figure 52 *Amount of coke formed per surface area catalyst as a function of the total amount of CO_2+CH_4 converted at 875K, ◆=Pt/ZrO_2, ■=Pt/TiO_2, ▲=$Pt/\gamma\text{-}Al_2O_3$*

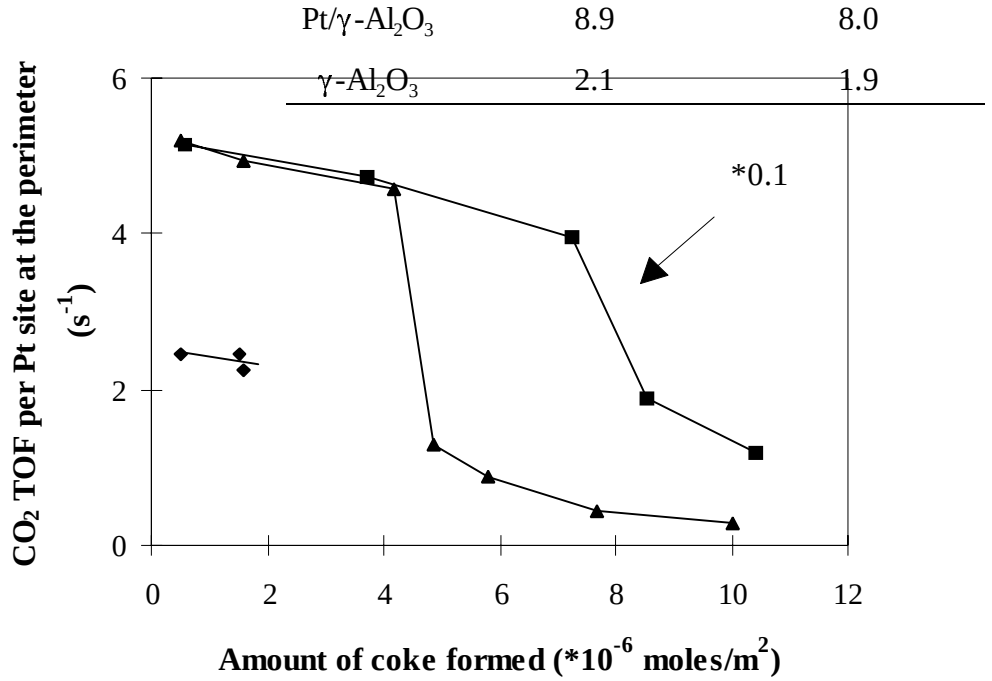

Figure 7 *Catalytic activity of different Pt catalysts as function of the amount of carbon deposited on the catalyst at 875K, ◆=Pt/ZrO_2, ■=Pt/TiO_2, ▲=$Pt/\gamma\text{-}Al_2O_3$*

coke content (as was shown in Chapter 5, the reaction rate is proportional to the amount of Pt on the Pt support perimeter). It can be seen from this figure that two types of deactivation exist on Pt/γ-Al_2O_3 and Pt/TiO_2. Initially, when coke is formed on these catalysts only a small deactivation was observed. At a certain coke concentration the catalytic activity dropped dramatically. For Pt/ZrO_2 this point of rapid deactivation was not reached after 180 hours time on stream.

Table 6 shows the amount of coke formed on the different catalysts after 25 hours of reaction. For comparison, also the amounts of coke formed on the blank supports, under reaction conditions, are included in the table. It is seen that coke was formed on the blank supports and on the catalysts (containing Pt). In the same table the amounts of coke formed on the catalysts are also compared on basis of the BET surface area of the catalysts. While Pt/ZrO_2 formed the least amount of coke, the differences between Pt/TiO_2 and Pt/γ-Al_2O_3 compared on basis of their surface area were less pronounced (see also Figures 5 and 6).

In Table 7 the amounts of coke formed on 0.5wt% Pt/ZrO_2 catalysts calcined at different temperatures (thus having different Pt particle sizes) are shown. It can be seen from this table that the amount of coke formed on the differently calcined catalysts was similar, when the calcination temperature was raised from 925K to 1125K. However, the

Table 22 *Coke deposition at 875K on 0.5wt% Pt/ZrO_2, calcined at different temperatures*

Catalyst	Hydrogen chemisorption capacity (H/Pt)	Pt-particle size[#] (nm)	Coke from CO_2/CH_4 after25 hours (*10^{-4} moles/g)	Coke selectivity[*] (*10^{-6} moles/mol)
925	1.1	1.0	0.31	9.4
1025	0.48	2.4	0.41	16
1125	0.33	3.3	0.43	28

*Coke selectivity = moles of coke formed per gram catalyst/moles of CO_2 +CH_4 converted
[#]particle sizes calculated on basis of hydrogen chemisorption according to ref. 21.

selectivity to coke (i.e., moles of coke formed/moles of feedgas converted) increased significantly (the amount of coke is similar on all catalysts, but the activity of the catalysts decreased with increasing calcination temperature (see Figure 3)).

Table 23 *Relative concentration of acidic sites on different Pt catalysts*

Catalyst	Relative concentration of acidic sites normalized per gram	Relative concentration of acidic sites normalized per m^2
Pt/ZrO_2	1.9	0.7
Pt/TiO_2	1	1
$Pt/\gamma\text{-}Al_2O_3$	11.6	0.7

For reactions involving hydrocarbons it is known that the concentration and the strength of acidic sites of the catalyst play an important role in C-C and C-H bond breaking on the acid sites [11-14]. To investigate the acidity of some of the catalysts, TPD of pyridine was measured. The resulting desorption traces are shown in Figure 8. The

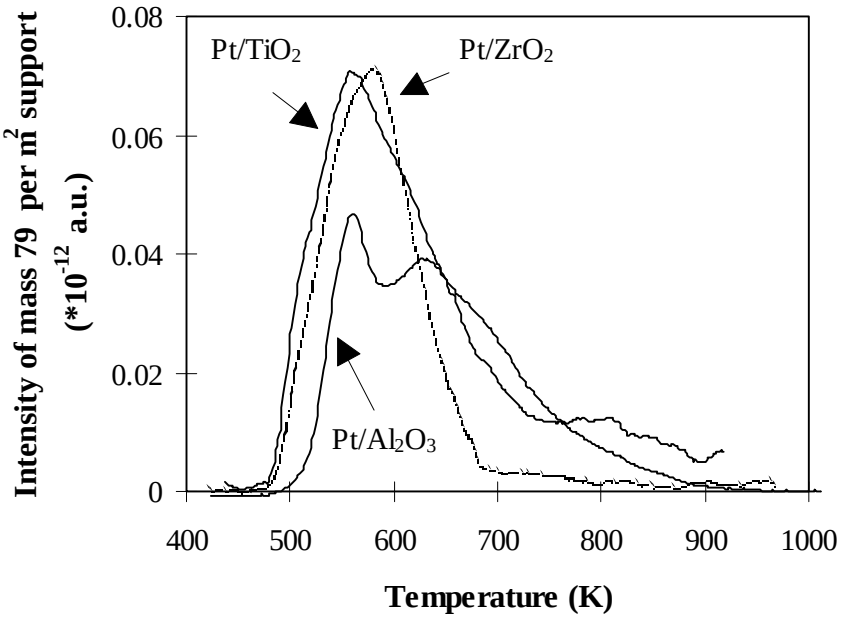

Figure 8 *Temperature programmed desorption of pyridine; pyridine adsorbed at 475K, heating rate 20K/min*

intensity of the signal at m/e=79, proportional to the rate of pyridine desorption, was normalized to the BET surface area of the catalyst. It can be seen in this figure that Pt/TiO_2 showed two desorption peaks with one maximum at 530K and a small peak at 810K. Pt/ZrO_2 showed only one desorption peak with the maximum at 580K. $Pt/\gamma\text{-}Al_2O_3$ showed at least two desorption maxima located at 550K and 640K. The relative areas of the desorption spectra are given in Table 8. The total concentration of acid sites (per m^2 catalyst) on the surface are comparable for all samples, on a weight basis $Pt/\gamma\text{-}Al_2O_3$ contained the highest concentration of acidic sites.

6.4 Discussion

6.4.1 Hydrogen chemisorption

Fresh catalysts

The results of the hydrogen chemisorption experiments and EXAFS on freshly reduced catalysts are summarized in Table 2. It was already shown in Chapter 4 that a SMSI state (i.e., the coverage of the metal particle with the partially reduced support) exists on Pt/ZrO_2 after high temperature reduction. However, this state is not retained under reaction conditions, because of the oxidation of partially reduced zirconia (decorating Pt) with oxygen formed by CO_2 dissociation. The fully oxidized support cannot decorate the Pt particle anymore. Therefore, the hydrogen chemisorption capacity of Pt/ZrO_2 reduced at low temperatures (i.e. in the absence of the SMSI state), assessing the full fraction of Pt, was used in the further discussions.

The SMSI state was originally reported for Pt/TiO_2 [15, 16] after high temperature reduction (>650K). This SMSI state does not occur after low temperature reduction (475K). In general, the apparent low hydrogen chemisorption capacity of high temperature reduced Pt/TiO_2 could be increased by an oxygen treatment followed by a

low temperature reduction. The Pt/TiO_2 samples used in our study showed a low hydrogen chemisorption capacity irrespective of the reduction temperature or oxidative treatment. Therefore, it must be concluded that the observed low hydrogen chemisorption capacity is the 'true' value and that Pt is poorly dispersed. This is also supported by EXAFS measurements on a used Pt/TiO_2 catalyst (see Table 5) which showed a high Pt-Pt coordination number from which a Pt dispersion of 26% was calculated. This is in good agreement with the Pt-dispersion calculated from hydrogen chemisorption (25%).

Table 3 shows clearly that the hydrogen chemisorption capacity of Pt/ZrO_2 decreased with increasing calcination temperature indicating that its fraction of exposed metal decreased. This was also observed when the fraction of metal exposed was calculated from the average particle size calculated from EXAFS. Thus we conclude that the increasing calcination temperature caused sintering of the Pt particles (see also Chapter 4).

Used catalysts

The hydrogen chemisorption capacity of catalysts after different stages of reaction are compiled in Table 4. After 25 hours of reaction the hydrogen chemisorption capacity of all catalysts was very low compared to the fresh catalysts. For Pt/TiO_2 and $Pt/\gamma\text{-}Al_2O_3$ this was accompanied by a decrease in activity (see also Figures 1 and 2). Because the hydrogen chemisorption capacity of the catalysts and their activity was restored after a mild oxidative treatment ($5\%O_2$/He at 675K) it was concluded that sintering did not occur during reaction. Moreover the Pt-Pt coordination numbers of used catalysts (without oxidative treatment) calculated from EXAFS did not differ from those of the freshly reduced samples (Table 5). Thus, it was concluded that the low hydrogen chemisorption capacity of the catalysts after 25 hours of reaction was caused by blocking of the metal by coke deposits. Because Pt/ZrO_2 did not deactivate, at least part of the coke on this catalyst is seen as an reactive intermediate. In contrast, $Pt/\gamma\text{-}Al_2O_3$ and Pt/TiO_2 lost almost

all their activity as the coke was deposited.

6.4.2 Coke formation on Pt catalysts

From the discussion above we concluded that coke formation is the primary cause for the deactivation of Pt catalysts for CO_2/CH_4 reforming. Figures 1 and 2 show that the deactivation of different Pt-catalysts depends crucially on the support. Therefore, the coking rates on supports and on Pt containing catalysts are compiled in Table 6. It can be seen that coke can be formed on the support and on the Pt containing materials. However, there is no simple relation between the amount of coke formed on the blank support and on the catalysts. For Pt/ZrO_2 and Pt/TiO_2 the amount of coke formed on the catalysts is lower then on the support alone. This is tentatively attributed to the coverage of the coke forming sites (possibly Lewis acidic sites) on the support during impregnation with Pt. This is effective for low surface area supports as TiO_2 and ZrO_2 but for $Pt/\gamma\text{-}Al_2O_3$ (high surface area) the concentration of Pt deposited seems insufficient. For this catalyst more coke is formed when Pt is present compared with the support alone. Barbier et al [17, 18] showed that two types of coke were present on cyclopentane reforming ($Pt/\gamma\text{-}Al_2O_3$) catalysts. The coke located on the metal could be removed in oxygen at 575K whereas the coke formed on the support was less reactive towards oxygen and could be removed at 725K. Figure 9 shows the results of oxygen pulsing at two subsequent temperatures over used $Pt/\gamma\text{-}Al_2O_3$. At 675K only 10% of the coke on $Pt/\gamma\text{-}Al_2O_3$ could be removed at 675K while the remaining 90% could be removed at 1125K. This indicates that a large fraction of the coke is located on the support.

The question to be answered now is why the coke formation on $Pt/\gamma\text{-}Al_2O_3$ is higher than on blank $\gamma\text{-}Al_2O_3$. Iglesia *et al.* [12, 13] reported that the rate determining step for the formation of aromatics from alkanes is the removal of the concomitantly formed hydrogen (from C-H scission of the alkane). The hydrogen desorption was claimed to be accelerated by providing “portholes” where the formed hydrogen atoms could recombine

and desorb as dihydrogen. A similar mechanism might occur on our Pt/γ-Al_2O_3 sample. In the absence of Pt, coking on the support is limited by the desorption of the hydrogen formed. When Pt is added, the hydrogen desorption is enhanced (*via* Pt) which could increase the coking rates on the support.

Because coke formation from hydrocarbons on oxidic materials is often related to the acidity of the material [11-14], the acidities of the catalysts used in this study were investigated by means of pyridine TPD. The TPD traces of pyridine (see Figure 8) from Pt/γ-Al_2O_3 and Pt/TiO_2 show two desorption maxima (550K and 640K for Pt/γ-Al_2O_3 and 530K and 810K for Pt/TiO_2) whereas Pt/ZrO_2 showed only one desorption maximum at 580K. This indicates that on Pt/γ-Al_2O_3 and Pt/TiO_2 stronger acid sites are present compared with Pt/ZrO_2. This explains the faster coke build up of Pt/γ-Al_2O_3 and Pt/TiO_2 (see Figures 5 and 6) on the support if we relate higher acidity of the support with more facile methane decomposition. Note that these sites of higher acid strength are of Lewis acid nature which are speculated to be important for dehydrogenation of alkanes [14]. The concentration of these sites decreases in the order Pt/γ-Al_2O_3 >Pt/TiO_2 >Pt/ZrO_2.

The coke formation on the support is also used to explain the faster deactivation of Pt/γ-Al_2O_3 after regeneration. Because low temperature oxidation restored the activity of the catalyst (Figure 4) it is concluded that the metal particle and the perimeter are accessible for reaction after regeneration. However, the regenerated catalyst deactivated much faster than the fresh one. As the perimeter of the coke formed on the support (surrounding the metal particles) may be active for methane decomposition [19, 20] it can be conceptually seen that it takes a much shorter time to block the active perimeter (for reforming) around the Pt particles on the support. Reactivation of Pt/γ-Al_2O_3 at a higher temperature (875K), in an attempt to remove all coke from the catalyst, caused a significant decrease in the activity of the catalyst in the second cycle. This attributed to sintering of Pt during the coke oxidation at this temperature. Note that during oxidation at high temperature, the actual temperature in the catalyst bed might be significantly higher than expected due to the exothermic reaction (hot spot) which might cause

sintering of the Pt particles.

The fact that most of the coke is located on the support explains also the induction periods seen in Figure 7. Initially the coke deposited has only a minor influence on the activity of the catalyst, because most of it is formed on the support and does not influence the availability of the metal particle perimeter for reaction. The slow initial deactivation it attributed to the small fraction of coke that is formed directly on the perimeter making the catalytic active sites unavailable for reaction. At a certain coke concentration it is speculated that the coke formed covers the metal-support perimeter which causes a significant drop in the activity of the catalyst.

The model proposed so far cannot fully account for the higher deactivation of Pt/ZrO_2 catalysts with larger Pt particles (Figure 3). Table 6 shows that the amount of coke formed on the Pt/ZrO_2 catalysts with different Pt-particle sizes is similar for all catalysts. Thus, the (low) amount of overall coke formed on catalysts with larger Pt-particles must act as a stronger poison, i.e., the coke covers the $Pt\text{-}ZrO_2$ perimeter with a higher selectivity. We wish to relate this to the lower perimeter/Pt metal area ratio. In Figure 10 the perimeter/area ratio for a hemisphere is plotted as function of the particle diameter indicating the perimeter/metal area ratio decreases with increasing metal particle size. Thus, a larger area (the outer surface of the hemisphere) becomes available for coke formation (CH_4 decomposition on Pt) while a smaller area (the perimeter) is available for

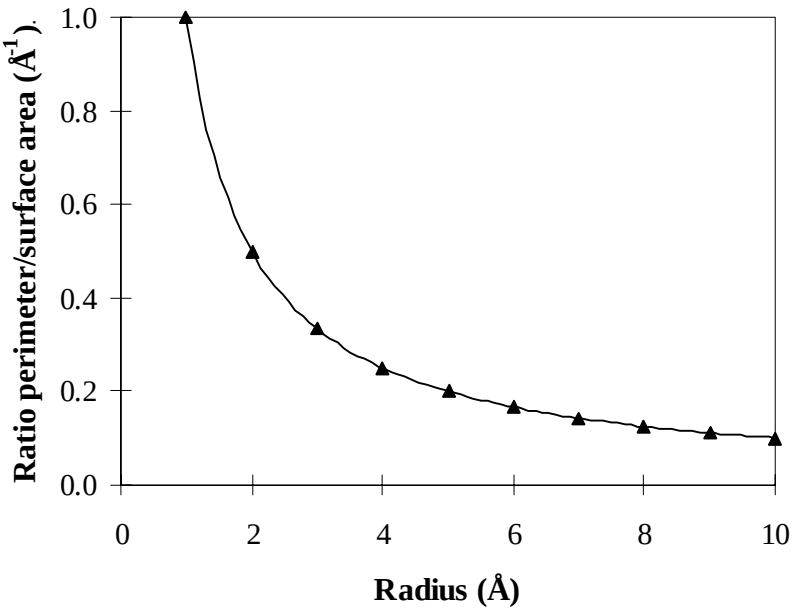

Figure 10 *Ratio between the perimeter and the surface area of a hemisphere as function of the radius*

the conversion of this coke to CO. This might cause an imbalance between the two reactions. More coke will be formed than can be removed by CO_2 causing blocking of the perimeter by coke originating from the metal rather than from the support.

6.5 Conclusions

The stability of Pt catalysts for dry CO_2/CH_4 reforming depends crucially on the support. The stability of the catalysts increased in the order Pt/γ-Al_2O_3<<Pt/TiO_2<Pt/ZrO_2. Pt/ZrO_2 is a stable catalyst and operates with only minor deactivation. The major cause for deactivation of these Pt catalysts is blocking of the active sites by carbonaceous deposits. Coke can be formed on the support and on the metal. When the rate of coke formation on the support is high, the catalysts tend to deactivate strongly due to a blanketing of the metal perimeter by coke which is formed on the strong acidic sites of the support. The rate of coverage of the metal-support

perimeter by coke increases with increasing Pt-particle size. This is explained by an imbalance in the rate of coke formation (on the metal) and the rate of coke removal on the perimeter, due to the lower perimeter/metal-area ratio in larger particles. In conclusion, Pt/ZrO_2 having 0.5wt% Pt and calcined at 875K is the optimal catalyst with a long time stability due to its relatively low acidity of the catalyst and small Pt-particle size (1nm).

6.6 Literature

1. N.R.Udengaard, J.-H. Bak Hansen, D.C. Hanson, J.A. Stal, Oil Gas J., 90 (1992) 62.
2. J.R. Rostrup-Nielsen, J.-H. Bak Hansen, J. Catal., 144 (1993) 38.
3. J.T. Richardson, S.A. Paripatyadar, Appl. Catal., 61 (1990) 293.
4. V.A. Tsipouriari, A.M. Estathiou, Z.L. Zhang, X.E. Verykios, Catal. Today, 21 (1994) 579.
5. K. Seshan, H.W. ten Barge, W. Hally, A.N.J. van Keulen, J.R.H. Ross, Stud. Surf. Catal., 81 (1994) 285.
6. S.T. Ashcroft, A.K. Cheetham, M.L.H. Green, P.D.F. Vernon, Nature, 352 (1991) 225.
7. H.M. Swaan, V.C.H. Kroll, G.A. Martin, C. Mirodatos, Catal. Today, 21 (1994) 571.
8. S. Teuner, Hydroc. Proc., 64 (1985) 106.
9. G. Kurz, S. Teuner, Erdol. Kohle, 43(5) (1990) 171.
10. A.N.J. van Keulen, PhD thesis, University of Twente, The Netherlands (1996).
11. J. Barbier, Appl. Catal., 23 (1986) 255.
12. E. Iglesia, J.E. Baumgartner, G.L. Price, J. Catal., 134 (1992) 549.
13. E. Iglesia, J.E. Baumgartner, Catal. Lett., 21 (1993) 55.
14. T. Narbeshuber, PhD thesis, University of Twente, The Netherlands (1995).
15. S.J. Tauster, S.C. Fung, R.L. Garten, J. Am. Chem. Soc., 100 (178) 170.
16. S.J. Tauster, Acc. Chem. Res., 20 (1987) 389.
17. J. Barbier, G. Corro, Y. Zhang, Appl. Catal., 13 (1985) 245.
18. J. Barbier, Appl. Catal., 23 (1986) 225.
19. German Patent 10789/36. Accepted 14 October 1937.
20. A.S. Hirschon, H.-J. Wu, R.B. Wilson, R. Malhotra, J. Phys. Chem., 99 (1995) 17483.
21. B.J. Kip, F.B.M. Duivenvoorden, D.C. Koningsberger, R. Prins, J. Catal., 105 (1987) 26.

7

Summary and General remarks

Samenvatting en Algemene opmerkingen

Summary

The most widely used process today to produce syngas is steam reforming ($CH_4 + H_2O \rightleftharpoons 3H_2 + CO$). However, the H_2/CO ratio in the produced syngas (=3) is too high for applications such as methanol synthesis ($H_2/CO=2$) or oxoalcohol synthesis ($H_2/CO=1$). In order to reduce the H_2/CO ratio in the product stream, steam reforming can be blended with carbon dioxide reforming. The latter reaction yields syngas with a H_2/CO ratio of 1 ($CH_4 + CO_2 \rightleftharpoons 2H_2 + 2CO$). The major drawback of CO_2/CH_4 reforming is the high thermodynamic driving force to form coke. Nowadays, two commercial processes which use CO_2-reforming have overcome the problem of coke formation exist. In the SPARG process (a mix of steam and CO_2 reforming) sulfur is added to the feed to reduce the Ni ensemble size of the catalyst because small Ni ensembles are less active for coke formation. The second process, using dry CO_2/CH_4 reforming, is the CALCOR process. For this process it is vaguely claimed that a special arrangement of the catalyst throughout the reformer tubes supresses coke formation.

Although the problems related to catalyst deactivation are minimized in the SPARG process, the negative aspect is that it operates in the presence of sulfur. Thus, traces of sulfur might be present in the syngas produced. When a pure syngas is required for further processing additional purification is necessary and this involves an additional investment. Therefore, a catalyst which operates carbon free without the necessity of sulfur addition is preferred. In case of the CALCOR process it is not exactly known how coke formation is prevented. With our research we aimed at the development of a stable catalyst for dry methane reforming and the understanding of the factors that influence the stability of the catalysts.

On noble metals, coke which is formed during the reaction covers the active sites and causes a significant loss of activity. In the case of Ni catalysts coke is formed as filaments with the Ni particle on top of it. The activity of these catalysts remains constant. However, a significant expansion of the catalyst bed occurs and causes severe operational

problems. Coke formation can be suppressed by adding steam to the feed (coupling with steam reforming), by adding oxygen to the feed (coupling with partial oxidation) or by the use of catalysts that kinetically suppress the formation of coke. Because the first two options increase the H_2/CO ratio in the product stream of CO_2/CH_4 reforming, the last option is preferred when low H_2/CO ratios are desired.

As early as 1928, Fischer and Tropsch showed that most group VIII metals show appreciable activity for CO_2-reforming. Since then, many authors investigated the reaction over different metals. It was shown that on noble metals coke formation occurs with a lower rate compared to non-noble metals. In general, Rh supported on γ-Al_2O_3 was preferred by most authors due to its good activity and stability. Ni catalysts, however, are commercially more interesting due to their lower price. Their main draw back is the high rate of coke formation. The use of Pt is a reasonable compromise because it is a noble metal with a good availability and a reasonable price compared to Rh.

In *Chapter 1* a general introduction on the production of syngas is given; also CO_2/CH_4 reforming and its potential uses are reviewed.

Chapter 2 describes the experimental methods used. Drawings of the experimental setups are included in this chapter.

Chapter 3 describes the selection and characterization of a stable and active catalyst for CO_2/CH_4 reforming. Pt and Rh on different inorganic carriers were compared with respect to their activity and stability for CO_2/CH_4 reforming. Rh/γ-Al_2O_3, Rh/ZrO_2 and Pt/ZrO_2 were found to be stable catalysts. The activity of the Rh catalysts was higher compared to that of Pt catalysts. However, due to the poor availability of Rh, Pt is preferred as the active component. The stability of the Pt catalysts depended crucially on the support and increased in the order Pt/γ-Al_2O_3 <<Pt/TiO_2 < Pt/ZrO_2. Thus, Pt/ZrO_2 was selected for further study. 0.5wt% Pt/ZrO_2 (calcined at 875K and reduced at 1125K) is an excellent catalyst for CO_2-reforming with respect to activity and stability. It operated for 180 hours without significant deactivation. When the metal loading exceeded 0.5wt% not all accessible Pt contributed equally to the activity of the catalyst. The fraction of less

active Pt increased with increasing Pt content. This was investigated in more detail in Chapter 4. Rh/SiO_2 deactivated with time on stream. Since this was accompanied by a loss in metal area it was concluded that for Rh catalysts the activity of the catalyst was predominantly determined by the accessibility of Rh. This was further supported by the fact that the influence of the support on the activity was significantly lower for Rh catalysts than for Pt catalysts.

An investigation of the influence of the reduction temperature of Pt/ZrO_2 on the activity showed that when all Pt is reduced (above 475K) its influence was insignificant, although ZrO_2 could be partially reduced at temperatures above 632K.

The reforming reaction is always accompanied by the reverse water gas shift reaction (RWGS, $CO_2 + H_2 \rightleftharpoons CO + H_2O$). The RWGS reaction decreased the H_2/CO ratio in the product stream to values lower than one and increased the CO_2 conversion compared to the CH_4 conversion. As a result of this reaction water was observed in the product stream. At higher temperatures (>900K) and conversions steam reforming of the water formed from the RWGS reaction became more significant. Because steam reforming yields syngas with a H_2/CO ratio of 3, the H_2/CO ratio in the product stream increased.

In *Chapter 4* the influence of the pretreatment and the metal loading on the activity of Pt/ZrO_2 was investigated in more detail. It was shown that not all accessible Pt atoms in Pt/ZrO_2 contribute equally to the activity of the catalyst for CO_2/CH_4 reforming. The Pt atoms on the Pt-ZrO_2 perimeter were shown to determine the activity of the catalyst. I.r. spectroscopy of CO_2 adsorption revealed the formation of carbonate species on the support. Therefore the linearity of the activity with the perimeter length is explained in terms of CO_2 activation *via* a carbonate species on the support that must be in the proximity of the Pt particles to react with the methane activated there. The Pt concentration on the perimeter could be changed either by changing the metal loading or by changing the calcination temperature of the catalyst. Increasing the calcination temperature caused the Pt-particles to sinter, i.e., the perimeter concentration to decrease.

The significance of the support for the activity was also manifested in the low activity of Pt black and Pt/SiO_2. These catalysts were incapable of forming carbonates on the support and showed a very low activity.

As was shown in Chapter 3, the reduction temperature of the catalyst did not have an influence on the stability of Pt/ZrO_2 although the support might be partially reduced at higher reduction temperatures. Increasing the reduction temperature (775-1125K) decreased the hydrogen chemisorption capacity of 0.5wt% Pt/ZrO_2. From EXAFS measurements it could be inferred that the Pt particle size did not increase at higher reduction temperatures. Therefore, it was concluded that a SMSI state (coverage of the Pt particles by the partially reduced support) occurs. The SMSI state is not relevant under reaction conditions because it can be destroyed by the oxygen left behind from CO_2 dissociation ($CO_2 \rightarrow CO + O_{ads}$) (Chapter 5).

Chapter 5 describes a more detailed mechanism for the CO_2/CH_4 reforming. In principal two mechanisms for CO_2/CH_4 reforming are discussed in the literature. An Eley Rideal type mechanism is suggested in which methane is adsorbed and decomposed on the metal (Rh) to H_2 and adsorbed carbon. The carbon on the catalyst reacts directly with CO_2 from the gasphase to yield CO. In the alternative mechanism methane is decomposed on the metal to yield a surface CH_x species and hydrogen. Upon sorption, carbon dioxide dissociates to CO and adsorbed oxygen. That oxygen reacts with the CH_x species to CO and hydrogen.

Transient kinetic measurements showed that methane is decomposed on the metal to form CH_x and hydrogen. In Chapter 4 it was shown that active catalysts formed carbonates on the support. On basis of these results a mechanism is proposed in which the carbonate on the $Pt\text{-}ZrO_2$ perimeter is reduced by CH_x species to form CO and a formate. In the next step the formate is decomposed to CO and an OH group. The latter remains on the surface of the catalyst under transient conditions. Under steady state conditions the OH-groups either can desorb as water or react further with methane to form CO and H_2 (steam reforming).

Chapter 6 describes the deactivation of different Pt catalysts. The stability of the catalysts depended crucially on the support and increased in the order Pt/γ-Al_2O_3<<Pt/TiO_2<Pt/ZrO_2. Hydrogen chemisorption and EXAFS studies on fresh, used and regenerated catalysts showed that blocking of the active sites by coke rather than sintering was the major cause of deactivation. Coke could be formed on the support as well as on the metal. The coke on the metal is reactive and reacts with the CO_2 activated on the support. When the rate of coke formation on the support is high the catalysts tend to deactivate strongly possibly due to a blanketing of the metal perimeter by coke formed on the strong acidic sites of the support. The rate of deactivation increased with increasing particle size. This is explained by an imbalance in coke formation (on the metal) and coke removal (on the perimeter). Larger Pt particles have a higher ratio between the surface area of the particle and the length of the Pt-ZrO_2 perimeter. A higher surface area/perimeter ratio increases the rate of methane decomposition compared to the reaction with CO_2 which causes a faster coke build up on the metal and the perimeter and, thus, a faster deactivation.

General remarks

The stability of Pt based catalysts for CO_2/CH_4 reforming depends crucially on the support. A strong acidic support favors carbon formation on the support which finally covers the metal particle and, thus, deactivates the catalyst. Therefore, a stable Pt catalyst should have a support which only possesses weak acid sites.

The mechanism of CO_2/CH_4 reforming over Pt based catalysts occurs in a bifunctional manner, CO_2 is activated on the support as a carbonate while methane is activated on the metal form a reactive coke and hydrogen. Recombination of the reactive coke with the carbonate species yields CO and water or a surface hydroxyl group. The activity of Pt catalysts which were not able to activate CO_2 on the support (Pt-black and

Pt/SiO_2) was two orders of magnitude lower than catalysts which were able to form the carbonate species (Pt/TiO_2, $Pt/\gamma\text{-}Al_2O_3$ and Pt/ZrO_2). Therefore, an active Pt catalyst for CO_2/CH_4 reforming should be able to activate CO_2 on the support as a carbonate.

Pt/ZrO_2 meets both requirements described above. It has weak acidic sites and is able to activate CO_2 by carbonate formation. Although Pt/ZrO_2 is an active and stable catalyst care has to be taken during the preparation of the catalyst. Increasing the Pt particle size (>1 nm) decreases the stability of the catalyst due to an enhanced rate of methane decomposition on the metal surface compared to the reaction of activated methane with the carbonate at the metal-support perimeter. When 0.5wt% Pt/ZrO_2 is calcined at 875K and reduced at 1125K the Pt particle size is small (1nm) and a stable catalyst is obtained.

Although Pt/ZrO_2 is an excellent catalysts for CO_2-reforming, other catalysts are suitable as well. It was shown in Chapter 3 that $Rh/\gamma\text{-}Al_2O_3$ and Rh/ZrO_2 are also active and stable catalysts for CO_2 reforming. Thus, depending on the availability and the price of these metals one can choose Pt or Rh as the active component. York *et al*. [1] reported a remarkable stability of WC and Mo_2C for CO_2/CH_4 reforming at elevated pressures (8.3atm). Although these authors cannot explain the stability of these catalysts they reported that these catalysts operated for 75 hours without significant deactivation. Consequently, these cheap materials are promising catalysts for CO_2/CH_4 reforming as well.

References

1. A.P. York, J.B. Claridge, A.J. Brungs, S.C. Tsang, M.L.H. Green, Chem. Comm., 1 (1997) 39.

Samenvatting

Op het moment is het meest toegepaste proces om synthese gas (CO en H_2) te maken de omzetting van stoom met methaan (steam reforming; $CH_4 + H_2O \rightleftharpoons 3H_2 + CO$). Het nadeel van dit proces is de hoge H_2/CO verhouding (3) van het geproduceerde synthesegas. Deze verhouding is te hoog voor het gebruik van dit synthesegas voor de synthese van methanol (H_2/CO=2) of oxoalcoholen (H_2/CO=1). De H_2/CO verhouding in het product kan worden verlaagd door steam reforming te mixen met CO_2-reforming welke een H_2/CO verhouding van 1 geeft ($CH_4 + CO_2 \rightleftharpoons 2H_2 + 2CO$). Het grootste probleem tijdens CO_2-reforming is de hoge thermodynamische drijvende kracht om kool te vormen waardoor de katalysator kan deactiveren (edel metalen) of er grote operationele problemen kunnen ontstaan door expansie (kooldraadvorming) van het reactorbed (Ni). Er bestaan twee commerciële processen die dit probleem opgelost hebben. In het SPARG proces (een mix van steam reforming en CO_2-reforming) worden zwavelhoudende componenten toegevoegd aan de voeding om de grootte van de Ni ensembles te verkleinen aangezien op kleine Ni ensembles kool moeilijker gevormd wordt dan op grote. Het tweede proces dat CO_2-reforming commercieel gebruikt is het CALCOR proces. Koolvorming wordt in dit proces voorkomen door een speciale pakking van de katalysator in de reactor. Het is echter niet duidelijk wat deze pakking precies inhoud.

Hoewel deze twee processen het probleem van koolvorming overwonnen hebben is het bezwaar van het SPARG proces dat zwavel toegevoegd moet worden aan de voeding wat uiteindelijk weer verwijderd moet worden uit het product. Van het CALCOR proces is niet bekend hoe de koolvorming tegen wordt gegaan. Daarom hebben wij gezocht naar een katalysator die geen kool vormt tijdens CO_2-reforming. Vervolgens werden criteria opgesteld waaraan aktieve en stabiele (Pt) katalysatoren voor CO_2-reforming moeten voldoen. De resultaten van dit onderzoek staan beschreven in dit proefschrift.

Al in 1928 lieten Fischer en Tropsch zien dat de meeste groep VIII metalen actief

waren voor CO_2-reforming. Sinds die tijd is er veel onderzoek verricht naar CO_2-reforming met gebruikmaking van verschillende metalen. Het voordeel van edelmetalen is hun lagere snelheid van koolvorming vergeleken met niet-edelmetalen. In het algemeen wordt $Rh/\gamma\text{-}Al_2O_3$ gezien als de meest geschikte katalysator door de hoge activiteit en goede stabiliteit van dit materiaal. Katalysatoren gebaseerd op Ni zijn economisch gezien echter meer aantrekkelijk maar het probleem is dat deze katalysatoren veel kool maken. Pt kan gezien vanuit een economisch perspectief (goede beschikbaarheid en relatief lage prijs) een goed compromis zijn.

In *Hoofdstuk 1* van dit proefschrif wordt een introductie gegeven in de productie van synthesegas. Ook wordt een beschrijving van CO_2-reforming en de mogelijke toepassingen van deze reactie gegeven.

Hoofdstuk 2 geeft een beschrijving van de experimenten gebruikt in dit onderzoek; tevens worden schematische tekeningen van de gebruikte apparatuur gegeven.

Hoofdstuk 3 beschrijft de selectie en karakterisering van een stabiele en actieve katalysator voor CO_2/CH_4 reforming. Pt en Rh op anorganische dragers werden met elkaar vergeleken op basis van aktiviteit en stabiliteit voor CO_2-reforming. $Rh/\gamma\text{-}Al_2O_3$, Rh/ZrO_2 en Pt/ZrO_2 bleken aktieve en stabiele katalysatoren te zijn. Aangezien de beschikbaarheid van Rh slechter is dan die van Pt is er voor gekozen om Pt als aktieve fase te gebruiken. De stabiliteit van gedragen Pt katalysatoren hangt sterk af van de gebruikte drager en nam toe in de volgorde $Pt/\gamma\text{-}Al_2O_3 << Pt/TiO_2 < Pt/ZrO_2$, Pt/ZrO_2 werd daarom gebruikt voor verdere studie. Een katalysator met 0.5gew% Pt/ZrO_2 gecalcineerd op 875K en gereduceerd op 1125K was een actieve katalysator die gedurende 180 uur slechts minimaal deactiveerde. Met het verhogen van de metaalbelading (hoger dan 0.5 gew%) nam de concentratie beschikbaar Pt van de katalysator toe, de activiteit daarentegen nam slechts marginaal toe. Hieruit blijkt dat niet alle bereikbare Pt atomen gelijk bijdragen aan de activiteit van de katalysator. De fraktie ‘minder actief’ Pt neemt toe bij hogere Pt concentraties (dit wordt verder uitgewerkt in hoofdstuk 4). Daarentegen bleek de deaktivering van Rh/SiO_2 direkt gerelateerd te zijn aan de beschikbaarheid van Rh. Voor

Rh katalysatoren lijkt de aktiviteit dus bepaald te worden door de beschikbaarheid van Rh. Dit wordt verder ondersteund door het feit dat de invloed van de drager op de activiteit van Rh katalysatoren gering is.

Wanneer de katalysator gereduceerd werd boven 475K was alle Pt gereduceerd en had verdere verhoging van de reduktietemperatuur geen invloed op de aktiviteit van de katalysator. Echter, boven een reduktietemperatuur van 632K kan de ZrO_2 drager gedeeltelijk gereduceerd worden.

Tegelijk met de CO_2-reforming reactie vindt ook de reverse watergas shift plaats ($H_2 + CO_2 \rightleftharpoons H_2O + CO$). Hierdoor is de H_2/CO verhouding in het geproduceerde synthese gas lager dan 1 en wordt een hogere CO_2 conversie waargenomen t.o.v. de CH_4 conversie. Ook is met deze reactie het ontstaan van water verklaard. Wanneer de reactietemperatuur hoger is dan 900K neemt het belang van de steam reforming ($CH_4 + H_2O \rightleftharpoons 3H_2 + CO$) toe en dus neemt de H_2/CO verhouding in het product toe.

In *Hoofdstuk 4* wordt de invloed van de voorbehandeling en de metaalbelading op de aktiviteit van Pt/ZrO_2 in detail beschreven. Er wordt aangetoond dat niet alle bereikbare Pt atomen gelijk bijdragen aan de totale activiteit van de katalysator. De Pt atomen op de rand van het Pt deeltje en de ZrO_2 drager bepalen de uiteindelijke activiteit van de katalysator. I.r. spectroscopie liet zien dat carbonaten op de drager gemaakt konden worden uit CO_2. Wanneer dit in de buurt van het Pt deeltje gebeurd, waar methaan geaktiveerd wordt, kunnen beide geactiveerde deeltjes met elkaar reageren op de rand van het Pt deeltje. Dit verklaart de afhankelijkheid van de activiteit van de katalysator van de Pt-ZrO_2 grensconcentratie. De Pt concentratie op de rand van het Pt deeltje kan worden gevarieerd door de Pt belading van de katalysator te veranderen of door de calcineringstemperatuur van de katalysator te veranderen (sintering). Het belang van de drager voor actieve katalysatoren werd ook aangetoond door gebruik te maken van katalysatoren die geen carbonaten konden maken op de drager (Pt/SiO_2 and Pt-black), deze katalysatoren waren twee orde groottes minder actief dan katalysatoren die wel carbonaten konden maken (Pt/γ-Al_2O_3, Pt/TiO_2 en Pt/ZrO_2).

In Hoofstuk 3 werd aangetoond dat de reduktietemperatuur geen invloed had op de aktiviteit van Pt/ZrO_2, hoewel de ZrO_2 drager gedeeltelijk gereduceerd kan worden bij hogere temperaturen. Wanneer de reduktietemperatuur verhoogd werd, werd een afname in de waterstof chemisorptie capaciteit van Pt/ZrO_2 waargenomen. EXAFS metingen daarentegen toonden aan dat de Pt deeltjes niet groter geworden waren. Hieruit werd geconcludeerd dat de Pt deeltjes gedeeltelijk bedekt waren door de gedeeltelijk gereduceerde ZrO_2 drager (SMSI). Deze toestand is niet aanwezig tijdens reactie omdat in dat geval de drager opnieuw geoxideerd wordt door de zuurstof die achterblijft van CO_2 ontleding ($CO_2 \rightarrow O_{ads} + CO$, zie Hoofdstuk 5).

Hoofdstuk 5 beschrijft het mechanisme van CO_2/CH_4 reforming in detail. Twee verschillende mechanismen zijn in de literatuur beschreven voor deze reactie. Een Eley Rideal type mechanisme werd gesuggereerd waarin methaan ontleedt op het metaal (Rh) onder vorming van H_2 en koolstof. Dit koolstof reageert met CO_2 uit de gasfase onder vorming van CO. In het tweede mechanisme ontleden zowel methaan (naar koolstof en H_2) en CO_2 (naar CO and O) op het metaal waarna koolstof en geadsorbeerd zuurstof met elkaar reageren tot CO.

Puls experimenten toonden aan dat methaan ontleed kon worden op Pt tot kool en waterstof. In Hoofdstuk 3 was aangetoond dat actieve katalysatoren carbonaten op de drager vormden uit CO_2. Op basis van deze resultaten is een mechanisme voorgesteld waarin uit methaan reactief kool gevormd wordt op Pt terwijl uit CO_2 een carbonaat gevormd wordt op de drager. Het reactieve kool op het metaal reageert met het carbonaat onder vorming van CO en een formaat. Dit formaat ontleedt naar CO en een OH groep op het oppervlak van de katalysator. Onder steady state condities kunnen OH groepen recombineren en desorberen als water of verder reageren met methaan naar CO en H_2 (steam reforming).

Hoofdstuk 6 beschrijft de deactivering van verschillende Pt katalysatoren. De stabiliteit van deze katalysatoren hing sterk af van de gebruikte drager en nam toe in de volgorde $Pt/\gamma\text{-}Al_2O_3 << Pt/TiO_2 < Pt/ZrO_2$. Waterstof chemisorptie metingen en EXAFS

studies toonden aan dat de deactivering van deze katalysatoren kan worden toegeschreven aan de bedekking van de aktieve plaatsen door kool en niet door een groei van de Pt deeltjes. Kool wordt voor het grootste gedeelte gevormd op de drager. Wanneer dit proces snel is deactiveert de katalysator snel door een bedekking van de aktieve plaatsen door kool gevormd op de zure plaatsen van de drager. Katalysatoren met grote Pt deeltjes deactiveren sneller dan katalysatoren met kleine Pt-deeltjes. Dit werd verklaard doordat grote deeltjes een relatief korte Pt-ZrO_2 grens hebben vergeleken met het totale buitenoppervlak van het deeltje. Hierdoor neemt de snelheid van methaanontleding (op het buitenoppervlak) toe vergeleken met de reactie van het geaktiveerde methaan met het carbonaat (op de Pt-ZrO_2 grens) waardoor de aktieve plaatsen bedekt worden met kool vanaf het metaal.

Algemene opmerkingen

De stabiliteit van op Pt gebaseerde katalysatoren voor CO_2/CH_4 reforming hangt sterk af van de gebruikte drager. Een drager met sterke zure plaatsen bevordert de vorming van kool op de drager wat uiteindelijk leidt tot een bedekking van de actieve plaatsen met kool. Een geschikte drager, voor Pt, mag dus alleen zwakke zure plaaten hebben.

De CO_2/CH_4 reforming reactie op Pt katalysatoren vindt plaats op de grens van het Pt deeltje en de drager. Methaan wordt geactiveerd op het Pt waar waterstof en reactief kool gevormd worden. Het gevormde koolstof reageert met een carbonaat, gevormd op de drager uit CO_2, onder vorming van CO. De activiteit van Pt katalysatoren die geen carbonaten konden vormen (Pt/SiO_2 en Pt-black) was twee orde groottes lager dan van katalysatoren die dat wel konden (Pt/γ-Al_2O_3, Pt/TiO_2 en Pt/ZrO_2). Een actieve Pt-katalysator moet dus methaan kunnen aktiveren (op het metaal) en CO_2 op de drager.

Pt/ZrO_2 voldoet aan beide hierboven geformuleerde eisen. ZrO_2 heeft alleen zwak

zure plaatsen en kan carbonaten vormen uit CO_2. Hoewel Pt/ZrO_2 een goede katalysator is moet wel enige voorzichtigheid in acht genomen worden tijdens de bereiding. Wanneer de Pt deeltjes te groot worden neemt de stabiliteit van de katalysator af door een naar verhouding snellere ontleding van methaan vergeleken met de reactie van het gevormde kool met het carbonaat op de drager. Wanneer 0.5gew% Pt/ZrO_2 gecalcineerd op 925K en gereduceerd op 1125K wordt gebruikt is aan alle hierboven beschreven voorwaarden voldaan en is de katalysator stabiel.

Hoewel Pt/ZrO_2 een zeer geschikte katalysator is voor CO_2/CH_4 reforming zijn ook andere materialen bruikbaar. In Hoofdstuk 3 is al aangetoond dat ook $Rh/\gamma\text{-}Al_2O_3$ een goede katalysator is. Afhankelijk van de markt (prijs en beschikbaarheid) voor deze twee metalen kan een keus gemaakt worden voor het goedkoopste alternatief. In dit opzicht is het werk van York *et al.* [1] erg interessant. Deze auteurs beschrijven het gebruik van WC en Mo_2C als katalysator voor CO_2-reforming. Deze katalysatoren zijn aktief en stabiel voor 75 uur bij 8.3 atm. Hoewel de aktiviteit en stabiliteit van deze katalysatoren niet verklaard kon worden zijn deze materialen veelbelovend als katalysator voor CO_2 reforming.

Referenties

1. A.P. York, J.B. Claridge, A.J. Brungs, S.C. Tsang, M.L.H. Green, Chem. Comm., 1 (1997) 39.

Curriculum Vitae

Harry Bitter werd geboren op 6 september 1969 te Zeist. In 1986 werd het HAVO diploma behaald aan het Duno College te Doorwerth. Vervolgens werd het Heldring College te Zetten bezocht waar hij in 1988 het VWO diploma behaalde. In dat zelfde jaar begon hij met de studie Scheikunde aan de Katholieke Universiteit Nijmegen alwaar in 1989 het propadeutisch examen werd behaald. Het doctoraal examen werd behaald in 1993 met als hoofdvak organische chemie en als bijvak anorganische chemie. Tijdens de hoofdvakstage werd gewerkt op de afdeling van Prof.dr. B. Zwanenburg aan de synthese van een kiemstimulant voor parasitaire onkruiden. Tijdens de bijvakstage werd op de afdeling van Prof.dr.ir. J.J. Steggerda gewerkt aan de synthese van een koolstof gebrugd heterobinuclear cyclopentadienyl metaal complex. Ook werd de predoctorale cursus vakdidaktiek gevolgd. Gedurende de studie was hij verschillende malen student-assistent op het praktikum voor eerste en tweedejaars scheikunde studenten.
In 1993 begon hij aan een promotie-onderzoek in de katalyse aan de Universiteit Twente (faculteit Chemische Technologie, vakgroep katalytische processen en materialen). Hier werd onder leiding van Prof.dr. J.A. Lercher gewerkt aan de bestudering van katalysatoren voor de omzetting van koolstofdioxide met methaan naar synthese gas. De resultaten van dit onderzoek staan beschreven in dit proefschrift.

List of Publications

J.W.J.F. Thuring, J.H. Bitter, M.M.K. de Kok, G.H.L. Nefkens, A.M.D.A. van Riel, B. Zwanenburg
N-Phthaloyl glycine derived strigol analogues. Influence of the D-ring on the seed germination activity of the parasitic weeds *Striga hermonthica* and *Orobanche crenata*.
J. Agric. Food Chem., submitted

W. Hally, J.H. Bitter, K. Seshan, J.A. Lercher, J.R.H. Ross
Problem of coke formation on Ni/ZrO_2 catalysts during the carbon dioxide reforming of methane.
Studies in Surface Science and Catalysis, **88**, 167 (1994)

J.H. Bitter, W. Hally, K. Seshan, J.G. van Ommen, J.A. Lercher
The role of the oxidic support on the deactivation of Pt catalysts during the CO_2 reforming of methane.
Catalysis Today, **29**, 349 (1996)

J.A. Lercher, J.H. Bitter, W. Hally, W. Niessen, K. Seshan
Design of stable catalysts for methane-carbon dioxide reforming.
Studies in Surface Science and Catalysis, **101**, 463 (1996)

K. Seshan, W. Hally, J.H. Bitter, J.A. Lercher
Carbon dioxide reforming of methane for syngas production - Promises and Pitfalls.
Proceedings of the International Conference on Catalysis and Adsorption and Environmental Protection, Poland, September 1996

J.H. Bitter, K. Seshan, J.A. Lercher
The state of zirconia supported Pt catalysts for CO_2/CH_4 reforming.
Accepted for publication in the Journal of Catalysis

J.H. Bitter, K. Seshan, J.A. Lercher
Mechanistic aspects of CO_2/CH_4 reforming over Pt/ZrO_2 catalysts.
In preparation.

J.H. Bitter, K. Seshan, J.A. Lercher
Deactivation of Pt catalysts for CO_2/CH_4 reforming.
In preparation.